Departament de Microelectrònica i Sistemes Electrònics

Novel methods and tools for corneal barrier function assessment through non-invasive impedance measurements

Autor: Anton Guimerà Brunet

Directors: Dra. Rosa Villa Sanz
Dr. Antoni Ivorra Cano

Tutor: Jordi Aguiló Llobet

Memòria de Tesi
presentada per optar al títol de
Doctor en Microelectrònica i Sistemes Electrònics

Bellaterra (Barcelona), Setembre 2013

Dra. Rosa Villa Sanz, Científica Titular del Consejo Superior de Investigaciones Científicas, Dr. Antoni Ivorra Cano, Recercador "Ramón y Cajal" del Departament de Tecnologies de la Informació i les Comunicacions de la Universitat Pompeu Fabra, i Dr. Jordi Aguiló Llobet, Catedràtic del Departament de Microelectrònica i Sistemes Electrònics de la Universitat Autònoma de Barcelona.

Certifiquen

que la Memòria de Tesi ***Novel methods and tools for corneal barrier function assessment through non-invasive impedance measurements*** presentada per Anton Guimerà Brunet per optar al títol de Doctor en Microelectrònica i Sistemes Electrònics s'ha realitzat sota la seva direcció a l'Institut de Microelectrònica de Barcelona pertanyent al Centro Nacional de Microelectrónica del Consejo Superior de Investigaciones Científicas i ha estat tutoritzada en el Departament de Microelectrònica i Sistemes Electrònics de la Universitat Autònoma de Barcelona.

Directors	Dra. Rosa Villa Sanz	.....
	Dr. Antoni Ivorra Cano	.....
Tutor	Dr. Jordi Aguiló Llobet	.....

……, a ……. de …….. de ……

A l'Anna,

a la Foix,

als meus pares

i a la meva germana

Abstract

The cornea is a hemispherical transparent structure located in front of the eye that allows the transmission of light and protects the ocular globe against external aggressions. Basically, it consists of three layers; the outer layer is the epithelium, the mean and thicker layer is the stroma and the endothelium is the innermost layer. The corneal transparency depends on the hydration of the stroma, which has to remain in a constant state of dehydration. This hydration level depends on a dynamic equilibrium between the ion fluxes through the endothelial and epithelial layer. Thus, the permeability of those layers plays the most important role to maintain the corneal homeostasis, and finally, the corneal transparency.

The quantitative assessment of the endothelial and epithelial permeability is of special interest to diagnose and monitor corneal diseases. Moreover, it is also important in the development of ophthalmologic drugs to improve their efficiency and security. However, there is a lack of proper non-invasive methods for assessing the corneal barrier function in *in vivo* conditions, and consequently in the clinical practice.

Since ionic permeability has a fundamental impact on the passive electrical properties of living tissues, methods based on the study of those properties have consistently been used in *in vitro* studies of the corneal layers functionality.

This dissertation is focused on the development and validation of a non-invasive method to assess the functional state of the main corneal layers in *in vivo* conditions. The proposed method is based on tetrapolar impedance measurements performed by electrodes placed on the corneal surface taking advantage of the progress made in the microtechnology field.

An electrical model of the cornea has been developed and analyzed by means of finite elements method (FEM). This model takes into account the main corneal layers together with the surrounding liquids like tear film and aqueous humour. It also implements a tetrapolar impedance measurement setup by means of electrodes placed on the corneal surface. The simulation results indicate that these measurements are indeed sufficiently sensitive to the changes in the electrical properties of the epithelial and endothelial layers, which are related with the permeability of such layers. It is also observed that the measurements are affected by the thickness of tear film existing between the impedance sensor and the corneal surface. From these results, an impedance sensor which allows the implementation of different electrode configurations was proposed in order to experimentally validate which one presents the best reliability.

The impedance sensor was firstly fabricated using a rigid Pyrex® substrate. Thus, in order to flatten the corneal curvature and ensure the electric contact between the electrodes and the corneal surface a reasonable pressure must be applied. However, the proper electric contact can only be achieved with the closest electrode configuration. Despite this limitation, the capability to *in vivo* assess the corneal barrier function was successfully evaluated by pharmacologically increasing the epithelial permeability of rabbits.

To overcome the limitations of the rigid substrate, a flexible impedance sensor has been developed using a polymeric SU-8 substrate. Therefore, the usability and performance of the proposed method is increased since no pressure is needed to place the sensor on the corneal surface. Its feasibility was evaluated *in vivo* by pharmacologically increasing the epithelial permeability and monitoring a corneal epithelium wound-healing process. The obtained impedance results of both experimental procedures were successfully compared to the measurements of permeability to sodium fluorescein, a well-known destructive method directly related with the permeability. It was also observed that the resolution of the performed measurements is mainly limited by variations in the tear film thickness between the sensor and the corneal surface. However, it was observed that the contribution of the tear film to the measured impedance can be minimized by increasing the separation between electrodes.

In parallel with the development of the *in vivo* system, it has been studied the possibility to apply the method to assess the endothelium barrier function of excised corneas. This new development could be a helpful tool for evaluating the corneal functionality before grafting. Moreover, it also can be applied to improve the behaviour of the preservation liquids used in the eye banks. The proposed method will allow the simplification of the currently used experimental procedures, which requires the remove of the epithelium to perform the measurement. The obtained impedance results were successfully compared with microscopy immunostaining techniques.

The multidisciplinary work described in this dissertation has given rise to a novel method for *in vivo* assessment of the corneal barrier function in a non-invasive way. The excellent results obtained in the experimental field have allowed transferring the proposed method to the clinical practice. Thus, the developed microsystem has been accepted as a medical device by Spanish Agency of Medicines and Medical Devices (AEMPS) to be used in humans. Currently, the developed method is clinical assay phase.

Resum

La còrnia és una estructura transparent ubicada a la part frontal de l'ull que permet la transmissió de la llum i protegeix globus ocular d'agressions externes. Les capes principals de la còrnia són: l'epiteli, l'estroma i l'endoteli. L'epiteli és la capa més superficial, està constituïda per cèl·lules de creixement ràpid que formen una estructura molt similar a la de les capes més superficials de la pell. La capa mitja i més gruixuda és l'estroma, format bàsicament per fibres de col·lagen que proporcionen a la còrnia les seves propietats òptiques i mecàniques. Finalment, la capa més interna és l'endoteli, format per una monocapa de cèl·lules amb molt poca capacitat regenerativa. La principal característica de la còrnia és la seva transparència, fet que la fa diferent de la majoria de teixits vius. Aquesta transparència depèn del nivell de hidratació de l'estroma, que ha de mantenir-se en un constant estat de deshidratació. Aquest nivell de hidratació depèn d'un equilibri dinàmic entre els fluxos iònics que travessen les capes endotelials i epitelials. Per tant, la permeabilitat d'aquestes capes resulta un factor determinant per mantenir la homeòstasis corneal i conseqüentment, la transparència corneal.

L'avaluació quantitativa de la permeabilitat endotelial i epitelial és important per diagnosticar i controlar les malalties corneals. De la mateixa forma, també és especialment interessant en el desenvolupament de medicaments oftalmològics per millorar la seva eficiència i seguretat. Malgrat això, no existeixen mètodes apropiats per avaluar la funció barrera corneal de forma no invasiva i que puguin ser utilitzats *in vivo* o en la pràctica clínica.

Ja que la permeabilitat iònica té molta importància en les propietats elèctriques passives dels teixits vius, els mètodes basats en aquestes propietats són àmpliament utilitzats en estudis *in vitro* de la funcionalitat de les capes corneals.

Aquesta tesis doctoral es centra en el desenvolupament i validació d'un mètode no invasiu per l'avaluació de l'estat funcional de les principals capes corneals que pugui ser utilitzat *in vivo*. El mètode proposat es basa en mesures d'impedància tetrapolars realitzades mitjançant elèctrodes col·locats sobre la superfície corneal gràcies a l'evolució en el camp de les tecnologies microelectròniques.

Per avaluar la viabilitat del mètode proposat s'ha desenvolupat un model numèric basat en elements finits (FEM) que té en compte les principals capes de la còrnia i el líquids que l'envolten, la llàgrima i l'humor aquós. Aquest model també implementa el sistema per realitzar mesures d'impedància tetrapolars mitjançant elèctrodes col·locats sobre la superfície corneal. Els resultats de les simulacions indiquen que les mesures són suficientment sensibles als canvis de les propietats elèctriques de l'endoteli i de l'epiteli, que es poden relacionar amb la permeabilitat d'aquestes capes. També s'ha observat que les mesures estan afectades pel gruix de la llàgrima que hi ha entre el sensor i la superfície corneal. A partir dels resultats obtinguts, s'ha proposat un sensor d'impedància que permet la implementació de diferents configuracions d'elèctrodes per tal d'avaluar quina d'aquestes funciona millor experimentalment.

Una primera versió del sensor d'impedància s'ha fabricat utilitzant un substrat de Pyrex®. De forma que s'ha d'aplicar una certa pressió per tal d'aplanar la curvatura corneal i assegurar

el contacte elèctric entre la superfície corneal i els elèctrodes. Malgrat la pressió exercida, sols es pot assegurar el contacte elèctric per la configuració d'elèctrodes més pròxima. Malgrat aquesta limitació, s'ha validat la capacitat del mètode per avaluar *in vivo* la funció barrera de la còrnia.

Per tal de superar les limitacions del substrat rígid, s'ha desenvolupat un sensor de impedància flexible basat en un substrat polimèric de SU-8. D'aquesta forma, la facilitat d'ús i aplicabilitat del mètode proposat milloren notablement ja que no es requereix pressió per aplicar el sensor. La viabilitat del mètode ha estat avaluada incrementant farmacològicament la permeabilitat epitelial de conills i monitoritzant el procés de cicatrització de l'epiteli. Els resultats obtinguts amb els dos procediments experimentals s'han comparat satisfactòriament amb mesures de permeabilitat a la fluoresceïna, un mètode destructiu que es relaciona directament amb la permeabilitat. També s'ha observat que la resolució de les mesures realitzades està principalment limitada per variacions en el gruix de la llàgrima entre el sensor i la superfície corneal. Malgrat això, també s'ha observat que la contribució de la llàgrima a la impedància mesurada es pot minimitzar augmentant la separació.

En paral·lel amb el desenvolupament del sistema *in vivo*, s'ha estudiat la possibilitat d'aplicar el mètode a l'avaluació de la funció barrera de l'endoteli en còrnies extretes. Aquest nou desenvolupament podria ser molt útil per avaluar la funcionalitat corneal abans d'un transplantament. Per altre banda, també pot ser aplicat a la millora del comportament dels líquids de preservació utilitzats en els bancs d'ulls. El mètode proposat permetrà la simplificació dels procediments experimentals utilitzats actualment, que requereixen de l'eliminació de l'epiteli abans de fer la mesura. Les mesures d'impedància obtingudes s'han comparat satisfactòriament amb tècniques microscòpiques de tinció immunològiques.

El treball multidisciplinar presentat en aquesta tesis doctoral ha resultat en un nou mètode per a l'avaluació *in vivo* de la funció barrera corneal de forma no invasiva. Els excel·lents resultats obtingut han permès la transferència tecnològica del mètode proposat a la pràctica clínica. D'aquesta forma, el microsistema desenvolupat ha estat acceptat com a dispositiu mèdic per l'Agència Espanyola dels Medicaments i Productes Sanitaris (AEMPS) per ser utilitzat en humans. Actualment, el mètode desenvolupat es troba en fase d'assaig clínic.

Agraïments

Són moltes les persones que d'alguna forma o altre han fet possible que aquesta tesis hagi arribat a bon port, algunes vegades de forma voluntària i d'altres sense adonar-se'n. En aquestes línies vull aprofitar per agrair a tots aquells que amb el seu suport i estima m'han ajudat a tirar endavant en els moments complicats.

Per començar m'agradaria donar les gràcies als meus dos directors. A la Rosa Villa, amb qui vam començar aquesta aventura, entre moltes d'altres, i en totes elles sempre m'he trobat recolzat i acompanyat. A l'Antoni Ivorra li haig d'agrair que m'injectés "el virus" de la impedància i de la ciència en els anys que vam coincidir al CNM, així com el suport i confiança rebuts en el transcurs d'aquesta tesi. També vull recordar al meu tutor, el Jordi Aguiló, que, a la seva manera, ha fet molt perquè jo hagi arribat fins aquí.

Haig d'agrair al MINECO el seu suport econòmic a través dels projectes CORBI (SAF2009-14724-C02-02) i CORBI II (SAF2012-40227- C02-02) que han permès finançar els treballs realitzats en aquesta tesis.

En el transcurs d'aquesta tesis, hi han hagut diferents grups de persones que han sigut claus per la seva evolució. El primero de ellos es el Dr. Miguel Maldonado, a quien quiero agradecer que invirtiera un día, sin saber a qué conduciría todo ello, en "presentarme" a un fantástico órgano, "la córnea". De alguna forma, Miguel y todos los miembros de su equipo en IOBA son muy culpables de todo esto, ya que desde los primeros pasos han creído ciegamente en esta aventura. Per altra banda, a meitat del projecte vaig tenir la sort de poder treballar amb l'Estefania Traver i a "les Carmenes", la Carmen Lagunas i la Carmen Herrero. A totes elles els haig d'agrair la relació gens comercial de la que he pogut gaudir, les discussions des de punts de vista aparentment molt allunyats i sobretot la feina ben feta. També vull agrair a Montserrat Rigol i Nuria Solanes del Institut Clínic del Tòrax del Hospital Clínic de Barcelona per haver-nos deixat fer proves dins el seu experimental de forma altruista i amb un somriure a la boca. I per finalitzar, agrair a Salvador Borrós i Laura Montero del IQS les deposicions de HEMA a última hora.

Vull agrair a la petita família que formem el Grup d'Aplicacions Biomèdiques lo fàcil que és treballar així. A la Gemma Gabriel perquè juntament amb la Rosa Villa són directament culpables de que jo estigui aquí. Al Xavi Illa per les converses al despatx i per les correccions d'anglès. A l'Eli Prats perquè amb el seu humor semàntic sempre t'arranca un somriure. Al Jose Yeste per les discussions electròniques i a l'Anna Moya per l'ànima juvenil que encomana. Per altra banda, també vull fer extensiu aquest agraïment a tothom del CNM que amb el seu treball han posat un petit gra de sorra en aquesta tesis.

Vull fer un agraïment amb un cert to de lamentació als companys de fatigues ciclistes. Porto un parell d'anys sense donar el callo, però adverteixo que tornaré.

També vull agrair a tota "la penya" el suport i caliu que generen espontàniament. Tot i que quan els parlo de "impedàncies" no em fan gaire cas, són els millors aliats per celebrar les victòries i ofegar les penes. Podria acabar aquest paràgraf de moltes formes, però crec que la

més idònia és amb la següent frase. Per tots ells i gràcies a un d'ells "Keep Calm & Impedància".

Tampoc em puc oblidar dels més pròxims. Així, només puc tenir paraules d'agraïment pels meus pares, que sempre m'han recolzat i animat a seguir endavant i pel Pere, la Janet i la Tània. Per acabar, a l'Anna i a la Foix pel suport incondicional en tots el reptes, siguin compartits o no.

Sant Marti Sarroca, Setembre 2013

Contents

Motivation & objectives

One of the current challenges in biomedical research is the development of non-invasive diagnostic tools. Generally, the conditions of the *in vitro* experiments are far from the real conditions, and the obtained results must be validated in *in vivo* conditions. Thus, the enhancement of obtained results depends on the quality of the diagnostic tools. In addition, this knowledge can also be applied in clinical practice to improve the quality of medical assistance.

The cornea is a very special tissue because of its transparency, which is maintained by the barrier function of main corneal layers. Methods based on the study of their passive electrical properties have consistently been used in *in vitro* studies of such layers. Thus, the aim of this dissertation is to develop a non-invasive *in vivo* method to assess the functional state of the main corneal layers. This development will take advantage of the progress made in microsystems to develop a diagnosis method based on the impact of ion fluxes on the passive electrical properties of the tissues.

This new development will satisfy the need for non-invasive diagnostic technology to determine the factors that alter the corneal barrier function, and thus, the corneal homeostasis. This is of special interest in the optimization of ophthalmologic drugs by improving the knowledge of their behavior. In clinical practice, it could be used to improve the current diagnostic methods to determine, for example, the suitability of a given patient for a corneal surgical procedure that may weaken the cornea, or the suitability of a given cornea for transplantation.

The main objectives of this PhD dissertation can be summarized as follows:

- To design and develop a sensing device able to perform non-invasive measurements of the corneal impedance in *in vivo* conditions.
- To obtain experimental results that shows the relationship between the impedance measurements and the functional state of the main corneal layers.
- To provide indicators related with the functional state of main corneal layers.

Thesis framework

The work presented in this PhD dissertation has been developed in the framework of project funded by Spanish Ministry of Science and Innovation and the European Regional Development Fund. The project SAF2009-14724-C02-02 entitled “Development of a new noninvasive diagnostic method of the cornea based on bioimpedace measurement using micro-nano-technologies” (CORBI) has two partners.

- Barcelona Microelectronics Institute (IMB-CNM CSIC), Bellaterra, Spain.
- Institute for Applied Ophthalmobiology (IOBA), University of Valladolid. Valladolid, Spain.

One of the first outcomes of the CORBI project resulted in a patent of the proposed method to non-invasive assessment of the permeability of the main corneal layers (Guimerà Brunet et al., 2011). This patent is held by Laboratorios SALVAT S.A. and its development is in the context of I+D contract with the IMB-CNM.

In order to continue with the research line started with this dissertation and in the framework of the CORBI project, two projects funded by Spanish Ministry of Economy and Competitiveness and the European Regional Development Fund have recently been started. One of them is a continuation of the CORBI project called CORBI-II (SAF2012-40227- C02-02). The other one is XXX IPT-2012-0438-010000 with the objective of study the dry-eye disease and study how the developed method can be used to assess it.

Dissertation outline

This dissertation is organized in six different chapters which are summarized below.

In the first chapter, *Chapter 1*, the main concepts needed to understand the results presented in this dissertation are introduced. Firstly, the basic concepts related with the bioimpedance monitoring are presented. In addition, a review of previously reported works related with the measurement of the corneal passive electrical properties is also given. Moreover, bearing in mind that the potential readers are not skilled in biology or medicine, a brief description of the corneal structure and physiology is given. Special attention is paid to the corneal barrier function, which is the phenomenon assessed by the method developed in this dissertation.

The feasibility of the proposed method for assessing the electrical properties of the corneal epithelial and endothelial layers is studied in *Chapter 2*. A bidimensional model consisting of the main corneal layers and a tetrapolar impedance measurement setup placed on the corneal surface is implemented and analyzed by means of the finite elements method (FEM). Simulation results show that the impedance measurements performed by means of external electrodes are indeed sufficiently sensitive to the changes in the electrical properties of the epithelial and endothelial layers, which can be related with their permeability.

To experimentally validate the numerical findings, an impedance sensor based on a Pyrex® substrate is presented in *Chapter 3* and its capability to assess the corneal barrier function is evaluated by increasing the epithelial permeability of rabbits. To overcome the limitations of the rigid substrate, a flexible impedance sensor is presented in *Chapter 4*. The usability and performance of the proposed method is increased since no pressure is needed to place the sensor on the corneal surface. Its feasibility is evaluated *in vivo*, and the experimental results are compared with measurements of the permeability to sodium fluorescein.

The possibility to apply the proposed method to assess the endothelium barrier function of excised corneas is studied in *Chapter 5*. It can be accomplished by placing the cornea directly over the rigid impedance sensor, with the endothelium side in contact with the electrodes. This procedure allows the assessment of the endothelium barrier function without

removing the corneal epithelium, simplifying the experimental procedures. The obtained results show that the impairment of tight junction integrity is detected by changes in impedance values that correlate with alteration observed after ZO-1 immunostaining.

Finally, the principal conclusions of this dissertation and the ongoing tasks intended for applying the developed method to endothelial permeability assessment are described in *Chapter 6*. In addition, the improvements that should be implemented in order to enable the use of the developed method in the clinical practice are also described.

Chapter 1

Introduction

The aim of this chapter is to introduce the main concepts needed to understand the results presented in this dissertation. Firstly, the basic concepts related with the bioimpedance monitoring are presented, showing what kind of physiological phenomena can be assessed using this technique. In addition, a review of previously reported works related with the measurement of the corneal passive electrical properties is also given. It is interesting to note the importance of the Translayer Electrical Resistance (TER) measurements in the *in vitro* studies of the corneal barrier function.

Moreover, bearing in mind that the potential readers are not skilled in biology or medicine, a brief description of the corneal structure and physiology is given. Special attention is paid to the corneal barrier function, which is the phenomenon assessed by the method developed in this dissertation. In addition, a review of the current methods used to assess the corneal barrier function is also included.

1.1 Bioimpedance basis

Electrical Bioimpedance Monitoring is one of the diagnostic methods based on the study of the passive electrical properties of the tissues. The study of such properties started at the end of the 19th century thanks to the development of new instrumentation and the setup of the electromagnetic field theory by James Clerk Maxwell (1831-1879) (McAdams and Jossinet, 1995). However, practical use of diagnostic methods based on these properties did not started until the middle of the 20th century. Currently, electrical bioimpedance monitoring is a consolidated tool for biomedical research and for clinical practice. The main advantages of these methods can be summarized as follows:

- It requires low-cost instrumentation.
- Its application is easy and quick.
- It allows on-line monitoring.

The potential applications of electrical bioimpedance monitoring (BI) in biomedical research are very wide. They can be found in the excellent published reviews (Grimnes and Martinsen, 2008a; Rigaud et al., 1996; Riu et al., 1999; Valentinuzzi et al., 1996) and can be summarized as follows:

- **Cellular measurements:** BI can be used to assess the cellular growth of cell cultures and its response to external agents such as drugs or toxins (Giaever and Keese, 1993). BI can also be used in cell suspensions, where the main application is as a coulter counter. For this, the cells are forced to pass through a capillary which changes its impedance as each cell passes.
- **Volume changes:** Since bioimpedance measurements depend on the electrical properties of the tissue and geometrical dimensions of the evaluated sample, it is possible to measure sizes or volumes when the electrical properties remain constant. This principle is applied to estimate blood volume changes in the extremities or to monitor respiratory air volumes.
- **Body composition:** Applying the above mentioned principle, BI is consistently used to estimate relative volumes of different tissues or fluids in the body by determining the total body water (Cornish et al., 1993).
- **Tissue classification:** Since different tissue types exhibit different electrical properties BI can be applied to characterize tissues (Parramon et al., 2007). The most interesting field in which these methods are applied is early cancer detection in an easy way (Laufer et al., 2010; Malich et al., 2007).
- **Tissue monitoring:** Since the electrical properties of the tissue are related to the metabolism of cells, BI can be used to perform a real time monitoring of ischemia processes (Casas et al., 1999; Ivorra Cano, Antoni, 2005). This can be used to assess the state of a given organ in a transplant procedure, especially in the clinical practice to determine its suitability for transplant (Genescà et al., 2005; Ivorra et al., 2005).

- **Electrical Impedance Tomography (EIT):** Using multiple electrodes to inject and record the voltages and currents it is possible to generate an image by applying a reconstruction algorithm. Although the resolution achieved is lower than other imaging methods (echography, X-ray tomography or Magnetic Nuclear Resonance), its use is justified in terms of cost and acquisition speed.
- **Skin impedance:** The analysis of the skin's electrical properties has two objectives. Firstly, in methods which use electrodes directly attached to the skin, the knowledge of skin properties will lead to a reduction of the undesired influence of the skin impedance (Martinsen et al., 1997). In addition, the skin's physio-pathological state can be studied in order to assess skin hydration, irritation or dermatitis (Martinsen et al., 2008).

1.1.1 Electrical characterization of materials

The electrical behavior of any material can be defined by its electrical properties, the conductivity and permittivity. However, the impedance measurement performed on a given material not only depends on its electrical properties, it also depends on the geometrical constraints. Ideally, the values of interest will be the electrical properties of the materials since they will be not dependent on the geometry used in each study. The cell constant is the scaling factor used to relate the measured impedance with the electrical properties of the material under study. Thus, the measured impedance can be described with the following expression.

$$1/Z = Y = G + jB = G + j\omega C = K(\sigma + j\omega\varepsilon)$$

Where:

- Z is the impedance expressed in Ω.
- Y is the admittance expressed in S.
- G is the real part of Y and it is called conductance, it is expressed in S.
- B is the imaginary part of Y and it is called susceptance, it is expressed in S.
- C is the capacitance expressed in F.
- K is the scaling factor of the measurement cell, in the case of a cube it can be calculated by dividing the area of its section by its length. It is expressed in m.
- σ is the conductivity of the material expressed in S/m.
- ε is the permittivity of the material expressed in F/m.

In some cases, like in the case of biological samples, the conductivity and permittivity are frequency dependent. In those cases, it must be noticed that the proper characterization of a dielectric material requires two parameters for each frequency.

1.1.2 Electrical bioimpedance

Electrical bioimpedance is defined as the measurement of the electrical impedance of a biological sample. This parameter is interesting for biomedical research since it can reflect some physiological conditions and events of the tissue under study. Schwan defined three frequency regions for the dielectric properties of biological materials, these regions are related with the observed dispersions of their electrical properties (Schwan, 1957). These frequency regions are shown in Figure 1-1 (Grimnes and Martinsen, 2008a; Schwan, 1988). Each of these regions is associated with different physical and physiological phenomena that can be summarized as follows:

- α **dispersion** (from 1 mHz to 1 kHz): Associated with diffusion processes of ionic species in the extracellular medium.
- β **dispersion** (from 1 kHz to 10 MHz): Associated with the dielectric properties of the cell membranes and their interactions with the extra and intra-cellular electrolytes.
- γ **dispersion** (from 10 MHz to 100 GHz): Associated with dipolar mechanisms of salts and proteins in polar media such as water.

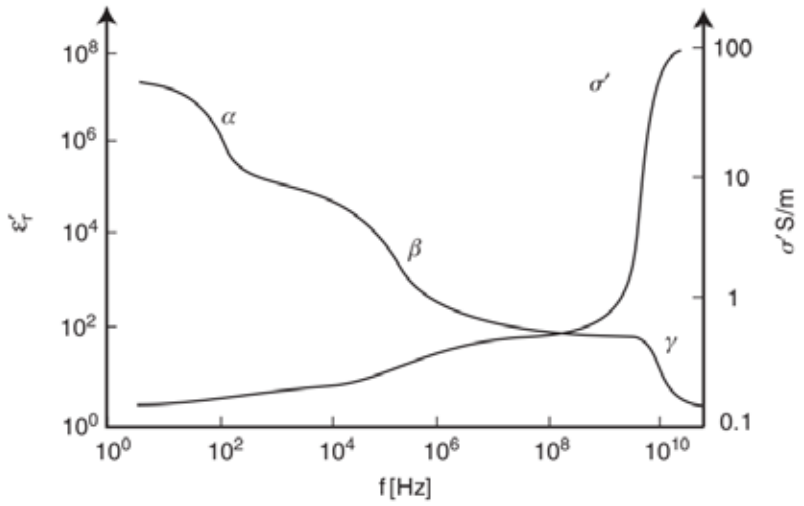

Figure 1-1 Idealized frequency dispersion regions (Source (Grimnes and Martinsen, 2008a, p. 90)).

1.1.2.1 Basis of the β dispersion

In order to assess the corneal barrier function, the studies presented in this dissertation are performed within the β dispersion frequency range. In this range, the passive electrical properties of the tissue basically depend on the cell membrane relaxation. From the electrical point of view, the tissue structure can be interpreted as two ionic solutions, the intra and extra-cellular medium, separated by a cell membrane.

The conductivity of the intra and extra-cellular medium depends on their ionic concentration and temperature. Although it is possible to find numerous membrane structures with completely different electrical responses inside the cell, for the sake of simplification, it is generally accepted that the intracellular medium behaves as a pure ionic conductor.

The cell membrane consists of the lipid bilayer with embedded proteins (≈ 7 nm thick). It has a passive role separating the extra and the intracellular medium, and an active role controlling the exchange of different chemical species. Its intrinsic electrical conductance is very low and it can be considered dielectric. Therefore, the structure formed by the extracellular medium, the cell membrane and the intracellular medium behaves as a capacitance (≈ 1 µF/cm2).

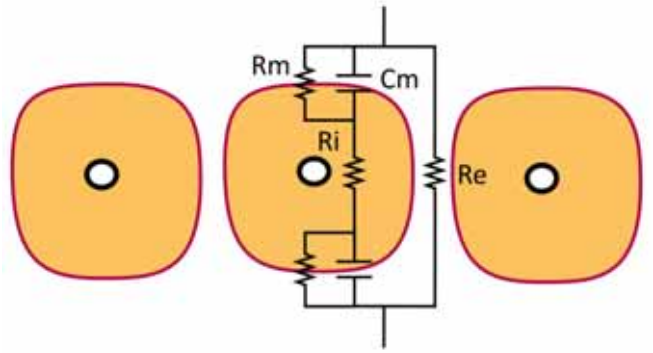

Figure 1-2 Schematic representation of a cell together with the equivalent circuit, where Cm is the membrane capacitance, Rm is the membrane resistance, Ri is the intracellular resistance and Re is the extracellular resistance.

For a better interpretation of the bioimpedance measurements, it is helpful to describe an equivalent circuit in which a physical meaning can be attributed to each component. Thus, in Figure 1-2 a basic circuit is depicted to explain the basic behavior of the bioimpedance measurements. As can be observed, taking into account that the resistivity of the membrane is very high, at low frequencies (<1 kHz) the current cannot penetrate into the intra-cellular medium. Thus, the impedance measured depends on the extra-cellular medium resistivity and more precisely on the spaces between cells. In the case of tissue measurement, these spaces are closely related with the tight and gap junctions between cells. Nevertheless, at high frequencies (>1 MHz), the current flows indiscriminately through both the extra and intracellular media.

The previous model works reasonably well for dilute cell suspensions, where the transition between low and high frequencies can be easily modeled by a capacitor. However, the tissue bioimpedance tends to be more complex and several dispersions can be observed. In such cases, another resistance-capacitance couple should be added to model the bioimpedance measurements. Moreover, to improve the agreement between the model and the bioimpedance results it is necessary to substitute the capacitance for a mathematical component called Constant Phase Element (CPE). Its impedance is described by the following expression:

$$Z_{CPE} = \frac{1}{(j \cdot 2\pi \cdot f \cdot C)^{\alpha}}$$

The α parameter is usually ranged from 0.5 to 1. Note that if its value is 1 the behavior of the CPE is exactly the same as a capacitance. When the CPE is included in the circuit described in Figure 1-2, the expression of the impedance measured is:

$$Z = R_{\infty} \frac{R_o - R_{\infty}}{1 + (j \cdot 2\pi \cdot f \cdot \tau)^{\alpha}}$$

This expression, called the Cole-Cole equation, was found by the Cole brothers in 1941 and is consistently used to describe the experimental results. It allows us to express the results using four parameters: R_∞, R_o, α and τ. As shown in Figure 1-3, R_∞ represents the impedance at infinite frequency, R_o the impedance at frequency 0 Hz, τ is the time constant (ΔR·C) and α is the α parameter of the CPE. The representation of the Cole-Cole equation on a Nyquist diagram results in a semicircle centered below the real axis. This displacement depends on the value of α the parameter.

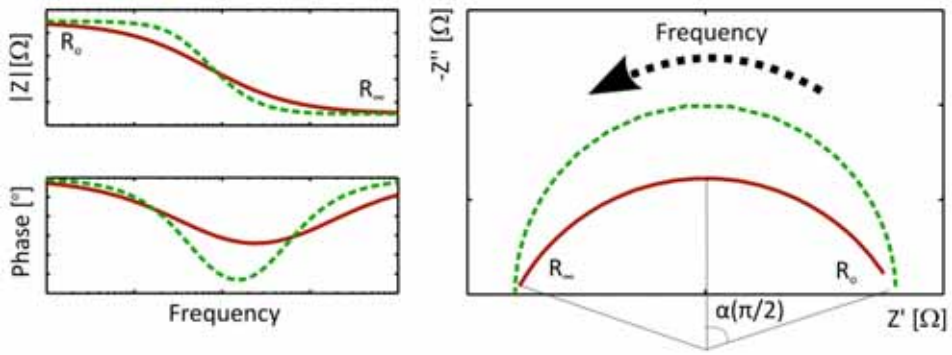

Figure 1-3 Comparison between the impedance of the equivalent circuit (Figure 1-2) with CPE component (red solid line) and with a pure capacitor (Green dash line).

Since the physical meaning of some parameters of the Cole-Cole equation such as the α parameter, has not yet been solved or explained, the use of equivalent circuits to analyze the experimental results have some drawbacks (McAdams and Jossinet, 1996). Moreover, the same impedance measurements can be interpreted as completely different circuits with different topologies and values. Thus, some authors choose a mathematical model (Cole-Cole equation) to describe their results without trying to interpret them.

1.1.3 Measurement methods and practical constraints

From a practical point of view, the sample under study must be connected to the proper instrumentation through electrodes to perform the bioimpedance measurement. Thus, the characteristics of both parts can alter the measurement and consequently produce errors in the proper interpretation of such measurement.

1.1.3.1 Electrode considerations

In order to avoid tissue damage or electrode degradation, most electrodes used for bioimpedance measurements are made of noble metals such us platinum or gold. To perform the measurement without altering the biological sample a small AC signal (less than 100 mV) is applied in order to avoid any electronic exchange reaction. In that case, the electrode-electrolyte impedance, also called interface impedance or electrode impedance, is quite similar to a capacitance (Fisher, 1996). This electrode impedance may disturb the bioimpedance measured, especially at low frequencies. Taking into account that the value of this capacitance is directly proportional to the electrode area, it can be understood that this constitutes the main limitation for the use of microelectrodes. This limitation can be overcome

by increasing the surface roughness in order to increase the surface area. This can be achieved by several methods such as the electrochemical depositions of metals (Gabriel et al., 2008, 2007).

1.1.3.2 Instrumentation considerations

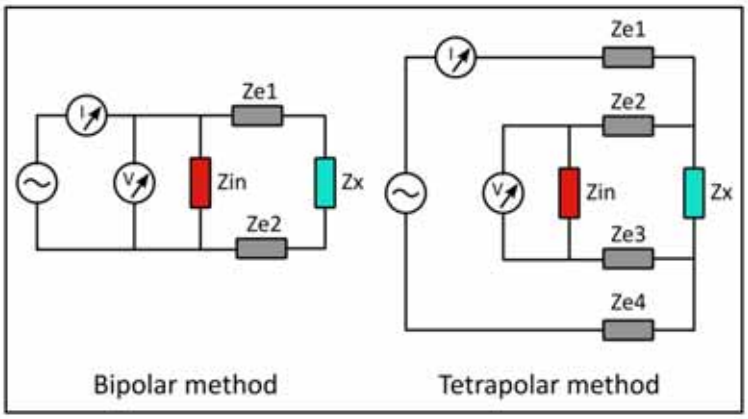

Figure 1-4 Schematic representation of the bipolar and tetrapolar measurement method, which shows the position of the main parasitic impedances.

The easiest way to measure the impedance of a given tissue is the bipolar method, which consists of attaching a pair of electrodes to the surface of the sample under study. In that case, both electrodes are used to inject the current and to measure the voltage drop. When this method is used the electrode-electrolyte interface impedances are in series with the sample impedance and, therefore, the measured impedance is the sum of the three impedances (Zx + Ze1 + Ze2). Thus, to obtain a measurement proportional only to the electrical properties of the sample, the electrode impedance must be much lower than the tissue impedance Zx. Unfortunately, this condition is not easy to accomplish when microelectrodes are used, especially at low frequencies. To overcome this limitations an alternative tetrapolar method can be used (Geddes, 1972; Schwan and Ferris, 1968). When this method is used, the current is injected by a pair of electrodes and the resulting voltage drop is measured using another pair of electrodes. However, the tetrapolar method is not free from errors. Other parasitic impedances such as capacitances between wires or instrumentation input impedances, combined with the electrode impedances can cause errors (Grimnes and Martinsen, 2007; Pallas-Areny and Webster, 1993). The main considerations that must be taken into account to avoid errors when the tetrapolar method is used can be summarized as follows:

- **Common mode voltage:** The electrode impedance of current-injecting electrodes produces a common mode voltage which must be rejected by the amplifier used to measure the voltage drop. The common mode rejection ratio (CMRR) of the commercially available instrumentation amplifiers is reduced by the capacitive behavior of the electrode impedance (Pallas-Areny and Webster, 1993). To overcome this, several improved instrumentation approaches have been developed, such as the balanced generation (Hinton et al., 1998) or the use of common-mode negative feedback (Yélamos et al., 1999).
- **Instrumentation input impedance:** The current leakages due to the input impedance of the instrumentation amplifiers and connection wires, together with the mismatch between the electrode impedance of the voltage-sensing

electrodes may also produce errors in the measurement. Performing a calibration process and subsequent correction of the measurement is a helpful alternative to reduce the error in the measurement. For greater accuracy, this process should include the connection wires (Guimerà et al., 2009). Furthermore, the use of active shielding techniques for the connection wires reduces the current leakage of the wires (Hinton et al., 1998).

1.2 Cornea

The cornea is a hemispherical structure located in the front of the eye which allows the transmission of light and protects the iris and lens against external aggressions (Figure 1-5). Together with the anterior chamber and the lens, the cornea constitutes the optical system of the eye which focuses the light on the retina. Its curvature refracts the light and provides most of the eye's focusing power. The human cornea has a diameter of about 11.5 mm and a thickness of 0.5–0.6 mm in the center and 0.6–0.8 mm at the periphery. It is mainly composed of three layers, the epithelium, the stroma and the endothelium, which are detailed in the following sections. These main layers are separated by two membranes, the Bowman's membrane located between the corneal epithelium and stroma and the Descemet's membrane located between the stroma and endothelium. Since these acellular membranes are mainly composed of collagen fibers, their impact in the corneal electrical properties can be considered negligible.

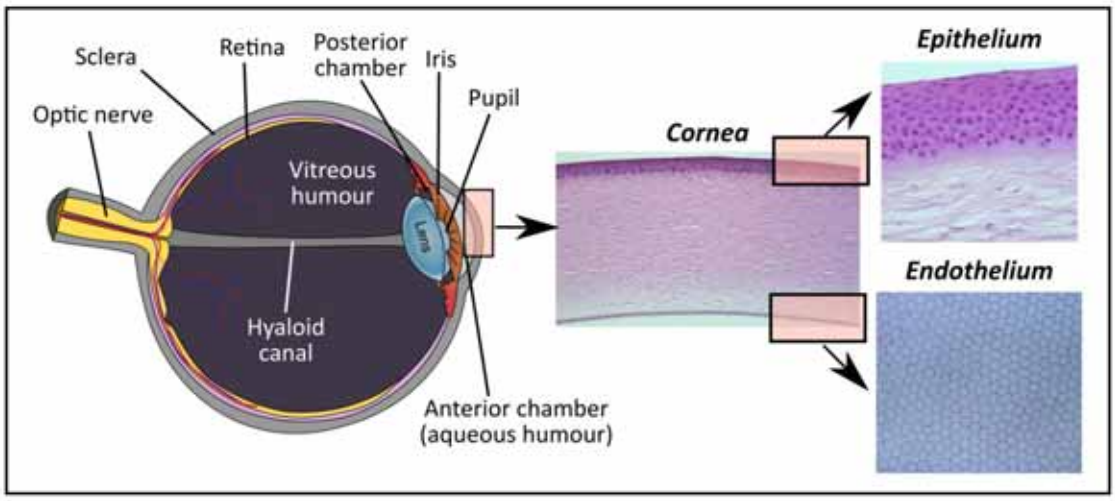

Figure 1-5 Schematic representation of the main parts of the ocular globe. Microscopic images of the cornea, epithelium and endothelium.

1.2.1 Corneal structure

The corneal epithelium covers the front of the cornea and plays an important role in determining the optical properties of the cornea. Along with the tear film components, it forms an excellent optical surface equivalent to any manmade lens. Like the skin epithelia, it presents a strong barrier for resisting the daily insults of the external environment. The central epithelium is five to six cells thick, and presents the most regular arrangement of stratified

epithelium in the human body. The most superficial layer consists of one to two layers of flattened, polygonal-shaped cells, which can vary in shape and size. These cells are joined by tight junctions (zonula ocludens), creating a barrier which is relatively impermeable. Below the superficial layer there is a layer of polyhedral cells, two to three cells thick. These cells, called wing cells, are transitional cells between the basal cylindrical cells and the flattened superficial cells. The deepest layer is the basal layer and consists of a single layer of cylindrical cells. Below this layer there is an acellular membrane, called basement membrane, which together with the Bowman's membrane help the cornea to maintain its shape and promote the adhesion of the epithelium basal cells. The corneal epithelium is a fast growing tissue, which undergoes a continuous renewal process. For this, basal and wing cells migrate from the basal layer to the surface layer, while squamous older cells are diluted into the tear film.

The corneal stroma is the central and thickest layer of the cornea, consisting of regular arranged collagen fibrils. To achieve the corneal transparency it remains in state of relative dehydration. It can be morphologically divided into an anterior and posterior lamellar stroma. The collagen fibrils in the anterior lamellar stroma appear as short narrow sheets with extensive interweaving, whereas in the posterior stroma they are long, wide and thick structures with minimal interweaving among layers. The stromal cells, called keratocytes, are dispersed between these structures and occupy only 3%-5% of the stromal volume. The keratocytes are a specialized fibroblast, which play the main role in synthesizing stromal components and healing wounds. The deeper stroma collagen fibers appear merged with the Descemet's membrane, a specialized basement membrane placed between the posterior stroma and the endothelium from which it is derived. It is composed of very regularly arranged stratified layers of filamentous material. Moreover, the stroma presents extensive innervation that works together with tear generation and the eyelid to protect the cornea against infections and aggressions.

The corneal endothelium is a monolayer of cells with poor regenerative capacity, which is attached to the Descemet's membrane and covers the entire back surface of the cornea. Its cells have a flat hexagonal shape, which yields the greatest efficiency for covering a given area. Due to their poor regenerative capacity, the number of cells decreases with age. When an endothelial cell disappears, the neighboring cells must expand to fill the gap. Consequently, the cell size, shape, and number are indicators of age and degree of stress.

Although it cannot be considered a part of the cornea, it is important give some details of the tear film since it plays an important role in the results obtained in this dissertation. The tear film is essential for maintaining the health of the cornea, offering protection and providing a smooth optical surface. It consists of three layers: a lipid outer layer, an aqueous middle layer and a mucous inner layer. The lipid layer is composed of low-polarity lipids with an average thickness of 0.1 µm. It helps to maintain the integrity of the tear film by providing a limiting hydrophobic barrier. Furthermore, it delays evaporation and prevents tears from running over the edge of the eyelid. The aqueous layer is composed of approximately 98% water and about 1.8% solid. It represents the bulk of the tear film with an average thickness of 10-20 µm (King-Smith et al., 2000; Prydal et al., 1992). The mucous layer is only 0.02-0.05 µm thick and converts the hydrophobic corneal epithelium into a wettable surface.

1.2.2 Corneal barrier function and transparency

Due to its transparency, the cornea is a very special tissue and this fact makes it different from the other body tissues. For this, it does not have blood vessels for its nourishment. The nutrients are supplied by diffusion through the epithelium and endothelium. As it has been commented, the transparency of the cornea depends on the level of hydration of the stroma, remaining in a constant state of dehydration. As shown in Figure 1-6, the hydration level of the stroma depends mainly of three different ion fluxes. Two of those fluxes are due to diffusion: one between tear film and stroma through the epithelium and another one between stroma and aqueous humour through the endothelium. Finally, an active flux is due to the metabolic pump function of the endothelium layer.

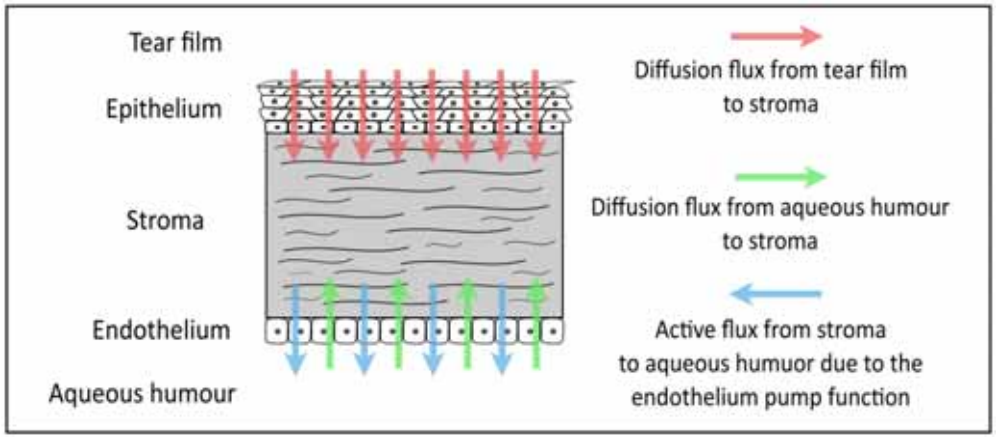

Figure 1-6. Schematic representation of the main corneal ion fluxes. The corneal homeostasis depends on the dynamic equilibrium between those ion fluxes.

These diffusion fluxes are regulated by the barrier function of the endothelium and epithelium layer. The basis of this barrier function is the existence of strong thigh junctions and gap junctions between cells (Ma et al., 2007). However, the endothelium metabolic pump function plays the most important role to extracting the waste products from the corneal stroma, balancing the leak rate of the barrier function, and finally, maintaining the corneal homeostasis[1].

The metabolic pump of the corneal endothelium is controlled by Na,K-ATPase located in the lateral membranes, there are about of three million of pump sites per endothelial cell. The pumping action is achieved by increasing the concentration of Na^+ ion in the extracellular spaces (Bonanno, 2003). Consequently, the concentration gradient between the extracellular

[1] *Homeostasis* is the property of a biological system that regulates its internal environment and tends to maintain a relatively constant condition of certain parameters such as temperature, pressure or hydration. Usually, it is the consequence of multiple adjustment and regulation mechanisms. In relation with the cornea it can also be stated as *deturgescence* and can be defined as the state of relative dehydration maintained by the normal cornea which is necessary for ensuring its transparency.

space and the humor aqueous produces an osmotic flux of water across the endothelium. To control this fluid flow the tight junctions maintains the space between endothelial cells.

1.2.3 Corneal pathologies

The corneal barrier function and thus the corneal homeostasis may be affected by several factors, most of which produce a decrease in the cell number or in the thigh junctions between cells. Table 1-1 summarizes the main diseases that may weaken the corneal barrier function according to the layer affected and their origin. Among the extrinsic factors it is interesting to note the impact of surgery procedures and the use of ophthalmologic drugs on the barrier function of epithelium and endothelium. Since it is an undesired effect resulting from the treatment of other diseases, a better characterization of such effects will be helpful to improve treatments and reduce these undesired effects.

Table 1-1 Relation of main corneal pathologies that can affect the corneal barrier function according to the layer affected and their origin. This table has been provided by Dr M.J. Maldonado based on his knowledge.

Cause	*Epithelium*	*Endothelium*
Extrinsic	**Chemical and physical insults** (i.e. abrasion, caustication, thermal burn, ultraviolet light or Swimming pool chlorine) **Ophthalmologic drugs** (i.e. contact lens solutions, topical anesthetics or generic topical medications) **Surgery procedures** (i.e. cataract, refractive surgery, trabeculectomy, keratoplasty or collagen cross linking) **Contact lenses wearing** **Ocular iontophoresis** **Infections**	***Surgery procedures*** (i.e. cataract, keratoplasty, radial keratotomy, hyphema or laser procedures to the anterior segment of the eyes) ***Intraocular ophthalmologic drugs*** (i.e. intracameral anesthetics, intracameral rtPA, irrigating solutions, Mitomycin-C or Silicone oil) ***Topical ophthalmologic drugs*** (i.e. antimicrobial voriconazol or antiglaucoma dorzolamide) **Detergent residue originating from irrigating cannulas** **Contact lenses wearing**
Intrinsic	***Dry eye*** (includes the Sjögren's and Stevens-Johnson syndrome) ***Allergic reactions*** (i.e. keratoconjuntivitis or atopic dermatitis) ***Dystrophies*** (i.e. Map-dot, Lattice or Meesmann´s) **Keratoconus** **Ocular cicatricial pemphigoid** **Limbal stem cell deficiency** **Neurotrophic keratopathy** **Diabetes mellitus** **Galactosemia**	Aging ***Dystrophies*** (i.e. Fuchs' or congenital hereditary) **Diabetes Type I** **Inmunulogic Rejection** **Corneal Endothelial Guttae** **Chronic anterior uveitis** **Pseudoexfoliation Syndrome**

In the case of topical ophthalmic drugs, the insult is produced by the preservative and surfactant components needed to enhance the effect and comfort of the topically instilled medication (Ayaki and Iwasawa, 2011). These undesired effects of the ophthalmologic

medicines become more serious in medicines and solutions that require long-term use, such as anti-glaucoma drugs, disinfecting and storage solutions for soft contact lenses or artificial tears. Several studies have been performed to evaluate their impact on the corneal barrier function (Cavet et al., 2010; Furrer et al., 2002; Lehmann et al., 2010).

Since Benzalkonium chloride (BAC) is one of the more common preservatives used in the formulation of ophthalmic medications in the present days, it has been chosen to increase the permeability of the corneal epithelium in the experimental sections of this dissertation. It is a quaternary ammonium compound whose antimicrobial activity arises from its ability to disrupt cell membranes and potentiate cell death. Besides its antimicrobial activity, BAC is cytotoxic to the corneal tissues as it induces the loss of tight junctions between cells, which is directly related to the increase of the epithelium permeability (Baudouin et al., 2010; Swan, 1944). Moreover, these changes appear to be both dose- and time-dependent (Chen et al., 2011).

1.2.4 Clinical corneal evaluation methods

As has been commented before, the permeability of the endothelium and epithelium layers plays the most important role in maintaining the corneal homeostasis. There are several methods to perform a direct evaluation of their permeability in *in vitro* conditions. However, the use of direct methods in *in vivo* conditions or in clinical practice is very limited. Consequently, the methods used to assess the permeability in daily clinical practice are based on indirect measurement methods. In the following lines is given a brief description of the available methods to assess the corneal physio-pathological state (Bourne and McLaren, 2004).

1.2.4.1 Permeability to fluorescein

The barrier function of the corneal epithelium and endothelium can be directly evaluated by measuring its permeability to fluorescein (Bourne and McLaren, 2004). This technique can be used *in vivo* and in clinical practice since it is non-invasive if the fluorescein is instilled topically. The fluorescein enters the corneal stroma through the epithelium, and after several hours when the dye becomes uniformly distributed through the cornea, it is measured in the cornea and anterior chamber by using a suitable fluorophotometer. This analysis requires accurate measurement of fluorescein concentration in the cornea and anterior chamber. The Ocular fluorophotometers have evolved over the years, and an instrument is available commercially (Fluorotron Master, Ocumetrics, Inc., Mountain View, CA, USA) that provides a profile of fluorescence in the cornea, anterior chamber and lens.

The main drawback of this technique is the substantial variability between repeated measurements which indicates that the single-drop procedure is unreliable for monitoring individual patient changes (McNamara et al., 1997). This fact, together with the time required to perform the measurement, reduces its application to experimental purposes only.

1.2.4.2 Corneal epithelial fluorescein staining

The macroscopic morphological state of the corneal epithelium can be easily assessed by performing a fluorescein test. It consists of a topical instillation of fluorescein, and after

blinking, the epithelial defects appear in bright green upon illumination by blue cobalt light (Figure 1-7). Due to its easy and quick application, this technique is commonly used in daily clinical practice. However, the information obtained cannot be directly related with the epithelium permeability since the staining does not fill the intercellular spaces, which are the structures responsible for maintaining the epithelium barrier function (Mokhtarzadeh et al., 2011; Wilson et al., 1995).

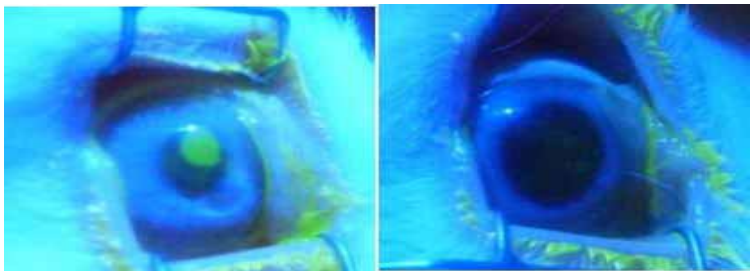

Figure 1-7 Example of how the corneal epithelial defects appear in bright green upon illumination by a blue cobalt light. Left image corresponds to a damged eye and right image to a normal eye.

1.2.4.3 In vivo microscopy analysis

The same principles that make the cornea transparent, and an ideal optical covering for the eye, render its structural components and cells nearly invisible. However, many of the cornea's cells can be made visible by specular reflection. This technique provides a powerful tool to obtain images of the main corneal layers (Figure 1-8). Taking into account that it is a non-invasive method, it can be used to examine the human cornea in the clinical practice. In order to standardize the provided images analysis, the recent trend is to develop of methods for quantifying image parameters such as the hexagonally, the cell density or the morphology of the corneal endothelium layer (V. Patel and N. McGhee, n.d.). Between these parameters, the endothelial cell density is the most widely used parameter for assessing the functional state of the corneal endothelium. However, in the case of cornea transplantation there are evidences that this parameter is unrelated to graft failure due to endothelial decomposition (Lass et al., 2010).

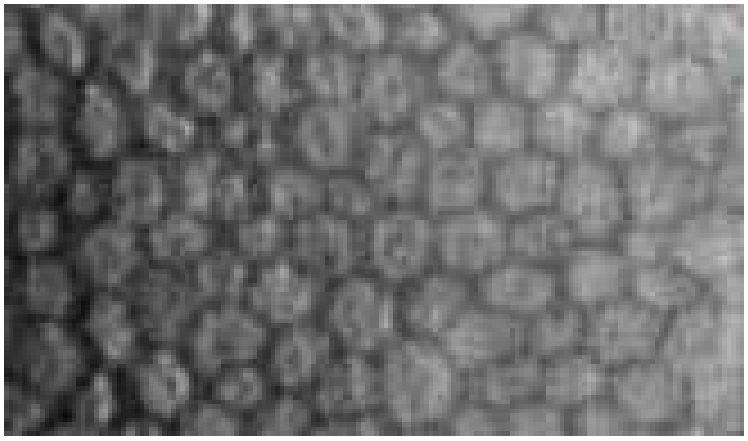

Figure 1-8 Image of the corneal endothelium obtained by specular microscopy, which shows its characteristic hexagonal cell shape.

1.2.4.4 Corneal thickness measurements

Any disorder in the barrier function of the epithelium or endothelium layer, which alters the corneal homeostasis, increases the hydration of the corneal stroma. Consequently, this hydration increase will lead in a corneal swelling. Thus, the measurement of the corneal thickness variation (corneal edema) is a powerful tool to indirectly assess the corneal barrier function. Ideally, corneal thickness should be measured to with an accuracy of 5 μm to assess the swelling and deswelling rate. Several methods have been developed to measure corneal thickness, and these can be divided in two categories, optical methods and ultrasonic methods (Doughty and Zaman, 2000).

The mechanism used by the optical systems to measure the corneal thickness is very wide, and there are a lot of instruments commercially available to perform this measurement. Specular and confocal microscopes have also been used to measure the corneal thickness (Bovelle et al., 1999). Images of the epithelial and endothelial surfaces can easily be identified by their bright reflex and characteristic appearance. This method is only accurate if the instrument accurately reports position of the focusing element, and the objective lens is stable with respect to the eye. Interferometry has also been used recently to measure corneal thickness. This method is based on a light source with a short coherence distance. Light reflected from surfaces of the cornea interferes with a beam from the reference arm of an interferometer. The length of the reference arm is scanned and only produces interference if the length of the arm corresponds to the path length of the light reflected from the surfaces of the eye. The accuracy of this method is around of a few microns. This principle has been used in ocular coherence tomography (OCT) to measure corneal thickness as well as other distances within the eye.

Ultrasonic pachometers are fast, simple to use, and provide repeatable measurements. The cornea must be contacted by a hand-held probe. Then, the corneal thickness is determined from the time required for a pulse of sound at 20 – 50 MHz to transit the cornea, reflect from the endothelium-aqueous humor interface, and return to be detected by the probe. Several commercial instruments are available and in use clinically

1.2.5 Experimental methods for corneal permeability evaluation

The most widely used setups for measuring the corneal permeability in *in vitro* conditions are based on the commercially available “cell culture inserts” such as Millipore® or Transwell®. As shown in Figure 1-9, these systems are based on a vertical side by side diffusion system across a semipermeable microporous membrane, allowing free passage of nutrients and diffusible factors between both compartments. In these setups, the permeability of the cultured layer can be evaluated using several techniques (Ma et al., 2007). They can be divided in two main groups, the chemical analysis of known molecules and the study of its passive electrical properties. The methods based on the passive electrical properties of living tissues such as Translayer Electrical Resistance (TER) measurement, taking advantage of the impact of the ion fluxes and tight junctions in such properties (Grimnes and Martinsen, 2008b). A detailed review of this kind of methods can be found in the following sections.

Related to the chemical analysis methods, the concentration of molecules in both compartments can be measured using the fluorescence properties of certain molecules such as fluorescein isothiocyanate–dextran (Kuang et al., 2004). Since the culture medium must be changed in order to introduce the fluorescein molecule, the main limitation of these techniques is the low throughput and the impossibility of perform a continuous monitoring along the time.

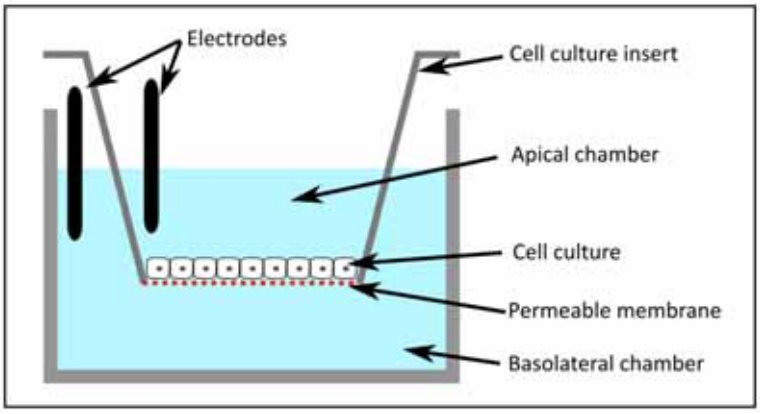

Figure 1-9 Schematic representation of a commonly used setup for a "cell culture insert".

The "cell culture inserts" can also be used to evaluate the permeability of excised corneas in *ex vivo* conditions. To perform the measurements the harvests corneas must be adapted to the cell insert. Moreover, to assess *ex vivo* the corneal endothelium permeability, the corneal epithelium must be removed in order to avoid its influence in the measurement, since it has a much lower permeability than the corneal endothelium (Kuang et al., 2001; Lim and Fischbarg, 1981).

1.3 Use of passive electrical properties for corneal valuation

The studies of the passive electrical properties of the different tissues that form the ocular globe are quite limited, and the application of such techniques within ophthalmology clinical practice is almost non-existent until the present. One of the first studies was performed by Pauly and Schwan, where the electrical properties of eye lens were studied. These measurements were made over excised lens from cow eyes (Pauly and Schwan, 1964). Later, Gabriel investigated the conductivity of the cornea, the retina, the choroids, the iris and the two parts of the lens (nucleus and cortex) (Gabriel et al., 1996, 1983).

In reference to the specific analysis of the cornea, Holt and Cogan evaluated for first time the permeability of excised cow corneas through impedance measurements performed at 1 kHz (Holt and Cogan, 1946). Later, Oksala and Lehtinen confirmed the findings of Holt and Cogan showing that the corneal epithelium presents most of the contribution to the corneal impedance (Oksala and Lehtinen, 1960). Following this research line, Lim and Fischbarg developed a method to remove the corneal epithelium of rabbit excised corneas and evaluate the endothelium impedance (Fischbarg, 1973; Lim and Fischbarg, 1981). Moreover, they proposed an equivalent circuit able to describe the impedance measurements. These achievements laid the basis of the Translayer Electrical Resistance (TER) measurements. As it

has been commented before, these measurements will be consistently used in subsequent *in vitro* studies of corneal permeability (Kuang et al., 2004; Ma et al., 2007). The most widely used systems for measuring TER are the commercially available "chopstick" electrodes or the more advanced cellZscope® system (nanoAnalytics, Germany). As it is shown in Figure 1-9, the measurements are performed by electrodes placed in each compartment. It allows a rapid and quantitative evaluation of the corneal permeability (Chen et al., 2011; Fischbarg, 1973). Alternatively, another approximation to evaluate TER in *in vitro* cell cultures is based on cell-substrate impedance sensing. With this method, better usability and higher throughput is provided (Srinivas, 2010; Tiruppathi et al., 1992).

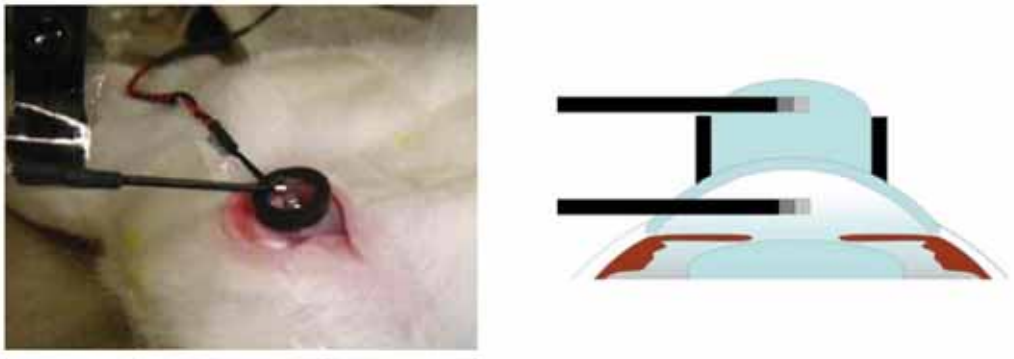

Figure 1-10 Image and schematic representation of how Uematsu performed TER measurements in in-vivo conditions (Uematsu et al., 2007).

The studies of the corneal electrical properties performed in *in vivo* conditions are quite limited. Biermann carried out *in vivo* measurements of normal and pathological corneas at 500 Hz (Biermann et al., 1991). The obtained results show an important decrease of the measured impedance in burned and pathological ones. However, although the obtained promising results, there are no further studies to determine the detection limit of this technique. Watanabe carried out impedance measurements of the cornea on a whole excised rabbit eye ball by placing electrodes on the corneal surface within the frequency range from 10 kHz to 100 MHz (Watanabe et al., 1993). The analysis of the obtained measurements were based on two-term Cole-Cole equation and suggested that one dispersion can be associated to the endothelial layer and the other one to the epithelium layer. More recently, Jürgens obtained EIT images of cornea and lens damaged chemically and thermally, and found a decrease in the measured impedance for the case of damaged corneas (Jurgens et al., 1996).

The last approach to perform *in vivo* measurements was carried out by Uematsu, who adapted the TER measurements in order to be implemented in living animals (Chen et al., 2012; Uematsu et al., 2007). As it is shown in Figure 1-10, the measurement is performed by two Ag/AgCl electrodes inserted into the anterior chamber of the eye through a small incision in the peripheral cornea. This technique allows the *in vivo* evaluation of the impact of ophthalmologic drugs in the corneal epithelium barrier function. However, the invasiveness of this procedure makes it impossible to be used in the clinical practice.

1.4 Conclusions

The major part of the studies of the corneal passive electrical properties presented up to the present are based on measurements made *in vitro*, where the methods based on the electrical properties are consistently used to assess the barrier function of cell cultures or excised corneas. As it has been commented, there are also some studies that performed *in vivo* measurements, but using very invasive methods, which generally translates into not being able to use the tissue for subsequent studies, nor they are applicable to human beings.

Since the evaluation of the corneal barrier function is important for assessing the behavior of ophthalmologic drugs in *in vivo* conditions and for the clinical practice, the aim of this dissertation is to develop a minimally invasive method to assess the corneal barrier function based on passive electrical properties. In this way, and taking advantage of the evolution in the microsystems field the developed sensor could be feasible for use in the ophthalmology clinical practice.

1.5 References

Ayaki, M., Iwasawa, A., 2011. Cell Viability of Four Corneoconjunctival Cell Lines Exposed to Five Preservatives and a Surfactant Used for Infection Control in Eyedrops. Biocontrol Sci. 16, 117–121.

Baudouin, C., Labbé, A., Liang, H., Pauly, A., Brignole-Baudouin, F., 2010. Preservatives in eyedrops: The good, the bad and the ugly. Prog. Retin. Eye Res. 29, 312–334.

Biermann, H., Boden, K., Reim, M., 1991. Measuring electrical impedance in normal and pathologic corneas. Fortschritte Ophthalmol. Z. Dtsch. Ophthalmol. Ges. 88, 17–20.

Bonanno, J.A., 2003. Identity and regulation of ion transport mechanisms in the corneal endothelium. Prog. Retin. Eye Res. 22, 69–94.

Bourne, W.M., McLaren, J.W., 2004. Clinical responses of the corneal endothelium. Exp. Eye Res. 78, 561–572.

Bovelle, R., Kaufman, S.C., Thompson, H.W., Hamano, H., 1999. Corneal thickness measurements with the Topcon SP-2000P specular microscope and an ultrasound pachymeter. Arch. Ophthalmol. 117, 868–870.

Casas, O., Bragós, R., Riu, P.J., Rosell, J., Tresànchez, M., Warren, M., Rodriguez-Sinovas, A., Carreño, A., Cinca, J., 1999. In vivo and in situ ischemic tissue characterization using electrical impedance spectroscopy. Ann. N. Y. Acad. Sci. 873, 51–58.

Cavet, M.E., VanDerMeid, K.R., Harrington, K.L., Tchao, R., Ward, K.W., Zhang, J.-Z., 2010. Effect of a novel multipurpose contact lens solution on human corneal epithelial barrier function. Contact Lens Anterior Eye 33, S18–S23.

Chen, W., Hu, J., Zhang, Z., Chen, L., Xie, H., Dong, N., Chen, Y., Liu, Z., 2012. Localization and Expression of Zonula Occludins-1 in the Rabbit Corneal Epithelium following Exposure to Benzalkonium Chloride. PLoS ONE 7, e40893.

Chen, W., Li, Z., Hu, J., Zhang, Z., Chen, L., Chen, Y., Liu, Z., 2011. Corneal Alternations Induced by Topical Application of Benzalkonium Chloride in Rabbit. PLoS One 6.

Cornish, B.H., Thomas, B.J., Ward, L.C., 1993. Improved prediction of extracellular and total body water using impedance loci generated by multiple frequency bioelectrical impedance analysis. Phys. Med. Biol. 38, 337–346.

Doughty, M.J., Zaman, M.L., 2000. Human corneal thickness and its impact on intraocular pressure measures: a review and meta-analysis approach. Surv. Ophthalmol. 44, 367–408.

Fischbarg, J., 1973. Active and passive properties of the rabbit corneal endothelium. Exp. Eye Res. 15, 615–638.

Fisher, A.C., 1996. Electrode Dinamics. Oxford University Press, Incorporated.

Furrer, P., Mayer, J.M., Gurny, R., 2002. Ocular tolerance of preservatives and alternatives. Eur. J. Pharm. Biopharm. 53, 263–280.

Gabriel, C., Gabriel, S., Corthout, E., 1996. The dielectric properties of biological tissues: I. Literature survey. Phys. Med. Biol. 41, 2231–2250.

Gabriel, C., Sheppard, R.J., Grant, E.H., 1983. Dielectric properties of ocular tissues at 37 degrees C. Phys. Med. Biol. 28, 43–49.

Gabriel, G., Erill, I., Caro, J., Gómez, R., Riera, D., Villa, R., Godignon, P., 2007. Manufacturing and full characterization of silicon carbide-based multi-sensor micro-probes for biomedical applications. Microelectron. J. 38, 406–415.

Gabriel, G., Gómez-Martínez, R., Villa, R., 2008. Single-walled carbon nanotubes deposited on surface electrodes to improve interface impedance. Physiol. Meas. 29, S203–S212.

Geddes, L.A., 1972. Electrodes and the measurement of bioelectric events. Wiley-Interscience.

Genescà, M., Ivorra, A., Sola, A., Palacios, L., Goujon, J.-M., Hauet, T., Villa, R., Aguiló, J., Hotter, G., 2005. Electrical bioimpedance measurement during hypothermic rat kidney preservation for assessing ischemic injury. Biosens. Bioelectron. 20, 1866–1871.

Giaever, I., Keese, C.R., 1993. A morphological biosensor for mammalian cells. Nature 366, 591–592.

Grimnes, S., Martinsen, Ø.G., 2007. Sources of error in tetrapolar impedance measurements on biomaterials and other ionic conductors. J. Phys. Appl. Phys. 40, 9–14.

Grimnes, S., Martinsen, Ø.G., 2008a. Bioimpedance and bioelectricity basics. Academic Press, New York.

Grimnes, S., Martinsen, Ø.G., 2008b. Chapter 4 - PASSIVE TISSUE ELECTRICAL PROPERTIES, in: Bioimpedance and Bioelectricity Basics (Second Edition). Academic Press, New York, pp. 93–137.

Guimerà, A., Gabriel, G., Parramon, D., Calderón, E., Villa, R., 2009. Portable 4 Wire Bioimpedance Meter with Bluetooth Link, in: Dössel, O., Schlegel, W.C. (Eds.), World Congress on Medical Physics and Biomedical Engineering, September 7 - 12, 2009, Munich, Germany, IFMBE Proceedings. Springer, pp. 868–871.

Hinton, A., Sayers, B., Solartron, V.R., 1998. Advanced Instrumentation for Bioimpedance Measurements. G. E. N. 1260, 1250–1253.

Holt, M., Cogan, D.G., 1946. Permeability of the Excised Cornea to Ions, as Determined by Measurements of Impedance. Arch Ophthal 35, 292–298.

Ivorra, A., Genescà, M., Sola, A., Palacios, L., Villa, R., Hotter, G., Aguiló, J., 2005. Bioimpedance dispersion width as a parameter to monitor living tissues. Physiol. Meas. 26, S165–173.

Ivorra Cano, Antoni, 2005. Contributions to the measurement of electrical impedance for living tissue ischemia injury monitoring. Universitat Politècnica de Catalunya, Barcelona.

Jurgens, I., Rosell, J., Riu, P.J., 1996. Electrical impedance tomography of the eye: in vitro measurements of the cornea and the lens. Physiol. Meas. 17, A187–A195.

King-Smith, P.E., Fink, B.A., Fogt, N., Nichols, K.K., Hill, R.M., Wilson, G.S., 2000. The Thickness of the Human Precorneal Tear Film: Evidence from Reflection Spectra. Invest. Ophthalmol. Vis. Sci. 41, 3348–3359.

Kuang, K., Li, Y., Wen, Q., Wang, Z., Li, J., Yang, Y., Iserovich, P., Reinach, P.S., Sparrow, J., Diecke, F.P., Fischbarg, J., 2001. Corneal endothelial NKCC: molecular identification, location, and contribution to fluid transport. Am. J. Physiol. Cell Physiol. 280, C491–499.

Kuang, K., Li, Y., Yiming, M., Sánchez, J.M., Iserovich, P., Cragoe, E.J., Diecke, F.P.J., Fischbarg, J., 2004. Intracellular [Na+], Na+ pathways, and fluid transport in cultured bovine corneal endothelial cells. Exp. Eye Res. 79, 93–103.

Lass, J.H., Sugar, A., Benetz, B.A., Beck, R.W., Dontchev, M., Gal, R.L., Kollman, C., Gross, R., Heck, E., Holland, E.J., Mannis, M.J., Raber, I., Stark, W., Stulting, R.D., for the Cornea Donor Study Investigator Group, 2010. Endothelial Cell Density to Predict Endothelial Graft Failure After Penetrating Keratoplasty. Arch Ophthalmol 128, 63–69.

Laufer, S., Ivorra, A., Reuter, V.E., Rubinsky, B., Solomon, S.B., 2010. Electrical impedance characterization of normal and cancerous human hepatic tissue. Physiol. Meas. 31, 995–1009.

Lehmann, D.M., Cavet, M.E., Richardson, M.E., 2010. Nonclinical safety evaluation of boric acid and a novel borate-buffered contact lens multi-purpose solution, Biotrue™ multi-purpose solution. Contact Lens Anterior Eye 33, S24–S32.

Lim, J.J., Fischbarg, J., 1981. Electrical properties of rabbit corneal endothelium as determined from impedance measurements. Biophys. J. 36, 677–695.

Ma, L., Kuang, K., Smith, R.W., Rittenband, D., Iserovich, P., Diecke, F.P.J., Fischbarg, J., 2007. Modulation of tight junction properties relevant to fluid transport across rabbit corneal endothelium. Exp. Eye Res. 84, 790–798.

Malich, A., Scholz, B., Kott, A., Facius, M., Fischer, D., Freesmeyer, M., 2007. The impact of lesion vascularisation on tumours detection by electrical impedance scanning at 200 Hz. Biomed. Imaging Interv. J. 3, e33.

Martinsen, Ø.G., Grimnes, S., Nilsen, J.K., Tronstad, C., Jang, W., Kim, H., Shin, K., Naderi, M., Thielmann, F., 2008. Gravimetric method for in vitro calibration of skin hydration measurements. IEEE Trans. Biomed. Eng. 55, 728–732.

Martinsen, Ø.G., Grimnes, S., Sveen, O., 1997. Dielectric properties of some keratinised tissues. Part 1:Stratum corneum and nailin situ. Med. Biol. Eng. Comput. 35, 172–176.

McAdams, E.T., Jossinet, J., 1995. Tissue impedance: a historical overview. Physiol. Meas. 16, A1.

McAdams, E.T., Jossinet, J., 1996. Problems in equivalent circuit modelling of the electrical properties of biological tissues. Bioelectrochem. Bioenerg. 40, 147–152.

McNamara, N., Fusaro, R., Brand, R., Polse, K., Srinivas, S., 1997. Measurement of corneal epithelial permeability to fluorescein. A repeatability study. Invest. Ophthalmol. Vis. Sci. 38, 1830–1839.

Mokhtarzadeh, M., Casey, R., Glasgow, B.J., 2011. Fluorescein punctate staining traced to superficial corneal epithelial cells by impression cytology and confocal microscopy. Invest. Ophthalmol. Vis. Sci. 52, 2127–2135.

Oksala, A., Lehtinen, A., 1960. Experimental and Clinical Studies on the Ohmic Resistance of the Cornea and the Sclera. Acta Ophthalmol. (Copenh.) 38, 153–162.

Pallas-Areny, R., Webster, J.G., 1993. AC instrumentation amplifier for bioimpedance measurements. IEEE Trans. Biomed. Eng. 40, 830–833.

Parramon, D., Erill, I., Guimerà, A., Ivorra, A., Muñoz, A., Sola, A., Fondevila, C., García-Valdecasas, J.C., Villa, R., 2007. In vivo detection of liver steatosis in rats based on impedance spectroscopy. Physiol. Meas. 28, 813–828.

Pauly, H., Schwan, H.P., 1964. The Dielectric Properties of the Bovine Eye Lens. Biomed. Eng. IEEE Trans. BME-11, 103–109.

Prydal, J., Artal, P., Woon, H., Campbell, F., 1992. Study of human precorneal tear film thickness and structure using laser interferometry. Invest. Ophthalmol. Vis. Sci. 33, 2006–2011.

Rigaud, B., Morucci, J.P., Chauveau, N., 1996. Bioelectrical impedance techniques in medicine. Part I: Bioimpedance measurement. Second section: impedance spectrometry. Crit. Rev. Biomed. Eng. 24, 257–351.

Riu, P.J., Rosell, J., Bragos, R., Casas, O., 1999. Electrical Bioimpedance Methods: Applications to Medicine and Biotechnology. New York Academy of Sciences, New york.

Schwan, H.P., 1957. Electrical properties of tissue and cell suspensions. Adv. Biol. Med. Phys. 5, 147–209.

Schwan, H.P., 1988. Biological effects of non-ionizing radiations: cellular properties and interactions. Ann. Biomed. Eng. 16, 245–263.

Schwan, H.P., Ferris, C.D., 1968. Four-Electrode Null Techniques for Impedance Measurement with High Resolution. Rev. Sci. Instrum. 39, 481–485.

Srinivas, S.P., 2010. Dynamic Regulation of Barrier Integrity of the Corneal Endothelium. Optom. Vis. Sci. Off. Publ. Am. Acad. Optom. 87, E239–E254.

Swan, K.C., 1944. Reactivity of the ocular tissues to wetting agents. Am J Ophthalmol 27, 1118–1122.

Tiruppathi, C., Malik, A.B., Vecchio, P.J.D., Keese, C.R., Giaever, I., 1992. Electrical method for detection of endothelial cell shape change in real time: assessment of endothelial barrier function. Proc. Natl. Acad. Sci. 89, 7919–7923.

Uematsu, M., Kumagami, T., Kusano, M., Yamada, K., Mishima, K., Fujimura, K., Sasaki, H., Kitaoka, T., 2007. Acute Corneal Epithelial Change after Instillation of Benzalkonium Chloride Evaluated Using a Newly Developed in vivo Corneal Transepithelial Electric Resistance Measurement Method. Ophthalmic Res. 39, 308–314.

V. Patel, D., N. McGhee, C., n.d. Quantitative analysis of in vivo confocal microscopy images: A review. Surv. Ophthalmol.

Valentinuzzi, M.E., Morucci, J.P., Felice, C.J., 1996. Bioelectrical impedance techniques in medicine. Part II: Monitoring of physiological events by impedance. Crit. Rev. Biomed. Eng. 24, 353–466.

Watanabe, M., Mokudai, Y., Ueno, H., Ando, M., Irimajiri, A., 1993. Dielectric measurements on the rabbit cornea using a surface electrode. Nippon Ganka Gakkai Zasshi 97, 569–574.

Wilson, G., Ren, H., Laurent, J., 1995. Corneal epithelial fluorescein staining. J. Am. Optom. Assoc. 66, 435–441.

Yélamos, D., Casas, Ó., Bragós, R., Rosell, J., 1999. Improvement of a Front End for Bioimpedance Spectroscopya. Ann. N. Y. Acad. Sci. 873, 306–312.

Chapter 2

Numerical study of non-invasive impedance measurements for corneal barrier function assessment.

Since ionic permeability has a fundamental impact on the passive electrical properties of living tissues, here it is hypothesized that bioimpedance methods can be employed for assessing the corneal barrier function in a non-invasive fashion. The aim of this chapter is to analyze the feasibility of the proposed method for assessing the electrical properties of the corneal epithelial and endothelial layers. Therefore, a bidimensional model consisting of the main corneal layers and a tetrapolar impedance measurement setup placed on the corneal surface has been implemented and analyzed by means of the finite elements method (FEM). From the performed simulations, the contribution of each layer to the measured impedance has been studied. Moreover, reasonable variations of the model parameters have been applied to study which measured parameter is able to mainly reflect the alterations of the epithelial and endothelial permeability. Simulation results show that the impedance measurements performed by means of external electrodes are indeed sufficiently sensitive to the changes in the electrical properties of the epithelial and endothelial layers. It is concluded that the method presented here can be employed as non-invasive method for assessing the corneal barrier function.

Most of the contents of this chapter have been published in the following article:

- Guimerà, A. Ivorra, G. Gabriel, R. Villa *"Non-invasive assessment of corneal endothelial permeability by means of electrical impedance measurements"*. **Medical Engineering & Physics** (2010) 32:1107–1115. doi: 10.1016/j.medengphy.2010.07.016

2.1 Introduction

The steady increase of computational power has made possible the emergence of simulations tools. The solution of very complex problems is now possible with commercially available computers. As a matter of fact, computer simulation has become an essential part of science and engineering. The Finite Element Method (FEM) is a numerical technique for finding approximate solutions to boundary value problems. It consists in dividing the domain of the problem into a collection of subdomains (finite elements), where each subdomain is represented by a set of differential equations related to the original problem. Then, a global system of equations for the final calculation is reached by recombining all sets of element equations. To obtain a numerical answer for the original problem, this global system of equations must be solved for the initial values. The implementation of this technique is often complex and requires a high level of mathematical knowledge. However, there are several software tools commercially available which implement the FEM techniques in a user friendly way. In particular, the work presented in this chapter has been carried out by employing the commercial FEM tool COMSOL® Multiphysics® and its associated application mode "Quasi-statics, Electric" of the "AC/DC module". By employing FEM methods it is possible to obtain information which would be difficult to obtain with real experiments such as, for instance, the current distribution in the measured sample. Information provided by numerical simulations allows a better comprehension of the system and facilitates design optimization.

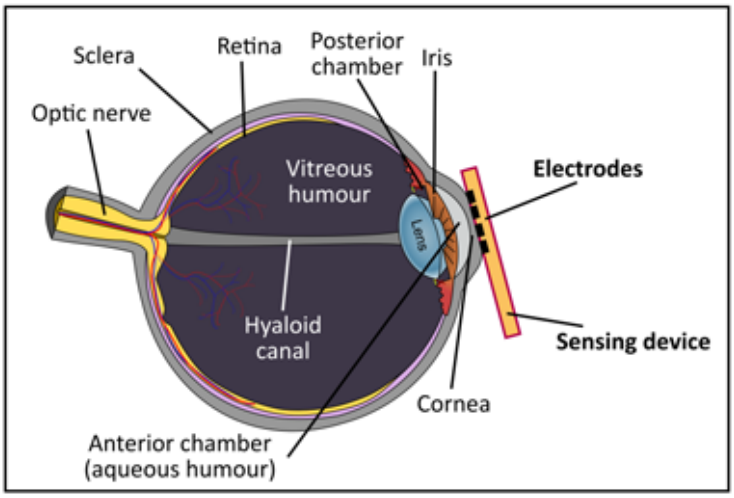

Figure 2-1 Schematic representation of the ocular globe, which shows the location of its main organs and the position of the proposed sensor.

In this dissertation, a non-invasive method to assess the corneal barrier function by placing electrodes on the corneal surface is proposed (Figure 2-1). In order to evaluate the feasibility of this approach a numerical study based on FEM simulations has been performed. Therefore, an electrical model of the main corneal layers was built and the corresponding electrical properties were selected from data reported in the literature. The study presented in this chapter is focused on how variations in the passive electrical properties of the endothelium and epithelium are reflected in the impedance measurements performed by electrodes placed on the corneal surface. Moreover, the proposed model also takes into account the stroma layer and the surrounding liquids, the tear film and the aqueous humour. Thus, the contribution of each layer to the total measured impedance has been studied. In

addition, reasonable variations in the model parameters have been simulated in order to study which measured parameter is able to reflect mainly the alterations of the endothelial and epithelial layer.

2.2 Methods

2.2.1 Simulation model

Figure 2-2 shows the geometry of the developed model. It is formed by the three main layers of the cornea and the electrodes. In addition, it also considers the surrounding fluids: tear film and aqueous humor. Taking into account the laminar structure of the cornea, which is composed of layers arranged in parallel to the surface, the model consist of a vertical cross section of such layers (Dewarrat et al., 2008). This approach simplifies the computational model because it can be reduced in one dimension, from 3D to 2D. Using this model, a 2D analysis within frequency range from 10 Hz to 1 MHz has been carried out.

To implement the impedance sensor it has been chosen the tetrapolar method. Compared to the simpler bipolar method, the tetrapolar method offers the advantage of minimizing, and ideally cancelling, the parasitic effects of the electrode-electrolyte interface impedances (Schwan and Ferris, 1968). To simulate impedance measurements, a constant AC current has been injected through the outer electrodes (I+ and I-) and the inner electrodes (V+ and V-) have been used to sense the voltage drop (Figure 2-1). Then, the impedance has been calculated using Ohm's law, Z=V/I. The electrodes have been modeled with a very high conductivity (6×10^7 S/m) so that the voltage in all points of the electrode is the same.

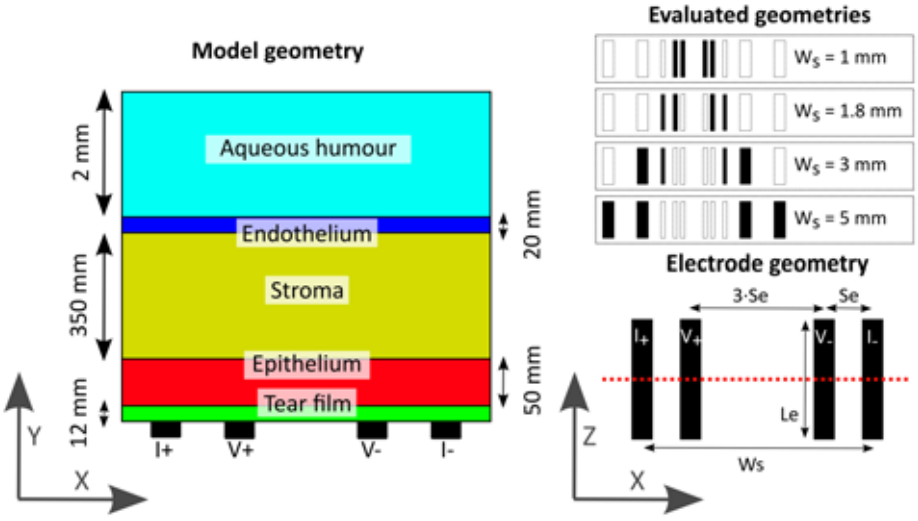

Figure 2-2 (left) Schematic representation (not to scale) of the simulated model, which shows the modeled layers and the electrode placement. (right) Schematic representation of the simulated electrodes geometry. Where I+ and I– are the current electrodes, V+ and V– are the voltage sensing electrodes. The dashed line indicates position of the modeled bidimensional vertical cross-section.

Four sets of electrode geometries have been tried in this study in order to identify the best configuration for detecting changes in the passive electrical properties of the endothelial

and epithelial layer. Figure 2-2 shows the geometry of the used electrode sets. In all electrode sets the separation ratio between the electrodes is the same; only the total sensor width differs between each set (3 mm, 5 mm, 1.8 mm and 1 mm). As it can be observed in Figure 2-2, these four tetrapolar configurations can be implemented by employing the same substrate with 10 electrodes, thus simplifying the fabrication of sensor prototypes. The distance between the inner electrodes is three times larger than the separation between the outer ones. This ratio of distances offers some advantages in terms of spatial resolution (Ivorra et al., 2001; Robillard and Poussart, 1979). The sensor width is related to the "penetration" of the measurement; it is advantageous to maximize this parameter in order to ensure that a significant amount of current goes through the endothelium. On the other hand, the sensor width is limited by the dimensions of the cornea (11 mm in diameter) and its curvature. Widths of 3 mm and 5 mm seemed a reasonable compromise between the penetration of the measure and the cornea dimensions.

2.2.2 Corneal electrical properties

Table 2-1. *Values for the conductivity, permittivity and thickness of the modeled layers for a healthy cornea.*

Layer	*Conductivity [S/m]*	*Relative Permittivity*	*Thickness [µm]*	*References*
Tear	1.5	80	12	(Prydal et al., 1992) (King-Smith et al., 2000) (López García et al., 2003)
Epithelium [a]	4×10^{-4}	1×10^{5}	50	(Klyce, 1972) (Gabriel et al., 1996) (Li et al., 1997)
Stroma	0.2	80	350	(Lim and Fischbarg, 1981) (Gabriel et al., 1996)
Endothelium [a]	6.6×10^{-3}	1.3×10^{4}	20	(Lim and Fischbarg, 1981)
Aqueous humor	1.5	80	2000	(Jurgens et al., 1996) (Gabriel et al., 1996)

[a] Frequency depending values. These values correspond to 10 Hz.

The electrical properties and thicknesses of the different modeled layers for a normal cornea are shown in table 2-1. The physical dimensions of rabbit cornea have been taken into account, because rabbit is the reference animal model for *in vivo* eye experimentation. The tear layer has been defined with the electrical properties of the saline solution and its influence must be taking into account since its conductivity is much higher than the conductivity of the epithelium. The thickness of this layer has been estimated to be around the 15 µm (López García et al., 2003; Prydal et al., 1992). The epithelium layer has been modeled with the same electrical properties as the skin (Gabriel et al., 1996) due to their similar histological structure. The endothelial and stroma layer have been modeled according

to the equivalent circuit proposed by Fischbarg (Lim and Fischbarg, 1981) which is shown in Figure 2-3. Considering the thickness of each layer, the resistivity values in Ω·cm^2 can be converted to a conductivity values in S/m, needed for the simulation inputs. The aqueous humour has been modeled with the electrical properties of the saline solution (Jurgens et al., 1996).

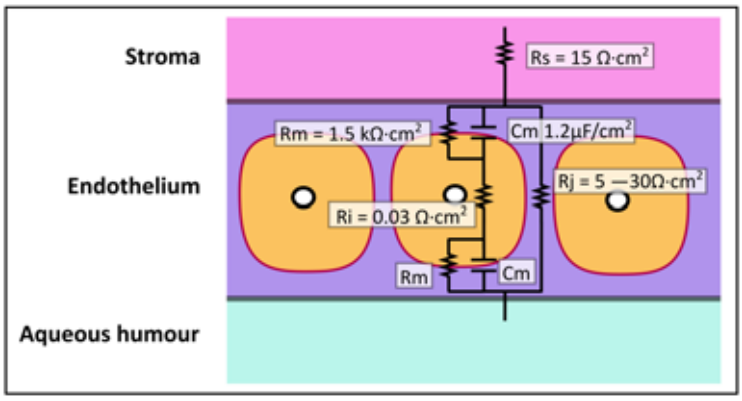

Figure 2-3 Schematic morphological representation of the corneal endothelium with the corresponding equivalent electrical parameters at the postulated locations (Lim and Fischbarg, 1981). Rm, cellular membrane resistance; Rs, resistance of the stroma; Rj, resistance of the tight junctions; Rc, resistance of the cytoplasm; Cm, capacitance of the cell membrane.

2.2.3 Endothelial and epithelial permeability model

For modeling the effect of endothelial and epithelial damage on their passive electrical properties, it has been assumed that the intercellular spaces between cells are widened according to the amount of damage, resulting in a decrease in its conductivity (Uematsu et al., 2007). Accordingly, it is proposed the following equations to describe the relation between damage and conductivity of each layer.

$$\sigma_{endo} = \frac{\sigma_{leak}}{H_{endo}} + \sigma_{cells} \quad (1)$$

$$\sigma_{epi} = \frac{\sigma_{leak}}{H_{epi}} + \sigma_{cells} \quad (2)$$

where the parameter H_{endo} and H_{epi} (for Health status) would be inversely related to the amount of damage in epithelium and endothelium respectively. σ_{leak} represents the normal contribution of the intercellular spaces to the conductivity and σ_{cells} correspond to the conductivity of cells. Note that σ_{cells} depend on frequency whereas σ_{leak} is frequency independent.

According to the reported changes of TER measurements when the endothelial permeability is pharmacologically increased (Bonanno, 2003; Ma et al., 2007), the simulated range values for parameter H must range from 1 to 0.1 (1 represents the normal permeability; 0.1 is related with a decrease of 10% of the normal TER measurement). Figure 2-4 shows the conductivity of the endothelial and epithelial layer as function of the frequency for some values of parameter H.

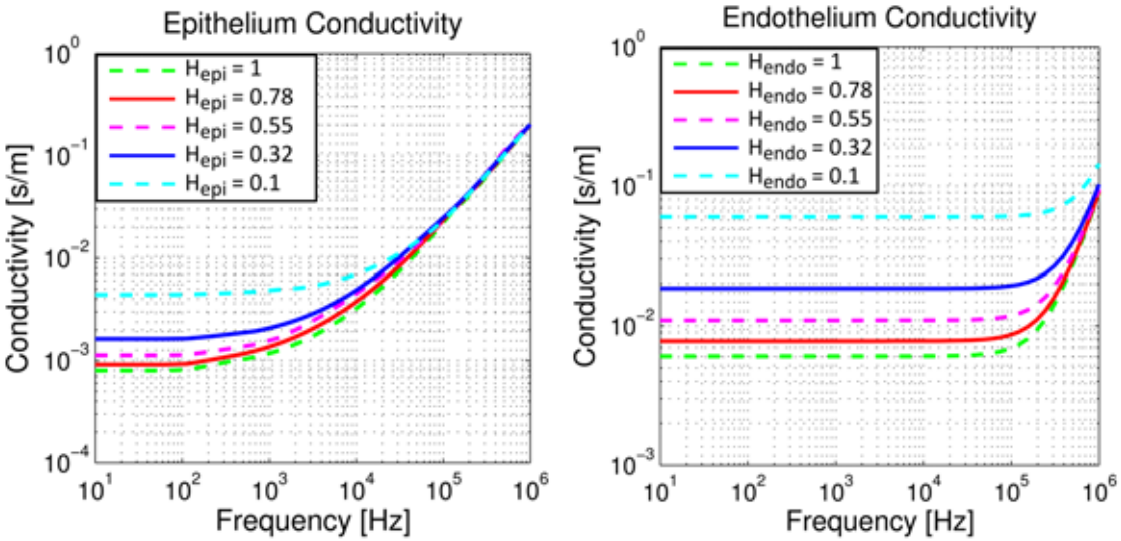

Figure 2-4 Endothelial and epithelial conductivity spectrogram for different values of parameter H (inversely to the endothelial and epithelial damage), evaluated according to Eq. (1-2).

2.2.4 Simulation strategy

In order to find a robust indicator for the endothelial and epithelial permeability, it must be taken into account that not only variations in the permeability will be present but also the value for the other parameters of the model will be different from the nominal values reported in Table 2-1. For instance, an increase in permeability of the endothelial or epithelial layer can produce an alteration of the ionic concentration in the stroma layer and, as a result, a change of its conductivity. Moreover, it can also produce a variation of the stroma thickness due to the increment of the water content of this layer (Kaye and Donn, 1965; Klyce, 1981). Besides, the tear layer thickness can be modified by the sensor placement or by the ambient conditions (Prydal and Campbell, 1992; Zhuang et al., 2010). Therefore, in order to obtain a robust indicator against these uncontrollable variations, it has been studied how the endothelium and epithelium conductivity contributes to the measured impedance together with the variation of the other layers of the model. Table 2-2 shows the variations applied on the model parameters.

Table 2-2. *Evaluated ranges for the conductivity and thickness of the modeled layers. The endothelium and epithelium conductivity is expressed according the equation (1-2).*

Layer	*Conductivity*	*Units*	*Thickness*	*Units*	*References*
Tear	1.5	S/m	5 — 15	µm	(Prydal and Campbell, 1992)
Stroma	0.1 — 0.5	S/m	325 — 425	µm	(Klyce, 1981)
Epithelium	H_{epi} = 1—0.1	—	55	µm	(Uematsu et al., 2007)
Endothelium	H_{endo} = 1—0.1	—	20	µm	(Ma et al., 2007)

2.2.5 Impedance sensitivity analysis

In a tetrapolar impedance measurement system, each portion of volume will have a different impact on the measured impedance depending on how currents are distributed within the tissues. It is intuitively understood that the volume portions close to the electrodes will contribute more than volumes far away from the electrodes. Therefore, choice of the electrode size and position is important in order to focus the measurement on the region of interest.

It can be defined a sensitivity parameter, S, that indicates the contribution of each infinitesimal volume of the sample to the total measured impedance. Such sensitivity parameter can be evaluated as follows (Geselowitz, 1971; Grimnes and Martinsen, 2007).

$$S = \frac{\vec{J}_1 \cdot \vec{J}_2}{I^2} \tag{3}$$

Where S is the sensitivity to the conductivity changes at point in the model, $\vec{J}_1$ is the current density vector when I is injected between the two current electrodes, and $\vec{J}_2$ would be the current density vector when the same current I is injected between the two voltage sensing electrodes. Thus, the sensitivity at each location depends solely on the angle and magnitude of these two vectors and can be either positive, negative or null. A positive value for the sensitivity means that, if the resistivity of this volume element is increased, a higher value of impedance is measured. A negative value means that, if the resistivity of this zone is increased, a lower value of impedance is measured. A higher absolute value for the sensitivity means a greater influence on the total measured impedance.

The measured impedance Z can be obtained as the integral of the sensitivity at each location weighted by the local complex resistivity ρ over the volume v. The local complex resistivity value ρ, depends of the frequency and is defined as equation (4). Where σ is the conductivity, ε_r is the relative permittivity, ε_o is the permittivity of the vacuum, and ω is the angular frequency. In the same way, the measured impedance due to each layer can be determined integrating each sub-volume v_i corresponding to each layer.

$$Z = \int_v \rho \cdot S \cdot dv \tag{4}$$

$$\rho = \frac{1}{(\sigma + j\varepsilon_r \varepsilon_o w)} \tag{5}$$

Another parameter, selectivity, was also analyzed in the present study (Kauppinen et al., 1998; Yang and Patterson, 2008). It provides the impedance of each layer as a fraction of the total impedance measured and is defined in equation (6). In other words, it analyzes the ability of a given electrode arrangement to detect changes in the conductivity of the layer of interest.

Therefore, this parameter is a convenient indicator for analyzing whether or not a set of electrodes is suitable to detect changes in the conductivity of the layer of interest.

$$Z_{v_i} = \int_{v_i} \rho \cdot S \, dv_i \tag{6}$$

$$Sel_{v_i} = \frac{Z_{v_i}}{Z} = \frac{\int_{v_i} \rho \cdot S \, dv_i}{\int_{v} \rho \cdot S \, dv} \tag{7}$$

2.3 Results and discussion

2.3.1 Simulation results from the impedance sensitivity analysis.

Sensitivity map for the sensor with a width of 5 mm is depicted in Figure 2-5. It shows the results for three different frequency values, 100 Hz, 6 kHz and 100 kHz. The represented zone corresponds only to the electrodes V- and I-, because of symmetry. It can be observed a negative sensitivity zone between the voltage electrode and the current electrode. It is interesting to note that the sensitivity of the interior layers (stroma, endothelium and aqueous humor) increases as frequency increases.

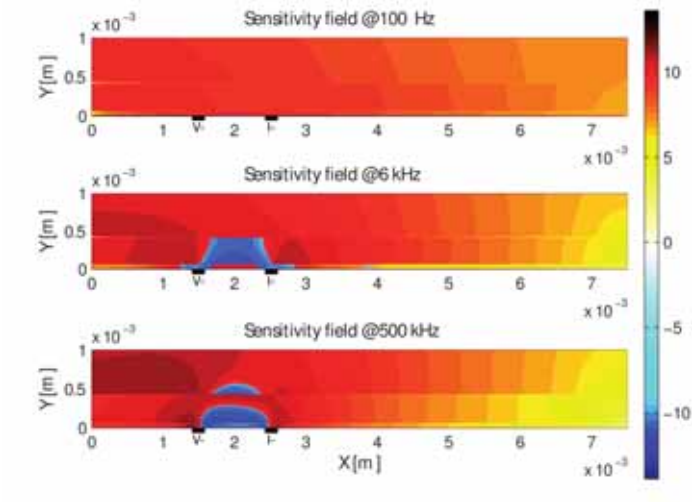

Figure 2-5 Representation of the sensitivity evaluated at three frequency points, 100 Hz, 6 kHz and 500 kHz. The sensitivity values are represented using a logarithmic scale color; positive sensitivities are visualized with a hot color map and negative with a cool color map.

Figure 2-6 shows the contribution of each layer to the total impedance magnitude as function of frequency. As expected, the contribution of each layer is different depending on the measured frequency. Three frequency ranges can be vaguely differentiated. In the low frequency band (up to frequencies of about 1 kHz), the measurement is only affected by the tear layer and by the epithelium layer. This observation can be explained as being the result of the fact that the resistivity of the epithelium layer is very high in this frequency range and, therefore, the current cannot pass easily through it. Therefore, the measured voltage drop is only due to the resistivity of these two layers. It is worth noting that a similar effect has been

reported in the case of skin impedance measurements (Martinsen et al., 1999). The second band of intermediate frequencies is limited in the frequency range from 1 kHz to 100 kHz. This band can be defined as a transition zone, the contribution of the exterior layers is decreasing and the contribution of the interior layers is increasing. As can be observed, the maximum contribution of the endothelium layer is reached in this band. Finally, the third band corresponds to high frequency range; it can be defined by frequencies above 100 kHz. In this frequency range the conductivity of the cellular layers is very low and the current can pass through them easily. Therefore, the layers with major contribution to the measure are the thickest layers, the stroma and the aqueous humour. Furthermore, it is interesting to note that the contribution of the tear layer is considerable across the whole spectrum, being higher at low frequency range and for the closest electrode configuration.

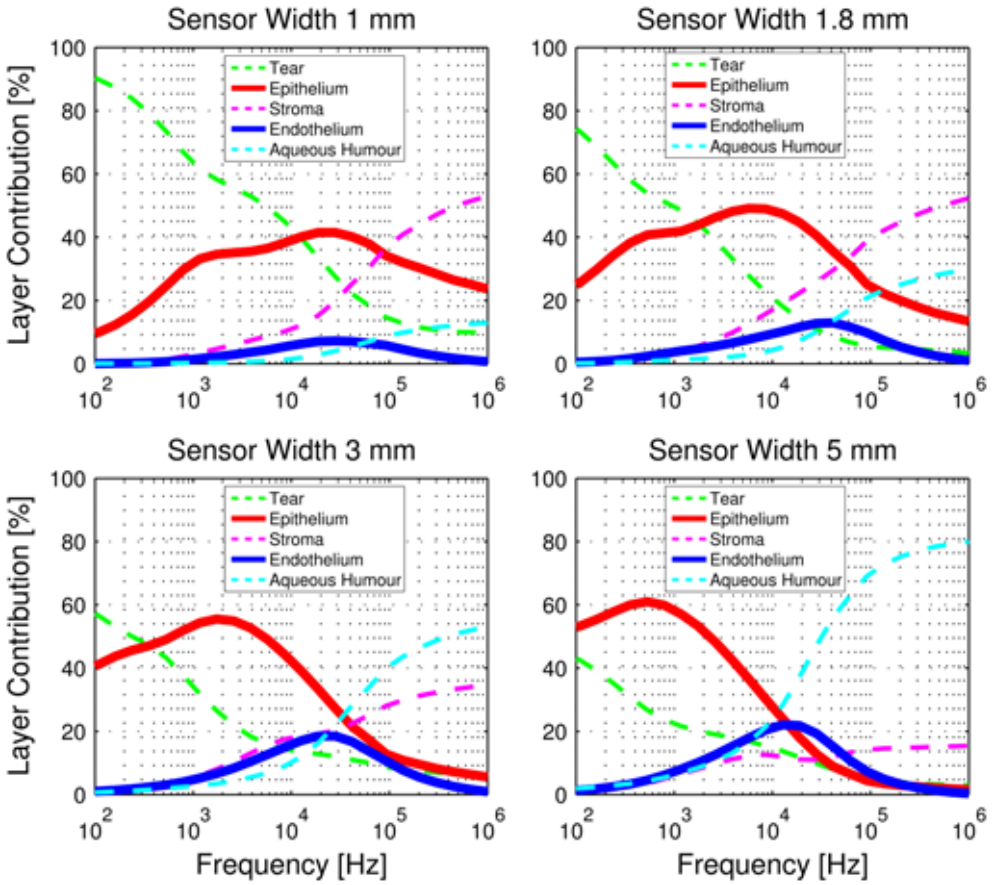

Figure 2-6 Contribution of each layer to the total measured impedance magnitude as function of frequency for the four studied sensor width. Note that the contribution of each layer has a large dependence on frequency. At intermediate frequencies is where the endothelium reaches its maximum contribution.

2.3.2 Simulation results when varying endothelial and epithelial permeability.

In relation to how the endothelium electrical properties will be reflected in the impedance measurements, Figure 2-7 shows the simulated impedance for the different values of parameter H_{endo}. According to the study of the contribution of each layer, the variation of the endothelium conductivity is reflected in the frequency range from 2 kHz to 12 kHz. The analysis of the impedance at this frequency range is quite complex because multiple factors contribute to it. On one hand, the conductivity of the aqueous humor layer is larger than the conductivity of the stroma layer and, consequently, the current will tend to go through the aqueous humour. On the other hand, the amount of current than can pass from the stroma to the aqueous humour layer is modulated by the conductivity of the endothelium layer. Therefore, the decrease in the measured impedance is not only due to a decrease in the conductivity of the endothelium layer, but also due to an increase of the contribution of the aqueous humor. Therefore, as can be observed, the variation of the measured impedance due to changes in the endothelium conductivity is larger when electrodes of 5 mm width are used since the profundity of the measurement is higher. In addition, the corneal impedance measurement presents two frequency dispersions, one due to the epithelial layer and another due to endothelial layer. The sensor width determines to some extent the frequency range of these two dispersions: a reduction of the sensor width produces an increase in the frequency of the epithelium dispersion, which ends up hiding the endothelium dispersion. Therefore, in order to observe the dispersion due to the endothelial layer and thereby to obtain information on its permeability, the sensor width has to be maximized. However, this parameter is limited by the size and curvature of the cornea. For this reason, the sensor width of 5 mm was the maximum size considered here.

Figure 2-8 shows how the epithelium electrical properties will be reflected in the simulated impedance. The results are depicted for different values of the parameter H_{epi}. As expected, the simulated impedance is lower when the damage in the epithelium layer increases (parameter H_{epi} decreases) in accordance with its conductivity decrease. Moreover, the variation of the epithelium conductivity is reflected in frequencies bellow 5 kHz (Figure 2-8). In this frequency range, the contribution of the tear film is also important and can alter the measurement. However, the tear film contribution can be minimized by increasing the separation between the electrodes. Consequently and as in the case of the endothelium layer, to obtain information on epithelium permeability, the sensor width has to be maximized.

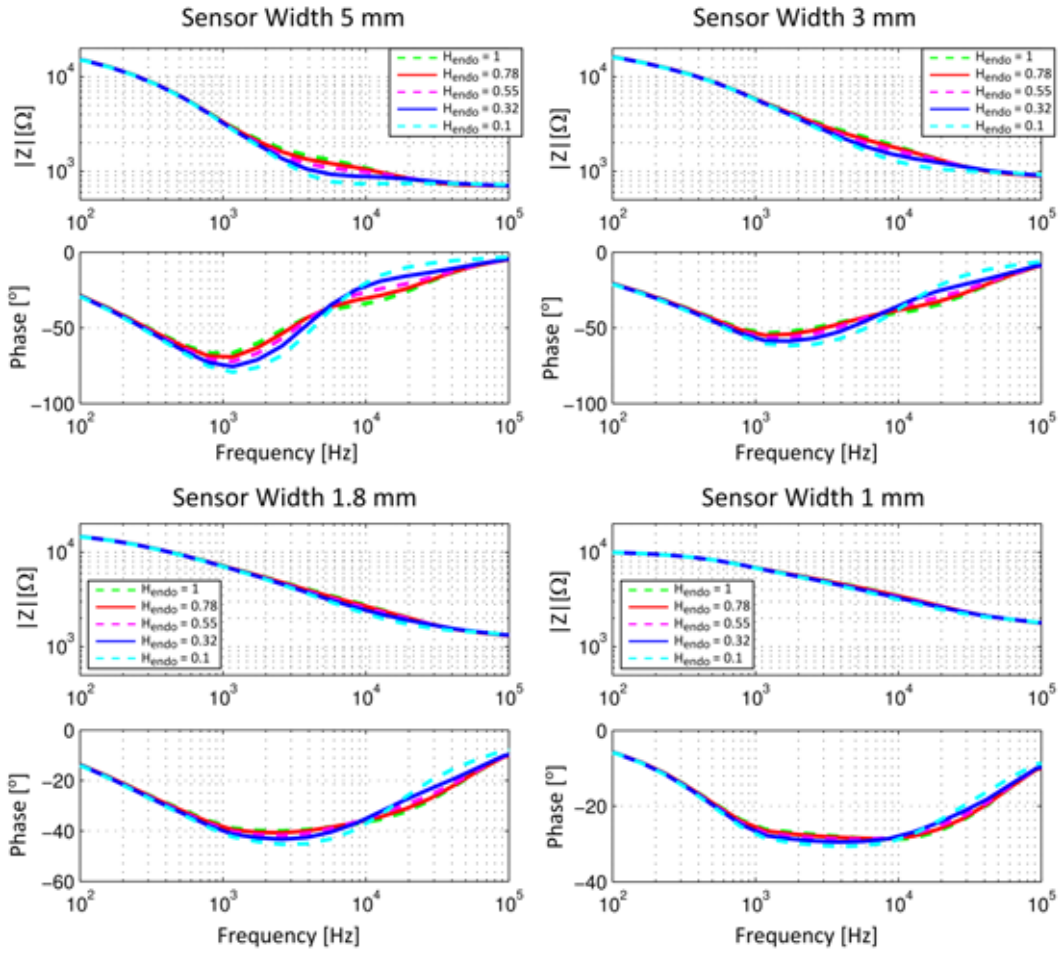

Figure 2-7 Calculated impedance modulus and phase shift for different values of parameter H_{endo}, showing the effect of the endothelial damage (inversely to parameter H_{endo}) in the measured impedance for the studied sensor widths. The major influence of the endothelial damage in the measured impedance is observed with a 5 mm sensor at the intermediate frequency range.

As described, the influence of the epithelial and endothelial electrical properties on the simulated impedance has been studied together with the variations of other parameters of the model (Table 2-2). Thus, Figure 2-9 shows the effect of the stroma layer on the simulated impedance. Changes in two parameters of this layer have been studied: the stroma conductivity and the thickness. According with the sensitivity analysis, the changes in its conductivity and thickness can be observed in frequencies above 10 kHz. The thickness variation produces slight alterations in the measured impedance and its effect is noticeable in frequencies above 100 kHz. On the other hand, the alterations produced by the stroma conductivity are more important and have influence in the frequency range where the endothelium conductivity can be detected. The stroma conductivity variations have a larger impact when narrower sensors are used because the contribution of this layer to the measured impedance is greater, as can be observed in Figure 2-6.

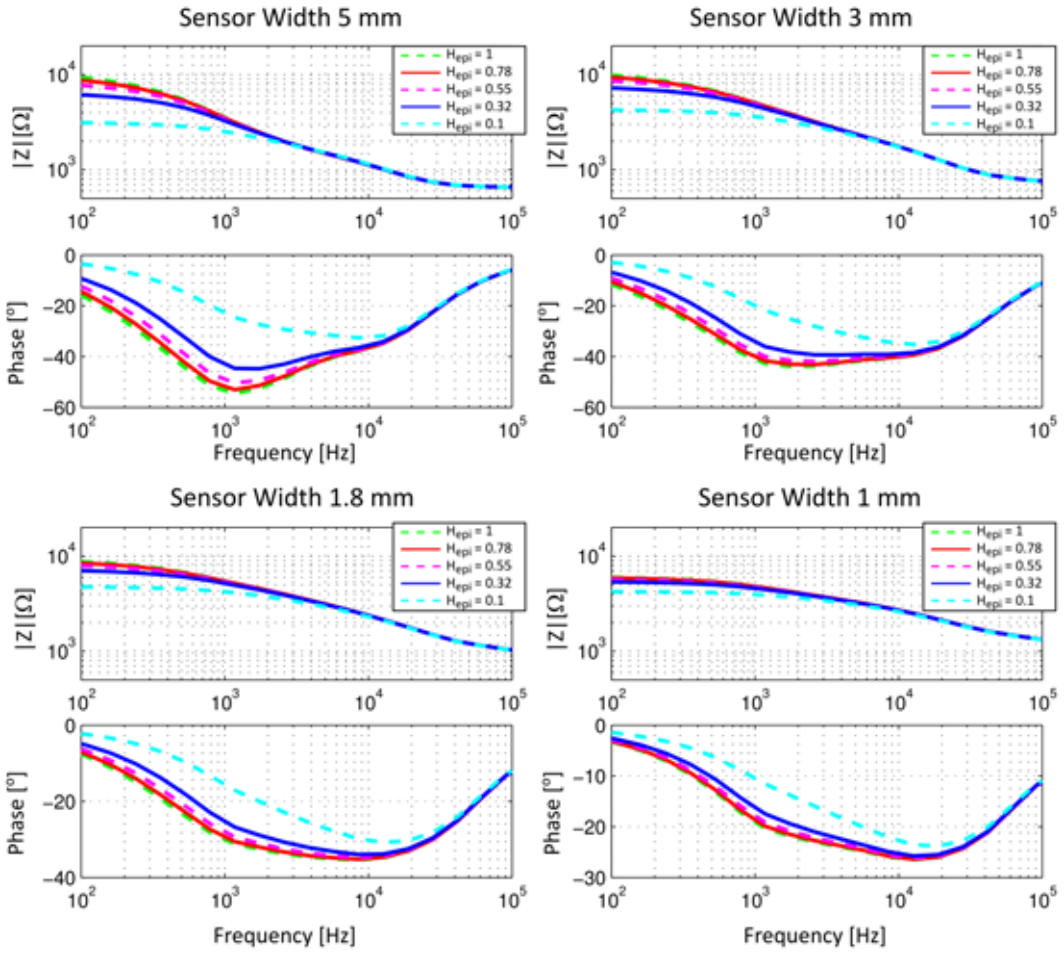

Figure 2-8 Calculated impedance modulus and phase shift for different values of parameter H_{epi}, showing the effect of the epithelial damage (inversely to parameter H_{epi}) in the measured impedance for the studied sensor widths. The major influence of the endothelial damage in the measured impedance is observed with a 5 mm sensor at the lower frequency range.

Figure 2-10 shows the simulated impedance for different values of tear film thickness, which is notable in all the frequency range. As in the sensitivity study, this layer has influence in a large frequency range, from 10 Hz to 100 kHz. As can be observed, the major influence of the tear thickness is on the phase shift measurement, reaching values minor than -90 degrees. At first thought, these phase shift values are inconsistent with knowledge about passive electrical properties of tissues. However, these phase values can be explained as being the consequence of large conductivity differences between the tear film, the epithelium and the stroma; such differences would produce two different paths for the current as it tends to go through the layers with lower conductivity, that is, the tear film and the stroma. Thus, the measured voltage drop is mainly due to the current that goes through the tear film, but the measured impedance is evaluated over the total current. Sverre Grimnes & Orjan G. Martinsen (2007) refer to this effect for explaining anomalous values of phase shift in the case of skin impedance measurements when tetrapolar electrodes are used.

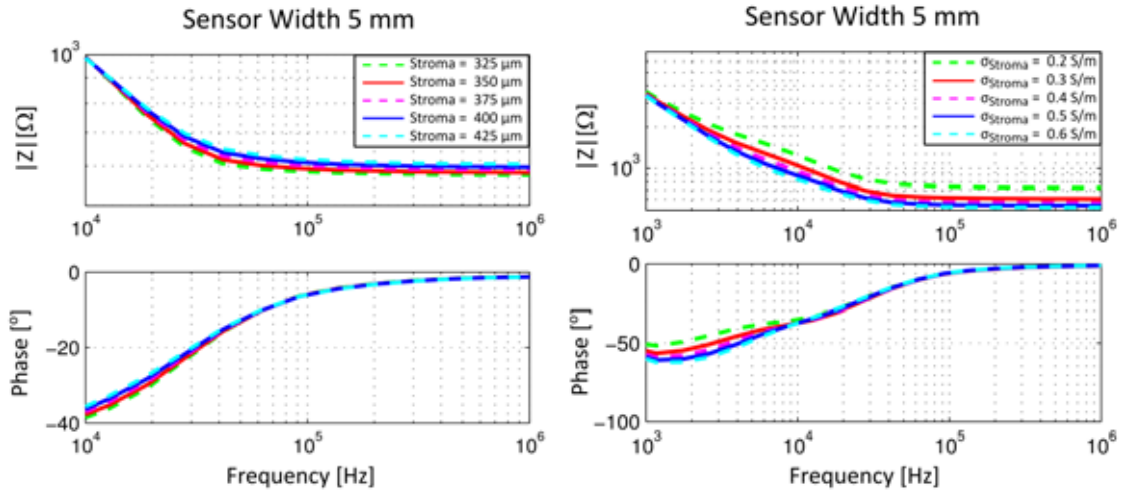

Figure 2-9 Calculated impedance modulus and phase shift for different stroma conductivities and thickness values using a 5 mm width sensor (left) for different values of stroma thickness (right) for different values of stroma conductivity. The variation of the stroma conductivity implies an alteration of the measured impedance in the same frequency range where the endothelial damage can be detected. However, the stroma thickness variation only modifies the measured impedance at high frequencies.

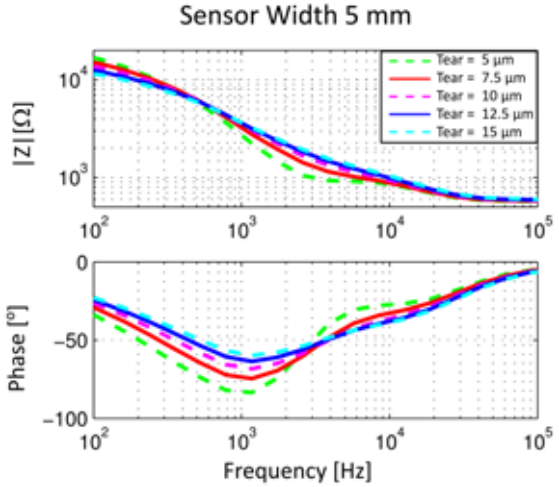

Figure 2-10 Calculated impedance modulus and phase shift of different values of tear thickness using a 5 mm width sensor. The variation of the tear thickness modifies the measured impedance at all frequencies. This alteration is very noticeable in the phase shift.

Several simulations have been carried out for finding out the most reliable indicator of the endothelial and epithelial damage. As mentioned, apart from the endothelial or epithelial damage (parameter H), it has been modified: the tear film thickness, the epithelium conductivity, the endothelium conductivity, the stroma conductivity and the stroma thickness. For each of these 5 parameters, 3 points nested sweeps in the specified range have been simulated in order to evaluate all combinations. Thus, a total of 81 measurements for each value of the parameter H have been obtained.

The impedance modulus measured at 6 KHz using the sensor width of 5 mm has been considered as an indicator of endothelial damage because at this frequency the contribution of the endothelial layer is largest. Represented in a boxplot, Figure 2-11 shows the measured impedance at 6 kHz as function of the parameter H_{endo}. As can be observed, the modulus of the impedance at 6 kHz presents a strong, and quite linear, correlation with the endothelial

permeability, but also presents a considerable dispersion. This dispersion is mainly due to the variation of tear film thickness and of the stroma conductivity

Since the contribution of epithelium layer to the measured impedance is largest in the low frequency range, the impedance modulus measured at 100 Hz using the sensor width of 5 mm has been considered as an indicator of epithelial damage. Figure 2-11 shows in a boxplot representation the impedance modulus simulated at 100 Hz as function of the parameter H_{epi}. As can be observed, it presents a good correlation with the epithelial damage. The measurements also present dispersion, in this case mainly due to the variations in the tear film thickness. It is worth noting that dispersion decreases as epithelial damage increases since the epithelium conductivity decreases reducing the effect of the two current paths.

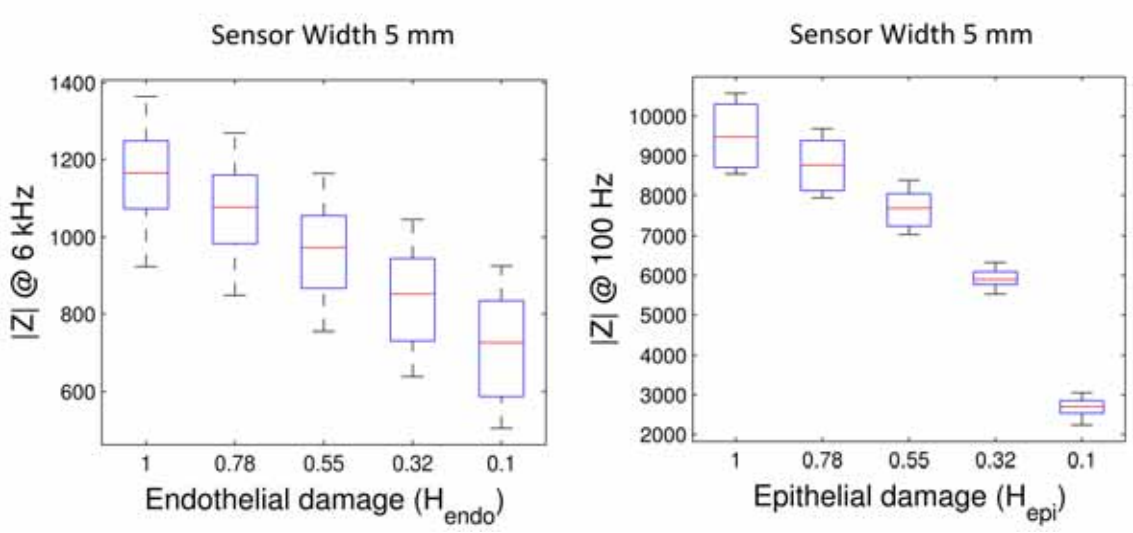

Figure 2-11 Representation of the different presented indexes for the assessment of the epithelium (left) and endothelium (right) permeability as a function of damage (inversely proportional to parameter H). The effect of the damage is presented together with the other variations of the model parameters. The boxplot representation shows the mean value, the dispersion of the measures grouped by quartiles (boxes and bars). The impedance magnitude measured at 6 kHz presents a strong linear correlation with the endothelial permeability and the impedance measured at 100 Hz presents a correlation with the epithelial permeability.

2.4 Conclusions

In this chapter, the feasibility of the proposed non-invasive method has been studied. For that, the influence of the epithelium and endothelium permeability on tetrapolar impedance measurements has been studied using FEM simulations. Simulated impedance measurements were performed by means of four electrodes placed on the cornea surface. It was found that the plausible variations in the epithelium and endothelium permeability will be detected by impedance measurements. In addition, it has been studied the influence on impedance measurements by other layers of no concern in the cornea. It was found that the influence of those layers can be minimized by increasing the sensor width. Moreover, indicators for the epithelium and endothelium damage have been proposed and it has been shown their potential for assessing damage despite the variability introduced by the layers of no concern. Therefore, it is concluded that the method presented here can be used as a non-invasive

method for assessing the corneal barrier function. This new method could be used in the clinical practice, filling the existing lack of this kind of methods.

2.5 References

Bonanno, J.A., 2003. Identity and regulation of ion transport mechanisms in the corneal endothelium. Prog. Retin. Eye Res. 22, 69–94.

Dewarrat, F., Falco, L., Caduff, A., Talary, M., 2008. Optimization of Skin Impedance Sensor Design with Finite Element Simulations, in: COMSOL Conference 2008 Hannover. Presented at the COMSOL Conference 2008 Hannover.

Gabriel, S., Lau, R.W., Gabriel, C., 1996. The dielectric properties of biological tissues: III. Parametric models for the dielectric spectrum of tissues. Phys. Med. Biol. 41, 2271–2293.

Geselowitz, D.B., 1971. An Application of Electrocardiographic Lead Theory to Impedance Plethysmography. IEEE Trans. Biomed. Eng. BME-18, 38–41.

Grimnes, S., Martinsen, O.G., 2007. Sources of error in tetrapolar impedance measurements on biomaterials and other ionic conductors. J. Phys. Appl. Phys. 40, 9–14.

Ivorra, A., Aguiló, J., Millán, J., 2001. Design considerations for optimum impedance probes with planar electrodes for biomimpedance measurements, in: Semiconductor Conference, 2001. CAS 2001 Proceedings. International.

Jurgens, I., Rosell, J., Riu, P.J., 1996. Electrical impedance tomography of the eye: in vitro measurements of the cornea and the lens. Physiol. Meas. 17, A187–A195.

Kauppinen, P.K., Hyttinen, J.A., Malmivuo, J.A., 1998. Sensitivity Distributions of Impedance Cardiography Using Band and Spot Electrodes Analyzed by a Three-Dimensional Computer Model. Ann. Biomed. Eng. 26, 694–702.

Kaye, G.I., Donn, A., 1965. Studies on the Cornea IV. Some Effects of Ouabain on Pinocytosis and Stromal Thickness in the Rabbit Cornea. Invest. Ophthalmol. Vis. Sci. 4, 844–852.

King-Smith, P.E., Fink, B.A., Fogt, N., Nichols, K.K., Hill, R.M., Wilson, G.S., 2000. The Thickness of the Human Precorneal Tear Film: Evidence from Reflection Spectra. Invest. Ophthalmol. Vis. Sci. 41, 3348–3359.

Klyce, S.D., 1972. Electrical profiles in the corneal epithelium. J. Physiol. 226, 407–429.

Klyce, S.D., 1981. Stromal lactate accumulation can account for corneal oedema osmotically following epithelial hypoxia in the rabbit. J. Physiol. 321, 49–64.

Li, H.F., Petroll, W.M., M\oller-Pedersen, T., Maurer, J.K., Cavanagh, H.D., Jester, J.V., 1997. Epithelial and corneal thickness measurements by in vivo confocal microscopy through focusing (CMTF). Curr. Eye Res. 16, 214–221.

Lim, J.J., Fischbarg, J., 1981. Electrical properties of rabbit corneal endothelium as determined from impedance measurements. Biophys. J. 36, 677–695.

López García, J.S., García Lozano, I., Martínez Garchitorena, J., 2003. Estimación del grosor de la capa lipídica lacrimal mediante colores interferenciales en distintos tipos de ojo seco. Arch. Soc. Española Oftalmol. 257–264.

Ma, L., Kuang, K., Smith, R.W., Rittenband, D., Iserovich, P., Diecke, F.P.J., Fischbarg, J., 2007. Modulation of tight junction properties relevant to fluid transport across rabbit corneal endothelium. Exp. Eye Res. 84, 790–798.

Martinsen, O.G., Grimnes, S., Haug, E., 1999. Measuring depth depends on frequency in electrical skin impedance measurements. Skin Res. Technol. 5, 179–181.

Prydal, J., Artal, P., Woon, H., Campbell, F., 1992. Study of human precorneal tear film thickness and structure using laser interferometry. Invest. Ophthalmol. Vis. Sci. 33, 2006–2011.

Prydal, J.I., Campbell, F.W., 1992. Study of precorneal tear film thickness and structure by interferometry and confocal microscopy. Invest. Ophthalmol. Vis. Sci. 33, 1996–2005.

Robillard, P.N., Poussart, D., 1979. Spatial Resolution of Four Electrode Array. IEEE Trans. Biomed. Eng. BME-26, 465–470.

Schwan, H.P., Ferris, C.D., 1968. Four-Electrode Null Techniques for Impedance Measurement with High Resolution. Rev. Sci. Instrum. 39, 481–485.

Uematsu, M., Kumagami, T., Kusano, M., Yamada, K., Mishima, K., Fujimura, K., Sasaki, H., Kitaoka, T., 2007. Acute Corneal Epithelial Change after Instillation of Benzalkonium Chloride Evaluated Using a Newly Developed in vivo Corneal Transepithelial Electric Resistance Measurement Method. Ophthalmic Res. 39, 308–314.

Yang, F., Patterson, R.P., 2008. A Simulation Study on the Effect of Thoracic Conductivity Inhomogeneities on Sensitivity Distributions. Ann. Biomed. Eng. 36, 762–768.

Zhuang, H., Zhou, X., Xu, J., 2010. A Novel Method for Pachymetry Mapping of Human Precorneal Tear Film Using Pentacam with Fluorescein. Invest. Ophthalmol. Vis. Sci. 51, 156–159.

Chapter 3

Rigid sensor for in vivo assessment of epithelium permeability

The aim of the study described in this chapter was to experimentally validate the numerical findings presented in the previous chapter. Therefore, an impedance sensor was developed which implements the proposed electrode configurations. Its capability to assess the corneal barrier function was evaluated by increasing the epithelial permeability of rabbits. Thus, a benzalkonium chloride (BAC) solution was instilled and its impact in the epithelium electrical properties was evaluated by performing *in vivo* and non-invasive impedance measurements. From the obtained results it can be concluded that the epithelium permeability may be evaluated through impedance measurements performed by four electrodes placed on the corneal surface.

Most of the contents of this chapter have been published in the following articles:

- A. Guimerà, G. Gabriel, M. Plata-Cordero, L. Montero, M.J. Maldonado, R. Villa *"A non-invasive method for an in vivo assessment of corneal epithelium permeability through tetrapolar impedance measurements"*. **Biosensors and Bioelectronics** (2012) 31:55–61. doi: 10.1016/j.bios.2011.09.039

- L. Montero, G. Gabriel, A. Guimerà, R. Villa, K.K. Gleason, S. Borrós *"Increasing biosensor response through hydrogel thin film deposition: Influence of hydrogel thickness"*. **Vacuum** (2012) 86:2102–2104. doi: 10.1016/j.vacuum.2012.06.002

3.1 Introduction

In order to experimentally validate the numerical findings shown in the previous chapter, the proposed electrode configurations were implemented in an impedance sensor. As mentioned, the corneal impedance measurement is to be performed by placing four electrodes on the corneal surface. The tetrapolar measurement method offers the advantage of minimizing, and ideally cancelling, the parasitic effects of the electrode-electrolyte interface impedances (Schwan and Ferris, 1968). Figure 3-1 shows the implemented electrode geometric relationships and the electrode configurations. In all configurations, the distance between inner electrodes was three times larger than the separation between the outer electrodes; this distance ratio is a compromise between the spatial resolution and signal-to-noise ratio (Robillard and Poussart, 1979; Ivorra et al., 2003). Thus, four different electrode configurations can be implemented using the 10 electrodes of the sensor, resulting in four different sensor widths.

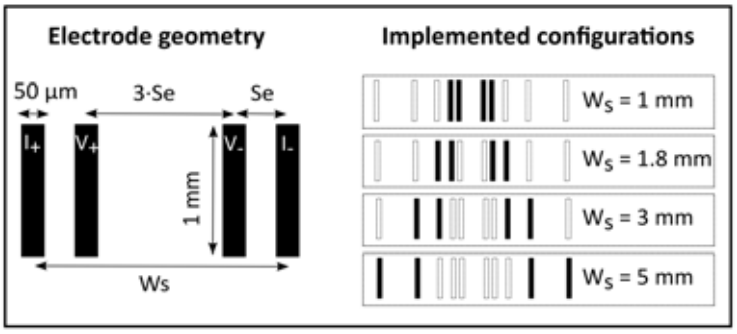

Figure 3-1 (Left) Schematic representation of the electrode geometry, where I+ and I- are the current carrying electrodes and V+ and V- are the voltage sensing electrodes. (Right) Schematic representation of the four electrode configurations implemented in function of the used electrodes (Black).

The impedance sensor has been fabricated based using Pyrex® as substrate. This substrate has been chosen for its transparency which allows the sensor to be properly located on the corneal surface. Since the Pyrex® substrate is not flexible the cornea must be flattened in order to ensure the proper electric contact between electrodes and corneal surface. Therefore, the impedance sensor has been attached to an applanation tonometer, which is used to apply a measured pressure (30 mmHg) on the corneal surface.

The capability of the proposed method to assess the epithelium permeability has been evaluated increasing the corneal epithelial permeability of rabbits by instilling a benzalkonium chloride (BAC) solution. BAC is one of the more common preservatives used in the formulation of ophthalmic medications in the present days, it is a quaternary ammonium compound whose antimicrobial activity arises from its ability to disrupt cell membranes and potentiate cell death. However, besides its antimicrobial activity, BAC is cytotoxic to the corneal tissues as it induces the loss of tight junctions between cells, which is directly related to the increase of the epithelium permeability (Swan, 1944; Baudouin et al., 2010; Chen et al., 2011). From the obtained results it can be concluded that the proposed method is able to discern the permeability increase produced by the installation of BAC solution (0.05%).

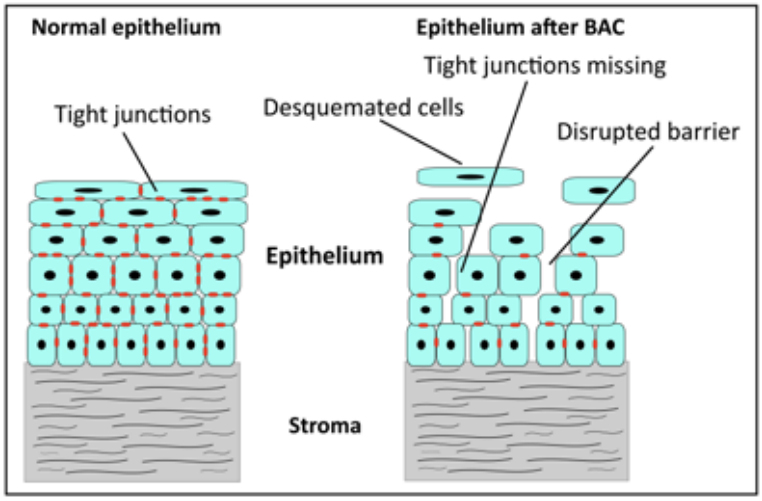

Figure 3-2 Schematic representation of how BAC breaks the epithelium barrier by inducing loss of cells and tight junctions. The increase in the extracellular spaces results in an increase of its conductivity and permeability.

3.2 Materials and methods

3.2.1 Sensor fabrication

As commented, the impedance sensor consists of 10 electrodes allowing four different electrode configurations depending on the chosen electrodes. Figure 3-1 shows the electrode geometric features of the impedance sensor. It was entirely fabricated in the clean room facilities at the Barcelona Microelectronics Institute (IMB-CNM) through standard photolithographic techniques using 500 µm thick Pyrex® 7740 wafers as the substrate material. As the process has been widely reported elsewhere (Heer et al., 2004; Hafizovic et al., 2007) it will not be described in detail. The main fabrication steps are depicted in Figure 3-3. Briefly, a photoresist was spin-coated and UV-exposed on a previously deposited Ni/Ti/Au layer (50/50/150 nm), defining the electrodes and their connection tracks (via wet-etching methods). Next, a passivation layer was deposited onto the wafer. For this layer, a SiO_2/Si_3N_4 (300/700 nm) layer was coated with plasma-enhanced chemical vapor deposition (CVD), and a second photolithographic step was used to etch the deposited layer into a pattern on the electrode area and connection pads.

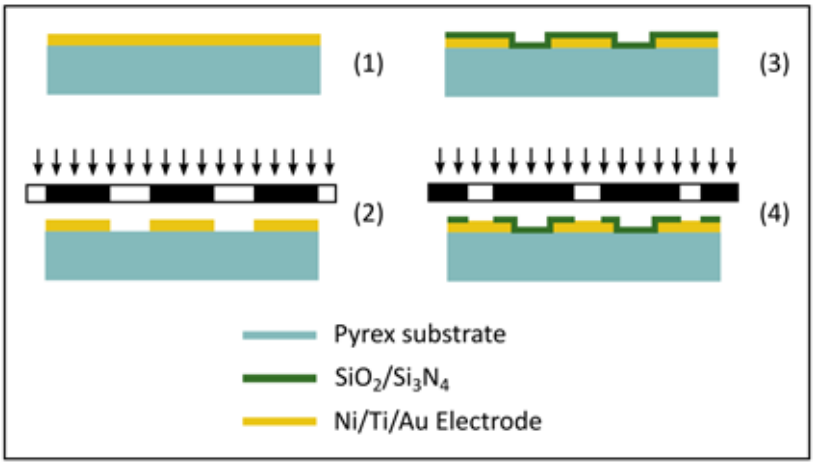

Figure 3-3 Schematic representation of the main fabrication processes. (1) Deposition of the Ni/Ti/Au layer (50/50/150 nm). (2) Etching of the Ti/Ni/Au layer to define the electrodes and connection tracks. (3) Deposition of SiO_2/Si_3N_4 layer used as passivation layer. (4) Etching the passivation layer on the electrodes and connection pads.

After the clean room processes, the wafer was sawed, then each impedance sensor was fixed on a Printed Circuit Board (PCB) and the connection PADs were connected to PCB tracks by wedge bonding. The packaging process ended with the covering of the PCB connection zone with an epoxy resin (Epo-Tek OG147-7) to waterproof the zone (Figure 3-4).

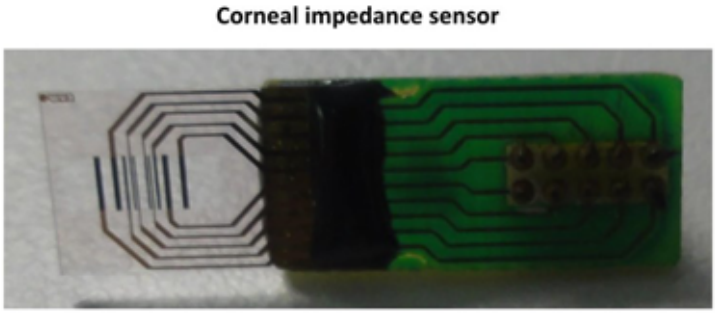

Figure 3-4 Image of the finished corneal impedance sensor.

3.2.1.1 Electrode modification with platinum black

The parasitic effects produced by the electrode–electrolyte impedance can be minimized using the previously described tetrapolar method. However, high impedance from the current-carrying electrodes leads to high common-mode voltage that must be rejected by the differential amplifier (Pallas-Areny and Webster, 1993). Furthermore, mismatched electrodes that are used to pick up voltage can introduce errors through a voltage drop by the polarization current in the differential amplifier (Hinton et al., 1998; Grimnes and Martinsen, 2007). To minimize these issues, a decrease in the electrode impedance is required. A well-known method for decreasing the impedance is to electrochemically coat the electrodes with a porous layer of platinum black (Marrese, 1987; Gabriel et al., 2007). Therefore, the fabricated gold electrodes were platinized using a customized process, wherein, after cleaning the electrode surface with ethanol, electroplating was performed simultaneously on the 10 electrodes in a platinum chloride solution (hydrochloric acid 0.1 M, 2.3% platinum (IV) chloride and 0.023% lead (IV) acetate 99%) at -0.2 V for 1 min. Figure 3-5 shows the electrodes before and after the platinum black deposition.

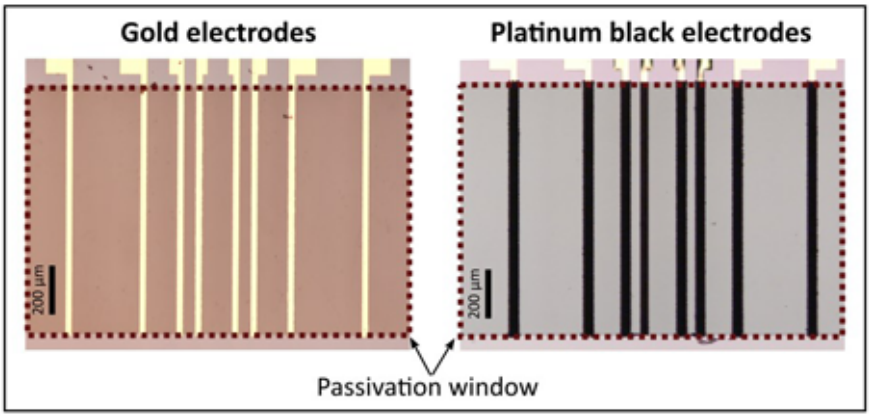

Figure 3-5 Images of the bare gold electrodes (left) and the electrodes with electrochemically deposited platinum black (right).

3.2.1.2 Electrode modification with pHEMA deposition

The resulting electrode–electrolyte impedance of the platinum black electroplated electrodes is low enough to reduce its parasitic effects in the impedance measurements.

However, the resulting surface is mechanically unstable, and the deposited material can become easily detached when it contacts with the tissue.

To improve the mechanical stability of the modified electrodes, an ultrathin film of hydrogel poly (hydroxyethyl methacrylate) (pHEMA) was deposited (Baxamusa et al., 2008). Figure 3-6 shows a schematic representation of the electrode modification applied processes. The pHEMA layer (100 nm) was deposited over the previously electrochemically deposited platinum black in order to reduce the platinum black detachment. Since this layer is permeable to ions its impact in the electrode-electrolyte impedance should be negligible. This development has been carried out in collaboration with Grup d'Enginyeria de Materials (GEMAT), Institut Químic de Sarrià.

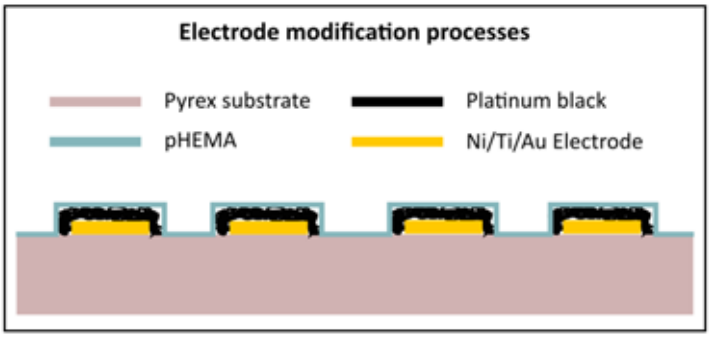

Figure 3-6 Schematic representation of the applied electrode surface modification processes.

Ultrathin films of pHEMA were deposited by initiated chemical vapor deposition (iCVD). For this process, a HEMA monomer (99 %) was used without additional purification. The liquid monomer was vaporized in a stainless steel jar, and its vapor was metered into the reactor. Likewise, the initiator TBPO (98%) was vaporized at room temperature and introduced into the reactor. The streams of both the monomer and the initiator were joined before entering the reactor, and their flow rates were regulated by needle valves, which were kept constant at 2 sccm for the monomer (HEMA) and 1 sccm for the initiator (TBPO). Once the streams reached the chamber reactor, polymerization occurred throughout the chamber. To initiate chemical vapor deposition, the reactor was equipped with a filament array, which provided thermal energy for the selective decomposition of molecules. In particular, the Nichrome filaments were resistively heated to 300 ºC.

3.2.1.3 Impedance sensor characterization

The electrode–electrolyte impedance has been measured in order to evaluate how it is affected by the electrode modification processes. The impedance sensor was immersed in a physiological saline solution (0.9 %wt. NaCl, resistivity at 298 K = 0.7 Ω m). Then, the electrode–electrolyte impedance was measured versus a platinum reference electrode (Radiometer Analytical) in the 100 Hz to 100 kHz frequency range using a custom made bipolar impedance analysis system (Guimera et al., 2008; Calderón et al., 2009), which allows the measurement of all electrodes at same time.

To evaluate the parasitic effects of the electrode–electrolyte interface on the measured impedance, tetrapolar impedance measurements were also performed using the same saline

solution. Analyzing these measurements, the frequency band where the parasitic effects of the electrode–electrolyte interface are minor will be determined. Thus, a custom-made tetrapolar impedance analysis system (Guimerà et al., 2009) was used to measure impedance spectroscopy from 100 Hz to 1 MHz. Moreover, to verify the stability of the electrodes, these measurements were performed before and after each series of *in vivo* experiments.

3.2.2 Experimental procedures

3.2.2.1 Experimental animals

The study was performed under the supervision of the University of Valladolid ethics committee and it conformed to the EU guidelines for handling and care of laboratory animals. For these experiments, a total of 10 New Zealand white rabbits that weighed between 2.5 and 3 kg were used. The rabbits were anaesthetized with an intramuscular injection of 50 mg/kg of ketamine (Imalgene 1000®, Merial) and 7 mg/kg of Xylazine (Rompun®, Bayer). Next, the animals were housed individually in cages, and their heads were stabilized to facilitate lateral access to the eyes, which simplifies the experimental processes and the impedance sensor application.

In each studied animal, one eye was used as control and damage was induced in the second one. Thus, the control group (CTR) and treated group (BAC) were each composed of 10 eyes. To avoid the influence of postural alterations, the control and treated eye were chosen alternately. For the treated group, damage was induced by applying one drop of BAC 0.05% solution (volume of each drop was approximately 50 µl) every minute over 5 minutes, for a total amount of 5 drops. In the control group, an innocuous physiological saline solution (0.9 %wt. NaCl) was applied using the same procedure.

After measuring impedance, each animal underwent a fluorescein test (Wilson et al., 1995; Mokhtarzadeh et al., 2011) in both eyes to macroscopically assess corneal damage. Thereafter, the animals were sacrificed by an intravenous injection of 200 mg/kg of pentobarbital sodium (Dolethal®, Vetoquinol) and their corneas were harvested.

3.2.2.2 Histopathology evaluation methods

To examine and evaluate the processed corneas, conventional optical microscopy was used. The corneal specimens were fixed in 10% neutral-buffered formalin (Panreac, Spain), and then paraffin was embedded. Multiple serial sections (3 µm) were stained with hematoxylin and eosin (H&E) and examined in an automated upright microscope (LEICA DM 4000 B, Leica, Germany). The images were recorded and processed using specific software (Leica Application Suite v.2.8.1, Leica, Germany).

The presence of the normal basal cell layer and the stratified layers in addition to the normal distribution and composition of the entire epithelium was evaluated. Similarly, the presence and integrity of the Bowman's membrane was also studied to observe the presence of scars on its surface. Finally, the microscope images were compared with the macroscopic

damage observed in the fluorescein tests, where defects in the corneal epithelium appear bright green upon illumination with blue cobalt light.

3.2.2.3 Impedance measurements.

Since the Pyrex® substrate of the impedance sensor is not flexible, the cornea must be flattened in order to ensure the proper electric contact between electrodes and corneal surface. Therefore, to perform the *in vivo* measurements, the sensor was attached to an applanation tonometer tip. The applanation tonometer is an instrument used in clinical practice to measure the intraocular pressure. In applanation tonometry, the intraocular pressure is inferred from the force required to flatten (applanate) a constant area (3 mm) of the cornea (Whitacre and Stein, 1993). In this study, the tonometer (AT 900®; Haag-Streit) was used to apply a measured pressure (30 mmHg) on the corneal surface in order to ensure the electric contact with the corneal surface.

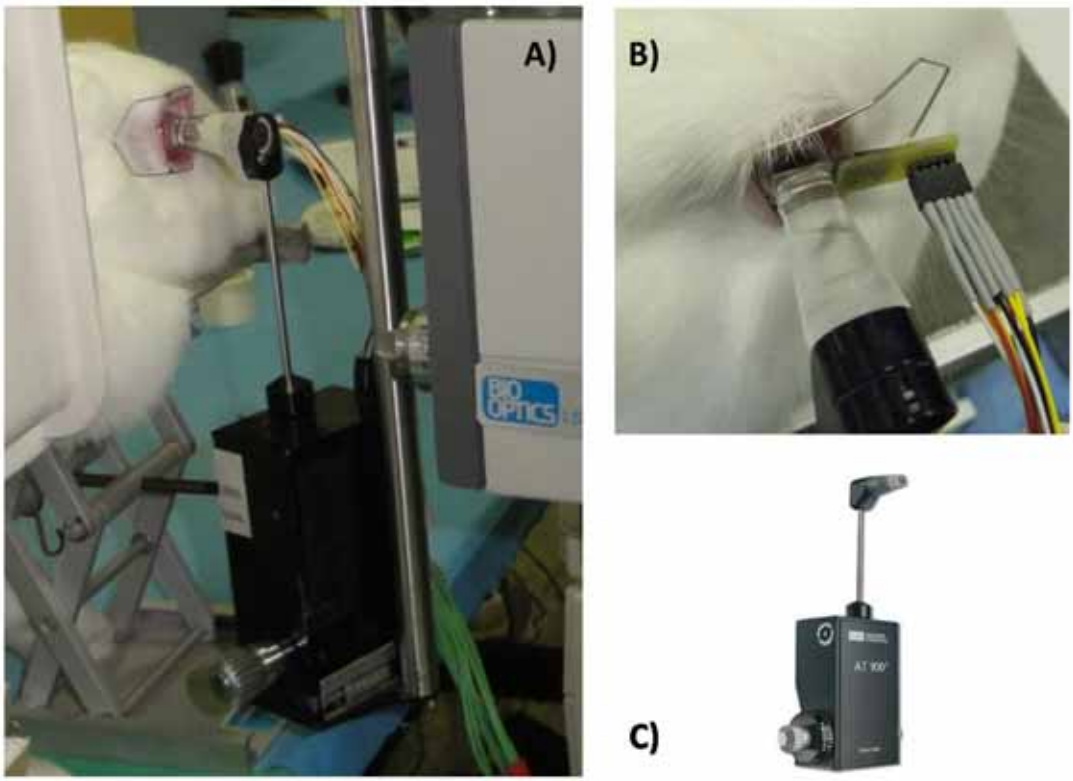

Figure 3-7 A) Image of the experimental setup, where it can be observed how the applanation tonometer was used to position the impedance sensor. B) Detail of impedance sensor placement on the corneal surface. C) Applanation tonometer Haag-Streit AT 900®.

The previously described custom-made tetrapolar impedance analysis system (Guimerà et al., 2009) was used to perform the impedance spectroscopy measurements. The design of this system made it possible to acquire 20 frequency points that ranged from 100 Hz to 1 MHz in just 10 seconds. Impedance measurements were always performed 10 minutes after application of the first drop to ensure damage stability. In order to evaluate the reproducibility of the measurement method, several impedance measurements were performed following a repetitive protocol. This procedure consisted of 3 repeated measurements without removing

the sensor followed by another 4 measurements in which the sensor was relocated before each new data acquisition. This relocation process, which consisted of removing the sensor, opening and closing the rabbit eyelid and then replacing the sensor, was intended to redistribute and homogenize the tear film and evaluate the impact of its thickness on the measurements.

3.3 Results and discussion

3.3.1 Impedance sensor characterization

The different electrode surface modification steps (platinum black, pHEMA) were first characterized by measuring the electrode–electrolyte impedance. The results are shown in Figure 3-8 where it should be noted that, as expected, deposition of the platinum black layer decreased the interface impedance (70 fold at 100 Hz) because the electrode roughness was increased; therefore, its surface area was increased maintaining its affective area. Moreover, the electrode–electrolyte impedance was slightly further decreased after the pHEMA was deposited. This is likely the result from increased hydration of the porous platinum black layer produced by the pHEMA film.

Results from the interface impedance measurements performed after each series of *in vivo* experiments showed only minor changes, which confirms the stability of the electrode modification processes (impedance was increased at 100 Hz < 25%, data not shown).

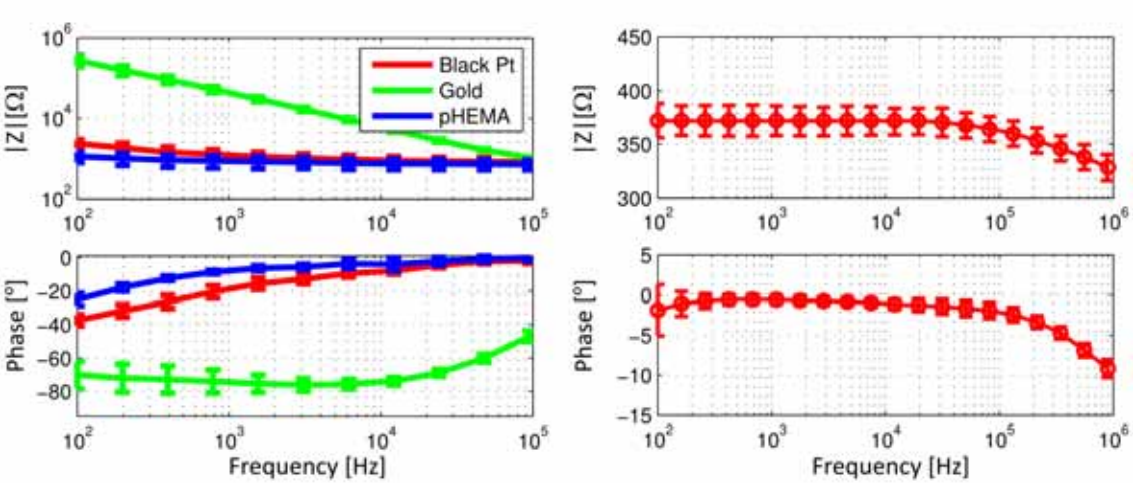

Figure 3-8 Results from the impedance sensor characterization: (Left) Electrode–electrolyte impedance modulus and phase shift measured in NaCl 0.9%wt. at different stages during the electrode modification; the bare gold electrode (dot line) after platinum black deposition (dashed line) and after pHEMA deposition (solid line). Results are expressed as mean ± standard deviation of 30 different electrodes. (Right) Bode representation of the measured impedance of a NaCl 0.9%wt. solution performed before each experimental usage (four-electrode measurement). Results are expressed as mean ± standard deviation of 20 different measurements.

Figure 3-8 shows the measured impedance (tetrapolar measurements) for a NaCl 0.9% wt. solution, performed before each experimental usage in order to ensure the correct behavior of the impedance sensor and the full measurement system. Ideally, in the analyzed frequency range , the measured impedance of a saline solution should be characterized by a flat modulus

and a phase shift of 0º for the entire spectrum (Grimnes and Martinsen, 2008). However, this expected behavior was not observed at frequencies greater than 300 kHz as the capacitive coupling of the wires has a strong influence on these measurements. Taking into account that these measurements were performed at different days, and therefore different solutions were used; the observed modulus deviation (lower than 5%) can be attributed to a small variations in the conductivity of the saline solution due to variations in the environmental conditions (i.e. temperature or saline solution concentration). Moreover, the deviation of the phase shift is greater in low frequency range since the influence of the electrode-electrolyte impedance is higher in this frequency range. Accordingly, from these results, it was concluded that the useful frequency band ranges from 100 Hz to 300 kHz.

3.3.2 Histopathology results

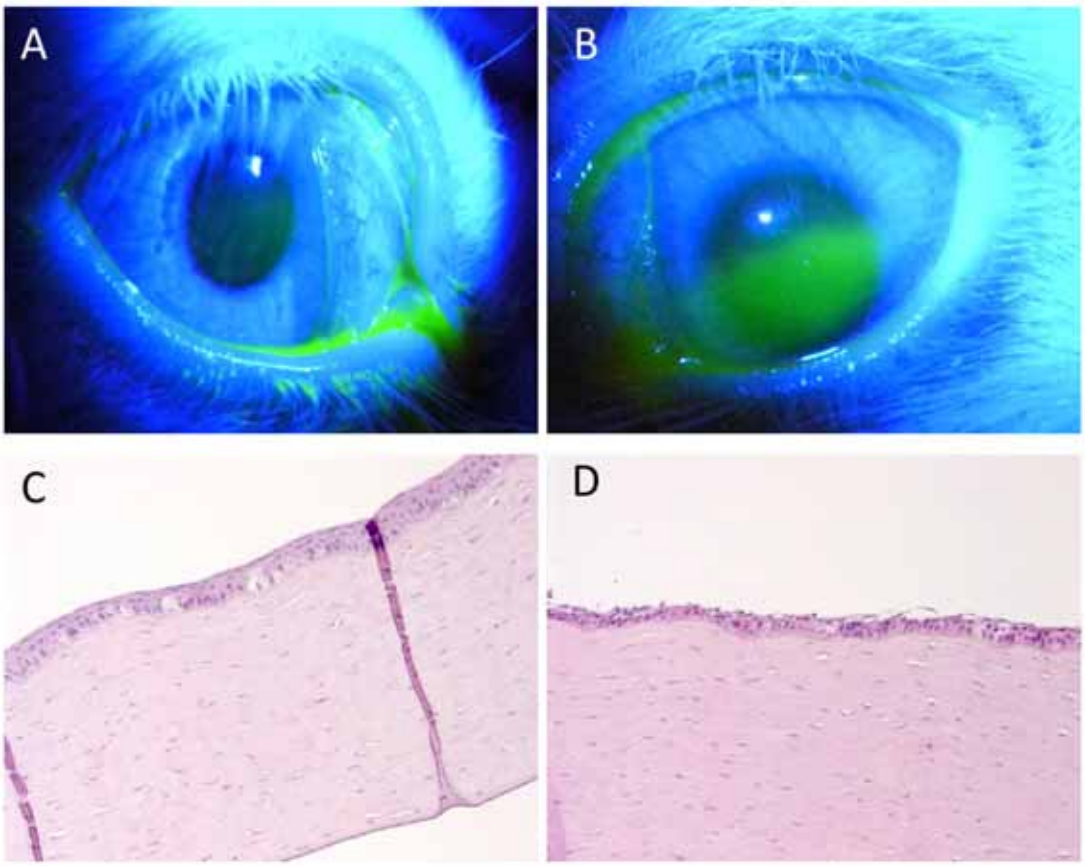

Figure 3-9 Images from the fluorescein test, wherein the corneal epithelial defects appear in bright green upon illumination by a blue cobalt light. (A) Image of a control eye; (B) image of an experimental eye. Optical microscopy images from a histopathological evaluation of a control (C) and an experimental epithelium (D).

Figure 3-9 shows different images of a rabbit's eyes and corneas after the experiments. The eye treated with saline solution (Figure 3-9A) showed no sign of macroscopic corneal damage: the cornea did not shine when it was stained with fluorescein. This was confirmed by observation of the corresponding non-keratinized squamous epithelium using optical microscopy (Figure 3-9C). In the image, a defined basal layer, several superficial layers and a normal Bowman's membrane along the entire cornea are easily distinguished.

On the other hand, the eye that was instilled with BAC (Figure 3-9B) showed a bright spot around the central cornea after it was stained with fluorescein, which revealed areas where the epithelium was damaged or partially absent. This was also observed by analyzing the same epithelium with an optical microscope (Figure 3-9D). Under the optical microscope, a partially non-cohesive epithelium and epithelial cell focal swelling, which primarily affect the basal layer, were observed.

3.3.3 Impedance measurement results

As reported, the impedance sensor was attached to an applanation tonometer in order to exert a controlled pressure when the sensor is placed on the corneal surface. Due to the corneal curvature, it is necessary to apply pressure in order to flatten the cornea and ensure a proper electric contact between the electrodes and the corneal surface. However, the application of an excessive pressure might result painful, and produce a compression of the ocular tissues that might affect their electrical properties. Therefore, and taking into account that the normal intraocular pressure is about of 13-15 mmHg (Sit, 2009)(values higher than 21 mmHg are considered pathological), it has been considered that the reasonable safety pressure should not exceed 30 mmHg. Thus, considering this limitation, a proper electric contact can only be achieved when the closest electrode configuration (W_S = 1 mm) is used. The measurements performed with the other configurations resulted in incongruous values and a high dispersion, which can be attributed to an unsuitable electric contact with the corneal surface during the measurement time (≈ 1 min). It is worth noting that it was found that the application of higher pressures did not ensure the electrical contact of the wider electrodes, since the pressure applied produces a rotation movement of the ocular globe, also resulting in non-proper electrical contact. Consequently, only the measurements acquired using the closest configuration are analyzed and reported. Besides this, the variation in the tear film thickness also produces errors in the measurements as demonstrated in the previous chapter. Here, the tear film between the sensor and the corneal surface may not be constant along the sensor due to the corneal curvature.

Figure 3-10 shows the impedance measurements for the control group and the treated BAC group. As predicted by the simulations performed in the previous chapter, an increase in the epithelium permeability produces a decrease in both phase shift and modulus, and this decrease is more notable at frequencies bellow 10 kHz. It is widely accepted that BAC instillation produces a loss in cohesion for the epithelial structure and a loss of tight junctions between the cells (Furrer et al., 2002; Chen et al., 2011, 2012). Thus, these alterations directly affect the electrical properties of the corneal epithelium and increase its electrical conductivity, as the current can pass through the extracellular gaps that are induced. Likewise, a decrease in the phase shift was also observed, as more current can pass through the extracellular spaces and reduce the capacitive effect produced by the cell membranes.

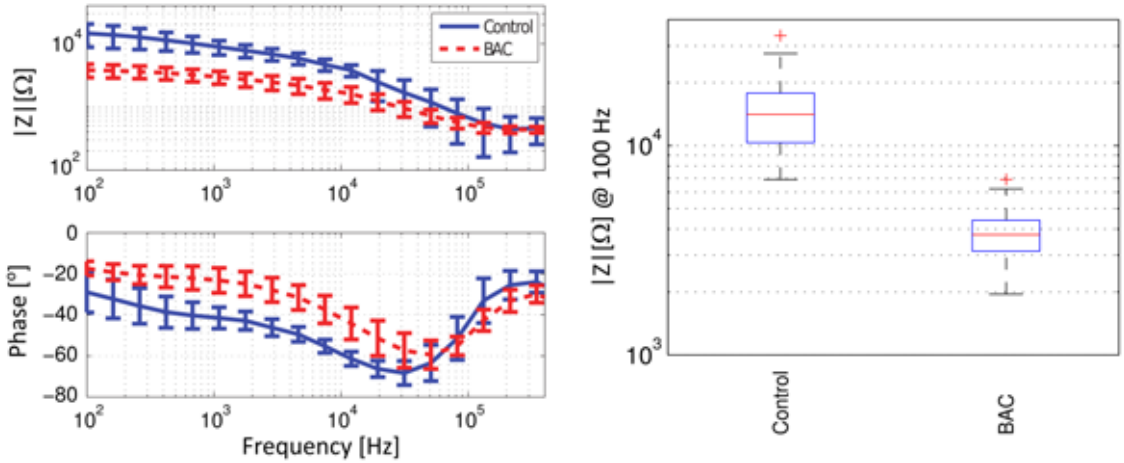

Figure 3-10 (left) Experimental impedance measurements for a control group (blue solid line) and a BAC group (red dashed line). Results are expressed as mean ± standard deviation (n=70). (b) Impedance modulus measured at 100 Hz; the boxplot representation shows the mean value, the dispersion of the measurements grouped by quartiles (boxes and bars) and the outlier values (as crosses) for the control group (n=70) and the group treated with BAC (n=70)

To analyze the resolution of this method, the impedance modulus at 100 Hz was used as an indicator of epithelial permeability. Figure 3-10 shows the results in a Boxplot representation for the control and BAC groups. The three-fold difference between the mean values for both groups (14 kΩ ± 5.8 kΩ against 3.8 kΩ ± 0.92 kΩ) would indicate that the impedance could provide high resolution damage assessment. However, this potential for resolution (i.e. capability to discern damage level) would be compromised by the large dispersion observed in the measurements. This dispersion can be explained by the variation in the tear-film thickness between each sensor application because the high conductivity of the tear film contrasts with the low conductivity of the epithelium, which facilitates the current movement through the tear film. As demonstrated in the previous chapter, a variation in the tear-film thickness (from 10 µm to 15 µm) produces a similar variation in the measured impedance. In addition, the simulated contribution from each layer to the total impedance measured showed a substantial contribution from the tear film at frequencies below 10 kHz.

It is difficult to compare the obtained results with previously reported studies of *in vivo* or *in vitro* permeability measurements because those have been performed using different experimental protocols and measurement methods. Previous studies have been based on TER measurements, using two electrodes placed on each corneal side, and the measurements values were reported in Ωcm^2. The use of Ωcm^2 allows the comparison of measurements performed with different methods with different cell constants. To perform the conversion from the measured impedance [Ω] to [Ωcm^2] is necessary to know the measured corneal area. In the case of previously reported *in vivo* TER measurements, this conversion is possible because the corneal area measured has been delimited with an isolating ring which is filled with saline solution and also contains the electrode (Uematsu et al., 2007). However, in the case of the method proposed in this dissertation, it is difficult to determine the measured area since it depends on the electrical properties of the corneal epithelium, decreasing with the decrease of the epithelium conductivity. Therefore, performing this conversion can induce errors, especially in the case of non-homogeneity electrical properties along the cornea, which

can be associated to different grades of damage in different corneal zones. Nevertheless, even taking into account the above considerations which limit the validity of comparisons between results reported here and in previous studies, it is worth mentioning that Uematsu et al. reported a decrease of around 80% of the initial value when a BAC concentration of 0.05% was instilled which would be in accordance with the decrease of around 75% observed here.

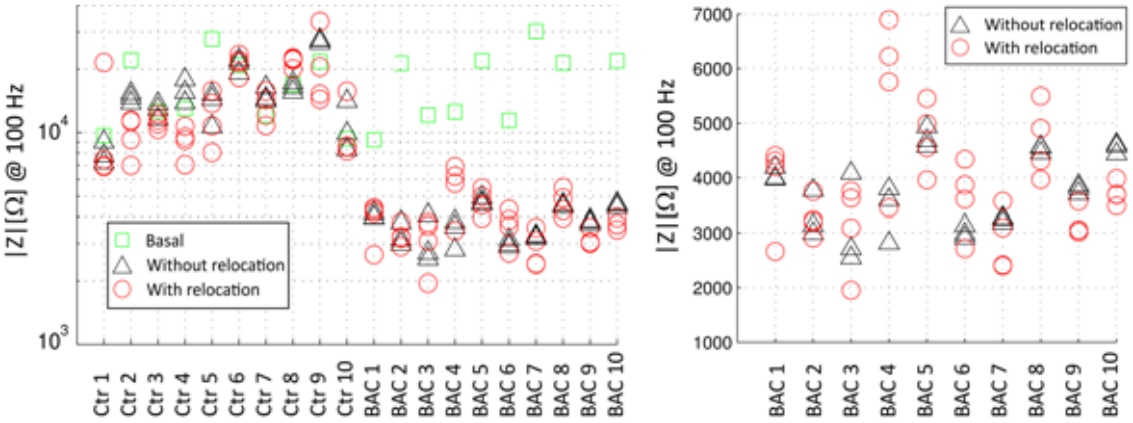

Figure 3-11 Impedance modulus measured at 100 Hz. (green squares) basal measurement, (black triangles) three repeated measurements performed without the relocating process and (red circle) four repeated measurements performed with the relocating process.

To assess the effect of the tear film on the measured impedance, several repeated measurements were performed. A total of seven measurements were performed in each eye after the treatment application; three measurements did not include a relocating process (explained in the experimental section), and the other four did use this process. The results from these experiments are shown in Figure 3-11, where the impedance modulus measured at 100 Hz is shown for each measurement. Within the dispersion shown, it can be assumed that the dispersion observed in the measurements performed without the relocation process was primarily due to the electronic equipment. On the other hand, the dispersion in the measurements performed with the relocation process was primarily associated with the small variations in the tear-film thickness produced by the eyelid action. From the results summarized in Table 3-1, it can be observed that the measurements performed without the relocating process have a lower dispersion than the measurements performed with this process. However, as can be observed in Figure 3-11, the deviation in the case of measurements performed without relocation process is also important, especially in the measurements BAC2 BAC3 and BAC4 where a higher deviation can be observed. This fact points out that other factors may affect the measurement. Thus, it can be considered that the tear film is redistributed during the sensor application as a consequence of the applied pressure. Then, variations in the tear film thickness between the sensor and the corneal surface during the measurement are produced. Besides, it can also be considered non proper electric contact along the electrode length due to the corneal curvature, inducing changes in the measured area, and consequently in the measured impedance. In addition, and as commented in the previous chapter, the larger conductivity difference between the tear film, the epithelium and the stroma produces a two current path phenomenon, magnifying the effect of the commented issues in the measured impedance (Grimnes and Martinsen, 2007).

Summarizing, the amount of the commented aspects limits the final resolution of the proposed method for detecting small alterations in the epithelium permeability. Nevertheless, the precision of the proposed method is enough to detect the alterations in the epithelium permeability produced by the instillation of BAC solution (0.05%). Thus, it can be concluded that the proposed approximation to perform non-invasive assessment of the corneal barrier function is feasible.

Table 3-1 Impedance modulus measured at 100 Hz for each data group as mean and standard deviation, and average for standard deviation for the measurements performed with and without relocation process.

		Without relocation	***With relocation***
Group	*Mean ± Std [kΩ]*	*Average deviation [kΩ]*	*Average deviation [kΩ]*
Basal	18.41 ± 8,08	--	--
Control	14.66 ± 5,83	1.42	2.67
BAC	3.82 ± 0,92	0.24	0.37

3.4 Conclusions

In this chapter an impedance sensor based on the numerical study performed in the previous chapter was presented. It was attached to an applanation tonometer in order to flatten the corneal curvature and ensure the electric contact between the electrodes and the corneal surface. Nevertheless, the applied pressure is not enough to make a proper contact with all the implemented electrode configurations and the electric contact can only be achieved with the thinnest configuration.

Impedance measurements performed with four electrodes placed on the cornea surface were sensitive enough to detect variations in the epithelium permeability after the cornea was damaged with a BAC solution. It was also observed that the impedance measurements were influenced by the tear-film thickness. However, the variation produced by the epithelial permeability is much higher than the variation from fluctuations in the tear-film thickness. In addition, the three-fold difference between the mean values for both groups would suggest that the presented method could provide high resolution damage assessment. Consequently, it can be concluded that the feasibility of a non-invasive method for assessing epithelial layer functionality.

3.5 References

Baudouin, C., Labbé, A., Liang, H., Pauly, A., Brignole-Baudouin, F., 2010. Preservatives in eyedrops: The good, the bad and the ugly. Prog. Retin. Eye Res. 29, 312–334.

Baxamusa, S.H., Montero, L., Dubach, J.M., Clark, H.A., Borros, S., Gleason, K.K., 2008. Protection of Sensors for Biological Applications by Photoinitiated Chemical Vapor Deposition of Hydrogel Thin Films. Biomacromolecules 9, 2857–2862.

Calderón, E., Melero, A., Guimerà, A., 2009. Portable Device for Microelectrode Array Bio-impedance Measurements, in: Dössel, O., Schlegel, W.C. (Eds.), World Congress on Medical Physics and

Biomedical Engineering, September 7 - 12, 2009, Munich, Germany, IFMBE Proceedings. Springer, pp. 883–886.

Chen, W., Hu, J., Zhang, Z., Chen, L., Xie, H., Dong, N., Chen, Y., Liu, Z., 2012. Localization and Expression of Zonula Occludins-1 in the Rabbit Corneal Epithelium following Exposure to Benzalkonium Chloride. PLoS ONE 7, e40893.

Chen, W., Li, Z., Hu, J., Zhang, Z., Chen, L., Chen, Y., Liu, Z., 2011. Corneal Alternations Induced by Topical Application of Benzalkonium Chloride in Rabbit. PLoS One 6.

Furrer, P., Mayer, J.M., Gurny, R., 2002. Ocular tolerance of preservatives and alternatives. Eur. J. Pharm. Biopharm. 53, 263–280.

Gabriel, G., Erill, I., Caro, J., Gómez, R., Riera, D., Villa, R., Godignon, P., 2007. Manufacturing and full characterization of silicon carbide-based multi-sensor micro-probes for biomedical applications. Microelectron. J. 38, 406–415.

Grimnes, S., Martinsen, Ø.G., 2007. Sources of error in tetrapolar impedance measurements on biomaterials and other ionic conductors. J. Phys. Appl. Phys. 40, 9–14.

Grimnes, S., Martinsen, Ø.G., 2008. Bioimpedance and bioelectricity basics. Academic Press, New York.

Guimera, A., Calderon, E., Los, P., Christie, A.M., 2008. Method and device for bio-impedance measurement with hard-tissue applications. Physiol. Meas. 29, S279–S290.

Guimerà, A., Gabriel, G., Parramon, D., Calderón, E., Villa, R., 2009. Portable 4 Wire Bioimpedance Meter with Bluetooth Link, in: Dössel, O., Schlegel, W.C. (Eds.), World Congress on Medical Physics and Biomedical Engineering, September 7 - 12, 2009, Munich, Germany, IFMBE Proceedings. Springer, pp. 868–871.

Hafizovic, S., Heer, F., Ugniwenko, T., Frey, U., Blau, A., Ziegler, C., Hierlemann, A., 2007. A CMOS-based microelectrode array for interaction with neuronal cultures. J. Neurosci. Methods 164, 93–106.

Heer, F., Franks, W., Blau, A., Taschini, S., Ziegler, C., Hierlemann, A., Baltes, H., 2004. CMOS microelectrode array for the monitoring of electrogenic cells. Biosens. Bioelectron. 20, 358–366.

Hinton, A., Sayers, B., Solartron, V.R., 1998. Advanced Instrumentation for Bioimpedance Measurements. G. E. N. 1260, 1250–1253.

Ivorra, A., Gómez, R., Noguera, N., Villa, R., Sola, A., Palacios, L., Hotter, G., Aguiló, J., 2003. Minimally invasive silicon probe for electrical impedance measurements in small animals. Biosens. Bioelectron. 19, 391–399.

Marrese, C.A., 1987. Preparation of strongly adherent platinum black coatings. Anal. Chem. 59, 217–218.

Mokhtarzadeh, M., Casey, R., Glasgow, B.J., 2011. Fluorescein punctate staining traced to superficial corneal epithelial cells by impression cytology and confocal microscopy. Invest. Ophthalmol. Vis. Sci. 52, 2127–2135.

Pallas-Areny, R., Webster, J.G., 1993. AC instrumentation amplifier for bioimpedance measurements. IEEE Trans. Biomed. Eng. 40, 830–833.

Robillard, P.N., Poussart, D., 1979. Spatial Resolution of Four Electrode Array. IEEE Trans. Biomed. Eng. BME-26, 465–470.

Schwan, H.P., Ferris, C.D., 1968. Four-Electrode Null Techniques for Impedance Measurement with High Resolution. Rev. Sci. Instrum. 39, 481–485.

Sit, A.J., 2009. Continuous Monitoring of Intraocular Pressure. J. Glaucoma 18, 272–279.

Swan, K.C., 1944. Reactivity of the ocular tissues to wetting agents. Am J Ophthalmol 27, 1118–1122.

Uematsu, M., Kumagami, T., Kusano, M., Yamada, K., Mishima, K., Fujimura, K., Sasaki, H., Kitaoka, T., 2007. Acute Corneal Epithelial Change after Instillation of Benzalkonium Chloride Evaluated Using a

Newly Developed in vivo Corneal Transepithelial Electric Resistance Measurement Method. Ophthalmic Res. 39, 308–314.

Whitacre, M.M., Stein, R., 1993. Sources of error with use of Goldmann-type tonometers. Surv. Ophthalmol. 38, 1–30.

Wilson, G., Ren, H., Laurent, J., 1995. Corneal epithelial fluorescein staining. J. Am. Optom. Assoc. 66, 435–441.

Chapter 4

Flexible sensor for epithelium permeability assessment

The impedance sensor presented in the previous chapter was fabricated using a rigid Pyrex® substrate. Thus, to ensure a proper electrical contact between the electrodes and the corneal surface a reasonable pressure must be applied. To overcome these limitations, in this chapter, a flexible impedance sensor is presented. Therefore, the usability and performance of the proposed method is increased since no pressure is needed to place the sensor on the corneal surface. Its feasibility has been evaluated *in vivo* by two experimental procedures. In the first one, different concentrations of benzalkonium chloride (BAC) solution were instilled on rabbit corneas. In the second procedure, the corneal epithelium wound-healing process was monitored. Finally, in both experimental protocols, the impedance measurements have been compared with measurements of the permeability to sodium fluorescein. From the obtained results, it has been found that the imaginary part of the impedance measured at 2 kHz is the parameter with the best reliability to assess the epithelium permeability. Moreover, the electrode configuration of 5 mm width presents the best resolution to assess the lower variations in the corneal epithelium permeability.

Most of the contents of this chapter have been published in the following articles:

- A. Guimera, X. Illa, E. Traver, S. Marchan, C. Herrero, C. Lagunas, M.J. Maldonado, A. Ivorra, R. Villa *"In vivo assessment of corneal barrier function through non-invasive impedance measurements using a flexible probe"*. **Journal of Physics: Conference Series** (2013) 434:012072. doi: 10.1088/1742-6596/434/1/012072

- A. Guimerà, X. Illa, E. Traver, M. Plata-Cordero, J. Yeste, C. Herrero, C. Lagunas, M.J. Maldonado, R. Villa "*Flexible probe for in vivo quantification of corneal epithelium permeability through non-invasive tetrapolar impedance measurements"*. **Biomedical Microdevices** (2013) 15:849–858. doi: 10.1007/s10544-013-9772-x

4.1 Introduction

The impedance sensor presented in the previous chapter was fabricated using a rigid Pyrex® substrate. To ensure a proper electrical contact between the electrodes and the corneal surface a reasonable pressure must be applied in order to flatten the corneal curvature. This fact constitutes its main limitation since the electrical contact cannot be ensured for the widest electrode configurations. Consequently, only the feasibility of the closest configuration (1 mm width) can be evaluated using the rigid sensor.

To overcome these limitations, in this chapter, a flexible impedance sensor is presented. It is based on SU-8, a well-known negative photoresist (Lorenz et al., 1997; Keller et al., 2008). The SU-8 has been chosen in preference to other possible polymeric substrates such as Polyamide or Cyclo-olefin Polymer (COP) because it can be easily implemented in the IMB clean room. The use of a polymeric substrate allows the increase of the usability and performance of the proposed method. Thus, the main weaknesses of the previous rigid probe will be overcome as no pressure is needed to ensure a proper electrical contact. Moreover, the flexible sensing device allows the use of wider electrode configurations, which is expected to results in an improvement in sensitivity. Figure 4-1 shows a comparison between the application of the flexible and rigid sensor. As represented in the sketch, it is expected that with the use of the flexible sensor the distribution of the tear film between the sensor and the corneal surface will be constant along the sensor width.

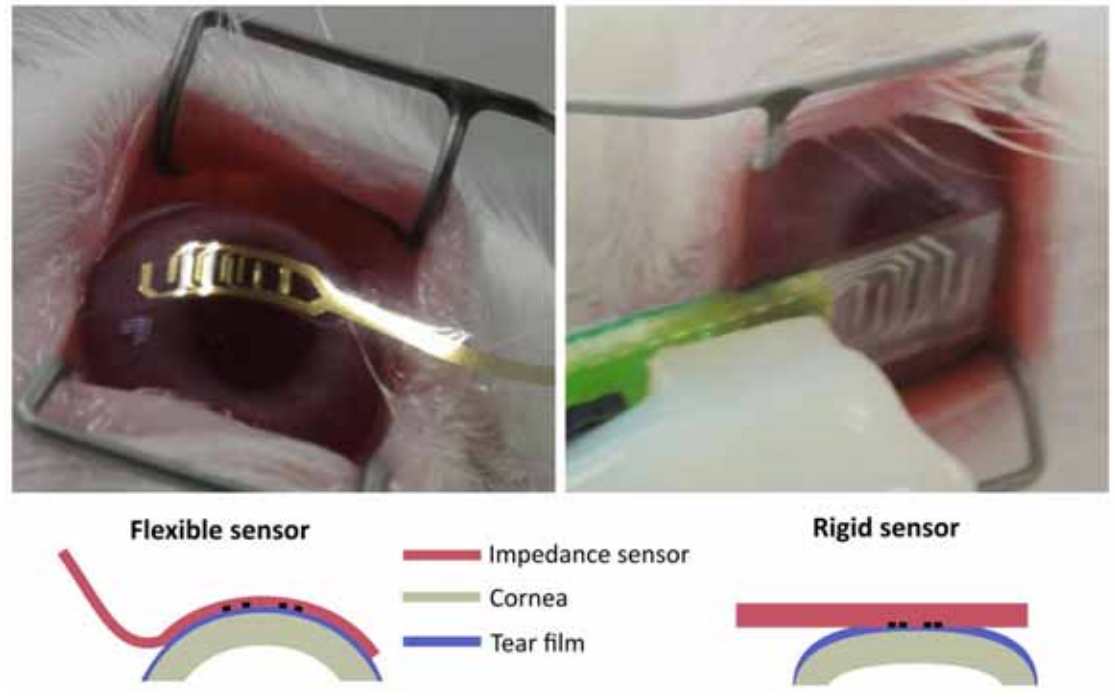

Figure 4-1 Image and sketch representation of how the impedance sensor is applied. It is interesting to note that the tear film distribution should be more homogeneous in the case of the flexible sensor.

Figure 4-2 depicts the geometrical dimensions of the impedance sensor. As in the case of the previous one, it consists of 10 electrodes that allow the implementation of 4 different

electrode configurations depending on the electrodes selected to perform the measurement. Since the sensor must be attached to the cornea by means of the surface tension of the tear film, the sensor is extended 2.6 mm beyond the last electrode in order to improve its electrical contact and ensure a constant tear film thickness along the sensor. In addition, taking advantage of the sensor's flexibility, the impedance sensor can be manually located on the corneal surface, avoiding the use of an applanation tonometer. This simplifies the experimental protocol and improves the usability of the sensor. Furthermore, the electrode width has been increased in relation to the previous rigid sensor in order to reduce the electrode-electrolyte impedance, especially in the case the most widely spaced electrodes since there is more free area.

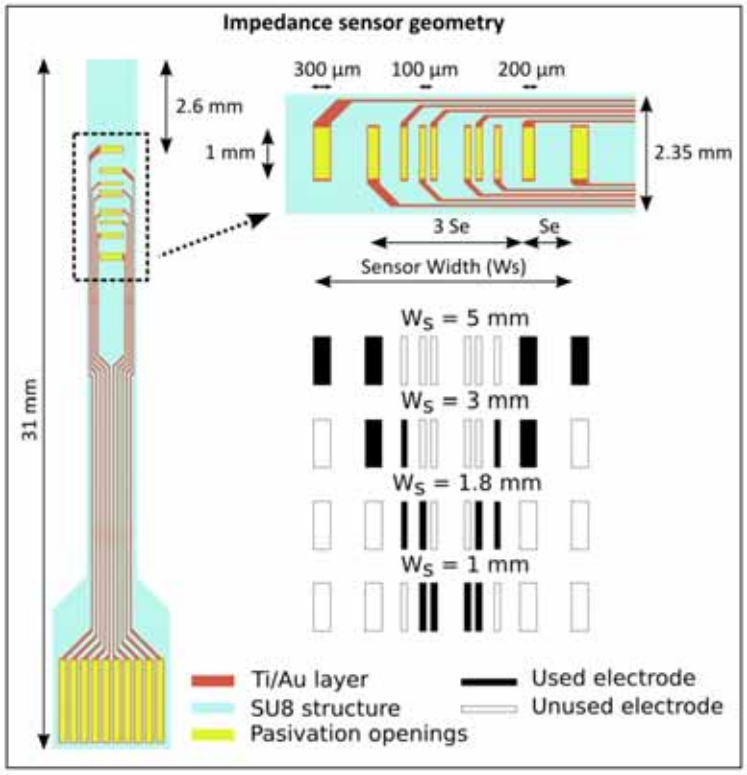

Figure 4-2 Layout and schematic description of the geometrical dimensions of the impedance sensor.

The feasibility of the corneal impedance sensor presented has been evaluated *in vivo* by two experimental procedures. In the first one, different concentrations of benzalkonium chloride (BAC) solution were instilled on rabbit corneas. This strategy produces different increases in the corneal epithelial permeability, which enables the discrimination of different degrees of corneal insult. In the second procedure, the corneal epithelium wound-healing process was monitored by performing impedance measurements at different times of the healing evolution. The non-invasiveness of the proposed method allows the monitoring of the process in the same eye for a sustained period of time. Moreover, the accurate assessment of the wound-healing process is of special interest for developing drugs for its treatment. These drugs are often used in the treatment of injuries produced by the LASIK (Laser-Assisted in situ keratomileusis) surgery (Jl et al., 1999; Dupps Jr. and Wilson, 2006) or the dry eye syndrome (Burgalassi et al., 2000; Versura et al., 2013). Finally, in both experimental protocols, the impedance measurements performed with the impedance sensor have been compared with

measurements of the permeability to sodium fluorescein. Since this measurement is directly related to epithelium permeability it can be used as a comparative method to evaluate the degree of the corneal insult (Chen et al., 2011, 2012).

4.2 Materials and methods

4.2.1 Impedance sensor

4.2.1.1 Sensor fabrication

The impedance sensor was entirely fabricated in the clean room facilities at the Barcelona Microelectronics Institute (IMB-CNM). Figure 4-3 shows a schematic representation of the main steps of the fabrication process. Thus, the fabrication of the flexible SU-8 impedance sensor starts with a thermal oxidation of a 4-inch silicon wafer. 400 nm of SiO_2 were grown to serve as a sacrificial layer for the final release of the devices. Then, the wafer was heated up to 200 ºC in a hotplate in order to enhance the adhesion of the silicon oxide to the SU-8 negative photoresist (2025, Microchem, USA) which was poured over the wafer. To obtain a 25 µm thick structural layer, the wafer was spin coated and baked at 65 ºC for 3 min and at 95 ºC for 20 min. UV-exposure was made through the mask where the device structure is defined using a dose of 140 mJ/cm^2. After the exposure, the wafer was heated up to 65 ºC for 1 min, ramped up to 95 ºC, baked at this temperature for 8 min and cooled down on the hotplate to ambient temperature. Afterwards, the wafer was developed in a propylene glycol methyl ether acetate (PGMEA)-based (mr Dev-600) bath for 3 min, rinsed with isopropyl alcohol (IPA) and dried with a N_2 gun. A hard bake at 120 ºC for 20 min in a hotplate was also applied to the wafer in order to finalize the photolithographic process.

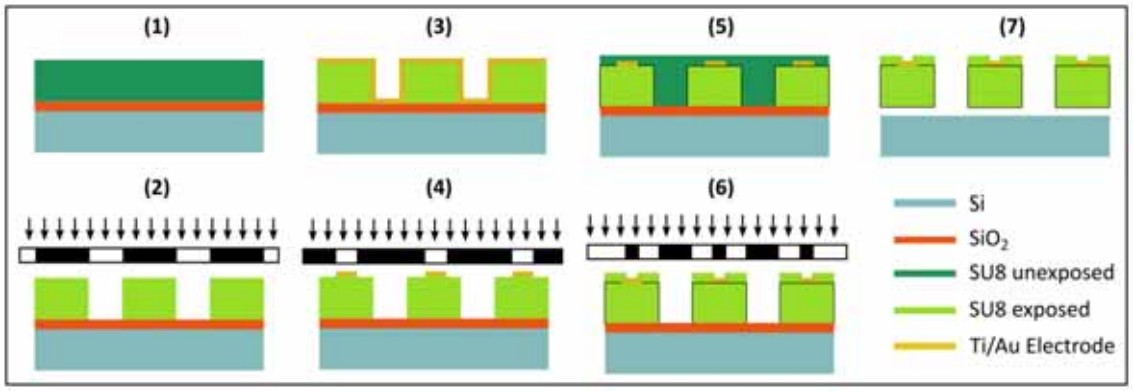

Figure 4-3 Schematic representation of the main fabrication processes. (1-2) Deposition and etching the structural SU-8 layer (20 µm). (3-4) Deposition and etching Ti/Au layer (20 nm / 100 nm) to define the electrodes and connection tracks. (5-6) Deposition and etching the passivation SU-8 layer (1 µm). (4) Etching the SIO2 sacrificial layer to release the final structures.

Evaporation of 20 nm of titanium (that acts as an adhesion layer) and 200 nm of gold were subsequently performed using an electron beam gun in a Univex 450B coating system (Oerlikon Leybold, Germany). However, before evaporation, a low-power oxygen plasma etching was applied to the wafer to improve metal adhesion to the SU-8 surface (Vilares et al.,

2010). Afterwards, patterning of the metal layer was performed by using a standard photolithography process and different selective wet chemical etchings.

In order to define the electrodes and connecting pads while insulating the metal tracks, a thin SU-8 layer (1 µm) was processed on top of the wafer. For that, firstly, the wafer was exposed again to low-power oxygen plasma to promote the adhesion between SU-8 layers. Then, SU-8 2005 was spin-coated and baked at 65ºC for 2 min and at 95 ºC for 10 min. The minimum thickness of this layer only required a UV-exposure with a dose of 80 mJ/cm^2 followed by a post-exposure baking made at 65 ºC for 1 min and ramped up to 95 ºC where the wafer was baked for 3 min. After being cooled down the wafer was developed in a PGMEA-based bath for 45 s, rinsed and dried as it had been done before. Again a hard bake at 120ºC for 20 min in a hotplate was also performed.

Finally, the whole wafer was immersed in a HF-based bath to etch the SiO_2 sacrificial layer, releasing the SU-8 flexible sensing devices. To facilitate the use of the corneal sensing devices, they were directly connected to a printed circuit board (PCB) by means of zero insertion force (ZIF) connectors. For that, the connecting pads of the sensing device were designed to match the specifications of a 10-channel ZIF connector. With this ready-to-use connector, no further encapsulation process was needed, resulting in valuable time and cost-savings. Figure 4-4 shows the impedance sensor ready to be used. As can be observed, the PCB was protected with an epoxy resin (Epo-Tek OG147-7) in order to waterproof the zone and facilitate the sensor manipulation.

4.2.1.2 Electrode modification with platinum black

Figure 4-4 (Left) Optical microscope image of a bare gold electrode just after the fabrication process and after being electrochemically coated with platinum black. (Right) Image of the packaged impedance sensor ready to be used.

As it is well-known, the use of the tetrapolar method minimizes the parasitic effects produced by the electrode-electrolyte interface impedance. However, problems when using high impedance electrodes appear due to the voltage drop produced by the polarization currents. To avoid this issue, a reduction of the electrode impedance is strictly neecessary. For this, among the different methods described in the literature, electrochemically coating of the electrodes with a porous layer of platinum black (Marrese, 1987; Ivorra et al., 2003) has been chosen because of its versatility, quickness and easy implementation in our laboratory. Therefore, a customized process to simultaneously platinize the ten gold electrodes of

individual devices was carried out by a 30 seconds electroplating in a platinum chloride solution (hydrochloric acid 0.1 M, 2.3% platinum (IV) chloride and 0.023% lead (IV) acetate 99%) at -0.2 V. The result of this coating is shown in Figure 4-4, where a bare gold electrode is shown together with an electrochemically coated with platinum black electrode.

4.2.1.3 Impedance sensor characterization

As in the previous chapter, in order to characterize the electrode-electrolyte interface impedance, a home-made impedance analysis system (Guimera et al., 2008; Calderón et al., 2009) was used. For that, the impedance sensor was immersed in a physiological saline solution (0.9%wt. NaCl, resistivity at 298 K = 71.3 Ωcm) where the electrode impedance was measured versus a platinum reference electrode (Radiometer Analytical) within the 100 Hz to 100 kHz frequency range.

To evaluate the parasitic effects of the electrode–electrolyte interface on the measured impedance, tetrapolar impedance measurements were also performed using the same saline solution. Analyzing these measurements, the frequency band where the parasitic effects of the electrode–electrolyte interface are minor will be determined. Thus, a custom-made tetrapolar impedance analysis system (Guimerà et al., 2009) was used to measure impedance spectroscopy from 100 Hz to 1 MHz. Moreover, to verify the stability of the electrodes, these measurements were performed before and after each series of *in vivo* experiments.

4.2.2 Experimental procedures

The ability of the proposed sensor to assess the corneal epithelium permeability was evaluated by using two different methods, both based on increasing the permeability of rabbit's corneal epithelium. The first one consists on the topical instillation of BAC at different concentrations, while the second one is based on the monitoring of a wound-healing process of the corneal epithelium. To verify the obtained results, the impedance measurements were compared with the measurements of epithelium permeability to sodium fluorescein. Moreover, all experimental procedures were conducted under the supervision of the University of Valladolid ethics committee, conformed to the EU guidelines for handling and care of laboratory animals and following the guidelines of the ARVO Statement for the use of animals in ophthalmic and vision research.

4.2.2.1 Increase of corneal epithelium permeability by topical BAC application

A total of 50 New Zealand white rabbits weighing between 2.5 and 3 kg were used for these experiments. The rabbits were anaesthetized with a single intramuscular injection of 50 mg/kg of ketamine (Imalgene 1000®, Merial) plus 7 mg/kg of Xilacine (Rompun®, Bayer). In each studied animal, one eye was used as control while the damage was induced in the other one (treated eye). Thus, both the control (S) and treated (B_x) group were composed of 50 eyes. Moreover, and to avoid the influence of postural alterations, the treated eye was chosen alternately. The insult induced in the treated eyes was accomplished by applying one drop (approximately 50 µl) of BAC solution every minute for 5 minutes up to a total of 5 drops. The

treated group was divided in 5 subgroups composed by 10 eyes. For each subgroup a different BAC solution concentration was used (B_1: BAC at 0.01%, B_2: BAC at 0.02%, B_3: BAC at 0.05%, B_4: BAC at 0.1% and B_5: BAC at 0.2%). Furthermore, in the control group an innocuous NaCl 0.9%wt. solution was applied using the same protocol. This protocol allows the induction of different grades of insult, which is helpfully to study the resolution of the method proposed. Moreover, impedance measurements were carried out at three different times; the first one was performed before the treatment (C) in order to measure the basal value, the second one just after the BAC solution instillation (S, B_x), and the last one 15 minutes after the application of the last drop (PB_x).

4.2.2.2 Monitoring a corneal epithelial wound healing process

To study the wound healing process, a total of 30 New Zealand white rabbits weighing between 2.5 and 3 kg were used. The rabbits were deeply anaesthetized following the same procedure described above. Here, both eyes were kept open by a blepharostat and a circular wound was performed in the central corneal epithelium by applying a 6 mm diameter paper disc soaked with 10 µl of n-heptanol for 30 seconds. After removing the paper disk, the cornea was rinsed with 10 ml of sterile saline solution. It has been reported that this protocol generates an epithelial wound with little or even no damage to the underlying stroma (Talarico, 2010; Burgalassi et al., 2011). To evaluate the wound healing, both impedance measurements and permeability to sodium fluorescein measurements were carried out before wounding and at 15 minutes, 24 hours, 40 hours and 48 hours after wounding. With this protocol, each group of measurements is composed by 6 eyes.

4.2.2.3 Impedance measurements.

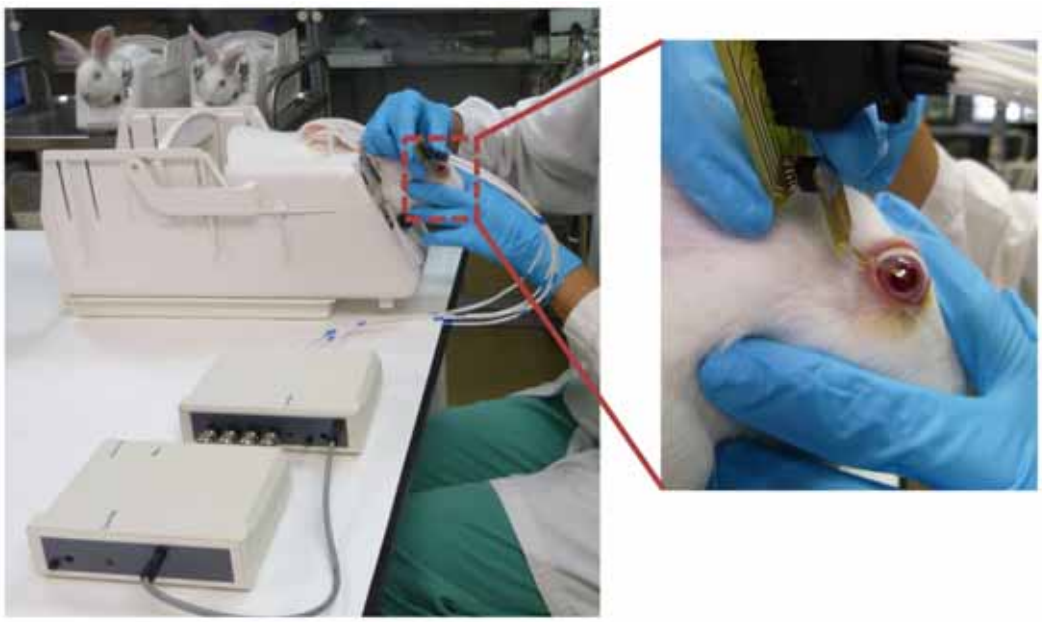

Figure 4-5 Image of how the impedance sensor is used in the experimental procedures. It is interesting to note that the rabbit is not sedated.

As it is shown in Figure 4-5 the impedance sensor can be easily placed on the corneal surface. In the case of the measurements performed to monitor the wound healing process, the impedance sensor was used without sedate the rabbits. This improvement, provided by the use of a flexible substrate, simplifies the experimental procedure and reduces its cost.

As it was described in a previous chapter, a home-made tetrapolar impedance analysis system (Guimerà et al., 2009) was used to perform the impedance measurements. In this chapter, this system was complemented with a home-made multiplexer allowing the acquisition of the impedance measurement of the 4 different electrode configurations in an automatic fashion. With the whole system, it takes approximately 1 minute to acquire 20 frequency points within the 100 Hz to 1 MHz frequency range. Since the impedance analysis system implements calibration procedures, the addition of the multiplexor has been possible without reducing the quality of the measurement. Thus, to reduce the parasitic effects produced by the current leakages, the whole system, including the connection wires, has been calibrated. In addition, other considerations have been taken into account to design the multiplexer in order to reduce the current leakages. Briefly, the multiplexer is based on relays since the current leakages and the coupling between channels is lower than in the case of solid state ones. Likewise, the active shield provided by the impedance analysis system is also multiplexed and extended until the sensor connector by means of coaxial wires.

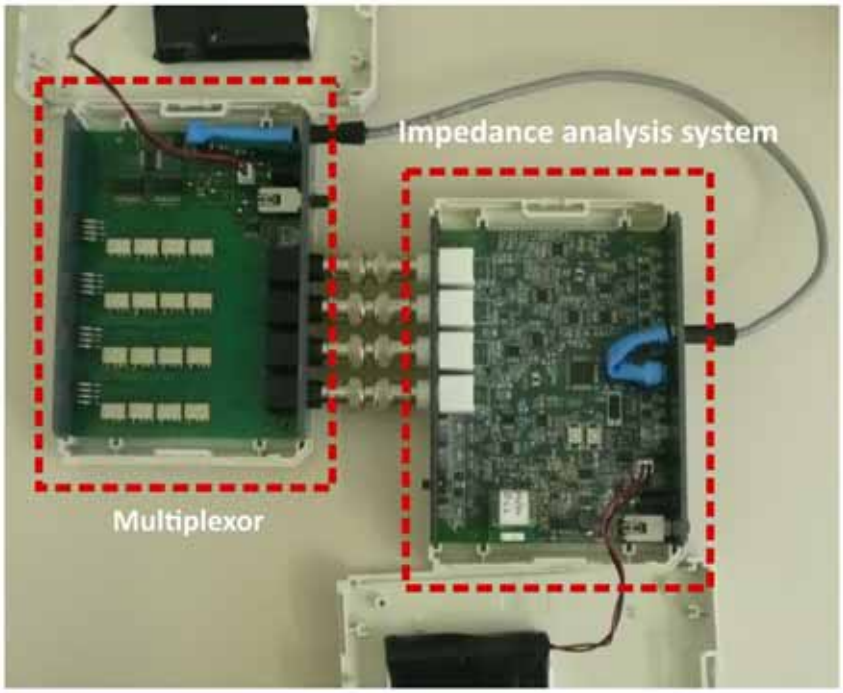

Figure 4-6 Image of the impedance analysis system and the multiplexor module

4.2.2.4 Statistical validation of epithelium permeability indicator

In previous chapters, it has been demonstrated that the resolution of the method presented is mainly limited by variations in the tear film thickness between each application of the sensor. Moreover, the FEM simulations performed in Chapter 1 showed that the contribution of the tear film to the impedance measured depends on the frequency. In this chapter, two statistical analyses have been performed in order to experimentally find a robust

indicator of epithelium permeability. This study was supervised by the applied statistical service of UAB.

The impedance measurements were acquired by triplicate in order to study the consistency of the proposed method. From this data experimentally obtained, the real part (Z'), the imaginary part (Z''), the modulus ($|Z|$) and the phase shift have been studied over the frequency range, in order to find the most reliable one. For this, the Intraclass Correlation Coefficient (ICC) was calculated for each impedance parameter at each used frequency (Bartko, 1966). In statistics, ICC is commonly used in the assessment of consistency or repeatability of quantitative measurements made by different observations measuring the same quantity (Shrout and Fleiss, 1979). In this case, the different observations are the three acquired impedance measurements. The ICC is ranged from 0 to 1, and can be interpreted as the proportion of total variance that is due to differences between subjects. Thus, for instance, in a dataset where the variance of the individual measurements is similar to the variance of the whole range of measurements, the ICC value is about 0.

Once established which impedance parameter is the most reliable, Dunnett's test was used to study the ability of selected parameter to discriminate between the different degrees of epithelium permeability (Dunnett, 1955). This test is performed by computing a Student's t-test statistic for each group in comparasion with a single control group. The Student's t-test is used to determine whether two sets of data are significantly different from each other, assuming a certain confidence interval.

4.2.2.5 Measurement of Epithelium permeability to sodium fluorescein

Corneal epithelium permeability to fluorescein was evaluated as an indicator of corneal epithelial integrity (Chen et al., 2011). In brief, 50 µl (1 mg/ml) of sodium fluorescein (Sigma, 46960) were applied to the ocular surface. Ten minutes after fluorescein administration, animals were euthanized with intravenous pentobarbital at 200 mg/kg (Sigma, P3761) and corneas were excised. Homogenization of each cornea was performed in 300 µl of PBS using an Ultra-turrax mixer (IKA) and samples were centrifuged at 14000 rpm and 4ºC during 10 minutes. Fluorescence in supernatants and in a fluorescein standard was measured using a Victor II plate reader (Perkin Elmer) by duplicate. The corneal fluorescein concentration (CFC) was expressed in mg per cornea.

4.2.2.6 Corneal epithelial fluorescein staining

The morphological state was also macroscopically assessed by a fluorescein test (Wilson et al., 1995). This evaluation is of special interest for the case of monitoring the wound healing, since it allows the macroscopic study of the healing process and the determination of the epithelium layer regeneration velocity. However, the information obtained is qualitative and cannot be directly related with epithelium permeability (Mokhtarzadeh et al., 2011). In brief, 40 µL of fluorescein (0.1%) solution was applied to the eye, which was followed by photography under a cobalt filter-attached slit-lamp. The images obtained were analyzed with image analysis software (ImageJ) to determine the area affected by the wound. The

fluorescein test (FITC) was expressed as the ratio between the area affected by the wound and the total corneal area.

4.3 Results and discussion

4.3.1 Impedance sensor characterization

As it has been mentioned in the previous section, electrode-electrolyte impedance measurements have been performed to characterize the electrode after being electrochemically modified with platinum black. In particular, these results at different stages of the electrode modification are shown in Figure 4-7. There, it can be seen that, as expected, the deposition of a platinum black layer decreases the electrode-electrolyte impedance values (70-fold at 100 Hz) due to the increase of the electrode roughness and, thus, its effective area. It is also worthy to note that the same measurements performed after each series of *in vivo* experiments presented only minor changes, proving the stability of the applied electrode modification process (impedance increase at 100 Hz < 25%, data not shown).

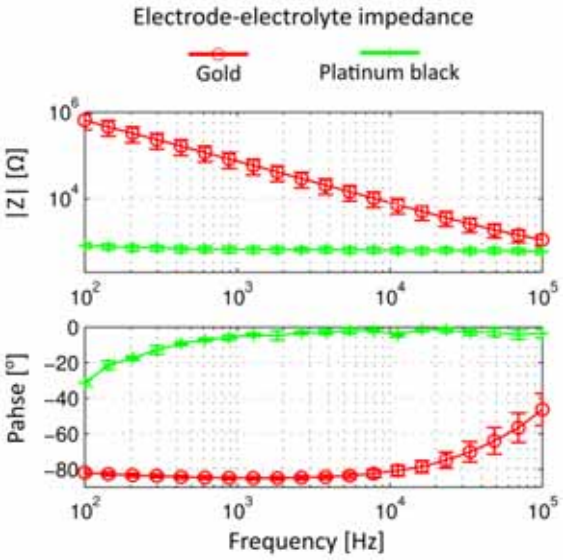

Figure 4-7 Results of the impedance sensor characterization. Bode representation of the electrode-electrolyte impedance measured in NaCl wt.0.9% at different stages of the electrode modification: bare gold electrode (red line) and after platinum black deposition (green line). Results are expressed as mean ± standard deviation (n=100).

The impedance sensor characterization was finished by performing tetrapolar impedance measurements of a NaCl 0.9 wt.% solution. Ideally, in the analyzed frequency range, the impedance measured of a saline solution should be characterized by a flat modulus and 0 º of phase shift (Grimnes and Martinsen, 2008) since it behaves as a pure resistance in the studied frequency range. Figure 4-8 shows the results of the tetrapolar measurements for a NaCl 0.9 wt.% solution using the different electrode configurations. It is interesting to note that the measurements performed with the bare gold electrodes do not present this behavior, especially in frequencies below 10 kHz. This undesired behavior it is due to the high values of the electrode-electrolyte impedance in this frequency range, which produce a high common mode voltage that cannot be rejected by the instrumentation amplifier used to measure the voltage drop. In contrast, the measurements performed after platinum black deposition, present the ideal behavior in the low frequency range, due to the decrease of the electrode-

electrolyte impedance. However, the ideal behavior cannot be accomplished at frequencies greater than 300 kHz. This can be attributable to the capacitive coupling and current leakages of the wires, which are strongly manifested in high frequency range; therefore, the useful frequency band ranges from 100 Hz to 300 kHz.

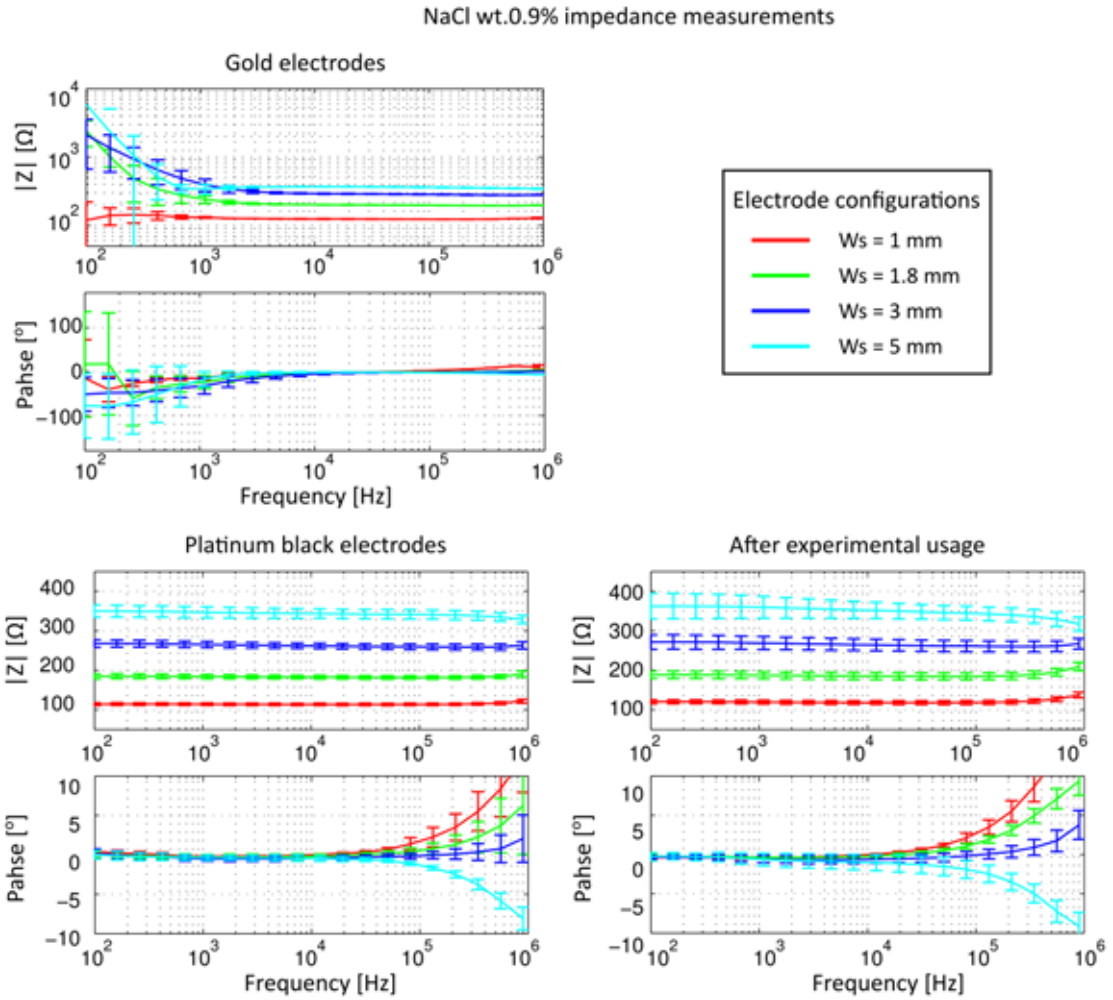

Figure 4-8 Results of the impedance sensor characterization. Bode representation of the Impedance measured in a NaCl wt.0.9% solution at different stages of the electrode modification (four-electrode measurement). (top) Impedance measurements performed with gold electrodes without platinum black modification. (bottom left) Impedance measurements performed with the final impedance sensor modified with platinum black. (Bottom right) Impedance measurements performed before and after each experimental usage in order to ensure the correct behavior of the impedance sensor. Results are expressed as mean ± standard deviation (n=10 for the case of gold and platinum black electrodes and n=1000 for the case of experimental usage).

As commented before, the electrode surface properties can be altered by the contact with the corneal tissue. Two key aspects must be taken into account to minimize the errors produced by the deterioration of the electrode surface properties. Firstly, in the tear film composition there are lipids and proteins (Tiffany, 1994; Bron et al., 2004) that can be attached to the electrode surface during the sensor application, resulting in an electrode passivation, and consequently, in an increase of the electrode-electrolyte impedance. To minimize this effect, a washing procedure after the sensor usage is required in order to remove the biological particles that can be attached to the electrode surface. Thus, the

impedance sensor was firstly cleaned by using Hellmanex® III (Hellma® analytincs) in order to dissolve the biological particles. Finally, was rinsed in distilled water to avoid the crystallization of diluted salts over the electrodes. On the other hand, the platinum black electrodeposited can be detached due to the mechanical friction with the corneal tissue, which also results in an increase of the electrode-electrolyte impedance. Consequently, to ensure the correct behavior of the impedance sensor during the experimental measurements, the sensor was tested before and after each experimental usage. Figure 4-8 shows these measurements, when comparing them with the measurements performed after platinum black deposition, only a slight increase in the dispersion of the impedance modulus can be observed. This increase can be attributed to slight variations in the conductivity of the saline solution since phase shift is about 0º over the frequency range measured. Therefore, it can be concluded that these results validate the experimental measurements obtained in the frequency range from 100 Hz to 300 kHz.

4.3.2 Statistical validation of the epithelium permeability indicator

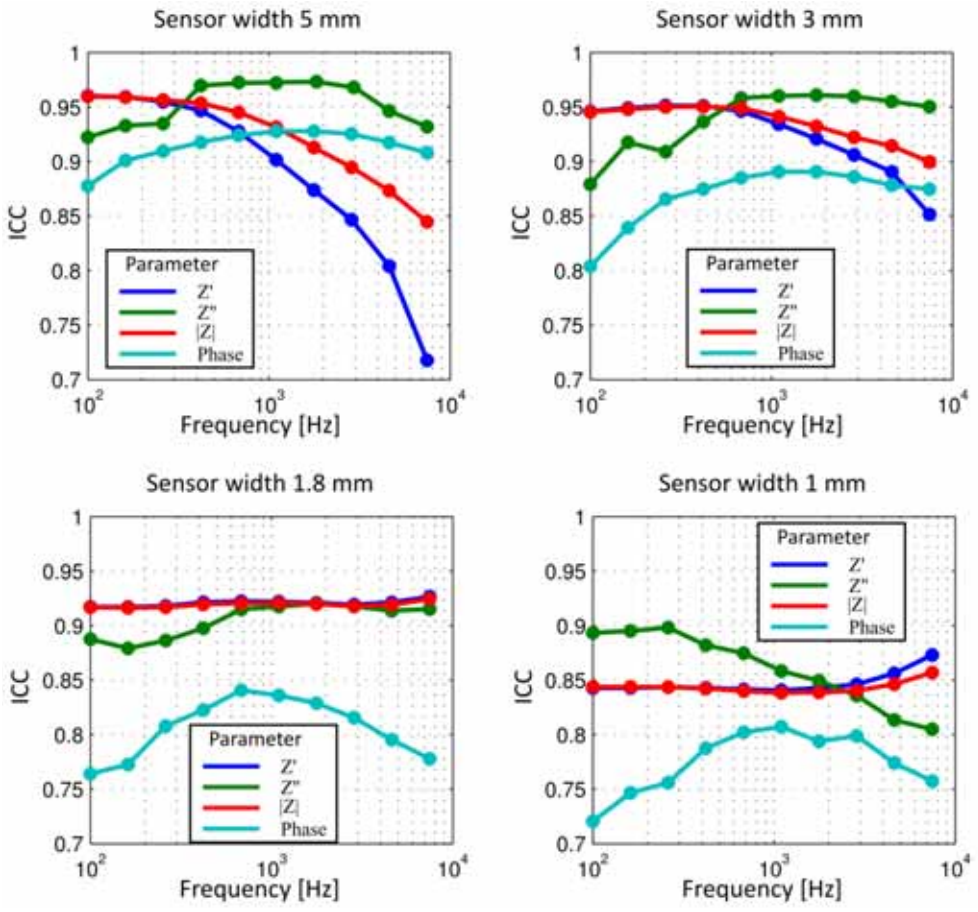

Figure 4-9 Results of the Intraclass Correlation Coefficient (ICC) evaluation in function of the frequency, for different impedance parameters (real part (Z'), imaginary part (Z''), modulus (|Z|) and phase shift). It is interesting to note that the imaginary part, measured in the frequency range from 500 Hz to 3 kHz, is the parameter which presents the best reliability for all the electrode configurations.

As commented, each impedance measurement has been acquired by triplicate in order to evaluate the consistency and repeatability of the method proposed. Therefore, the ICC has

been evaluated for different impedance parameters in function of frequency. The obtained results are shown in Figure 4-9, and they have been used to choice the parameter with the best feasibility as a prospective indicator of the epithelium permeability.

Table 4-1 ICC values for different impedance parameters measured with the electrode configuration of 5 mm.

Frequency [Hz]	***Interclass Correlation Coefficient (ICC)*** *Parameters analyzed*			
	Z'	*Z''*	*|Z|*	*Phase*
100	0,960	0,922	0,960	0,878
161	0,959	0,933	0,959	0,901
261	0,955	0,935	0,956	0,910
421	0,947	0,970	0,953	0,918
680	0,927	0,971	0,945	0,924
1098	0,902	0,973	0,931	0,928
1773	0,874	***0,975***	0,913	0,928
2861	0,847	0,968	0,895	0,925
4616	0,804	0,946	0,873	0,917
7467	0,718	0,932	0,845	0,908

As a conclusion of the previous chapter, it was stated that the variability of the measurements performed is mainly due to variations in the tear film thickness between different sensor applications. Therefore, it can be assumed that the ICC value can be related with the contribution of the tear film to the impedance measured. This hypothesis are in agreement with the findings of Chapter 2 (Figure 2-6), where it is shown that the contribution of the tear film is lower when the electrode separation increases. Therefore, as can be observed, the imaginary part measured in the frequency range from 500 Hz to 3 kHz is the parameter which presents the best reliability for all the electrode configurations, being maximum when the electrode configuration of 5 mm is used. Consequently, the imaginary part of the impedance measured at 2 kHz was chosen as a prospective indicator of the epithelium permeability. Although the real part and the modulus present a similar ICC value (Table 4-1), it was chosen the imaginary part because of it can be measured in a higher frequency range, where the parasitic effects of the electrode-electrolyte impedance are lower. Moreover, as it is shown in Figure 2-6, the contribution of the epithelium to the total impedance is maximum in this frequency range. Likewise, the tear film should not contribute to the imaginary part since it can be considered like a saline solution. Therefore, it is expected that the main contribution to the imaginary part should be due to the epithelium cells. However, this hypothesis can be limited by the two current paths phenomenon produced by the tear film, which can also produce alterations in the imaginary part (Grimnes and Martinsen, 2007), as it has been showed in the Chapter3.

4.3.3 Results of topical BAC application

Different BAC dilutions have been instilled in rabbit's eyes in order to produce different degrees of corneal epithelium permeability. The experimental results obtained with the 5 mm sensor width configuration are shown in Figure 4-10 in a Bode and Nyquist representations.

These results are presented as mean of all the performed measurements for each group. As expected, a decrease in both the impedance modulus and phase, which is inversely proportional to the applied BAC concentration, is clearly observed.

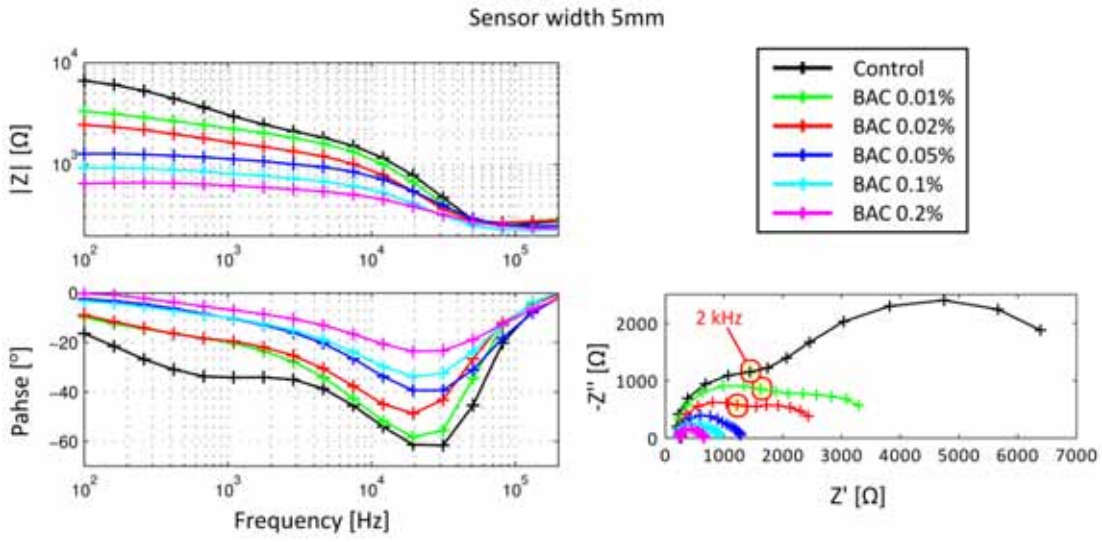

Figure 4-10 Experimental impedance measurements for the eyes insulted with different BAC dilutions, which are showed in a (Left) Bode and (right) Nyquist representation of the mean values for each group.

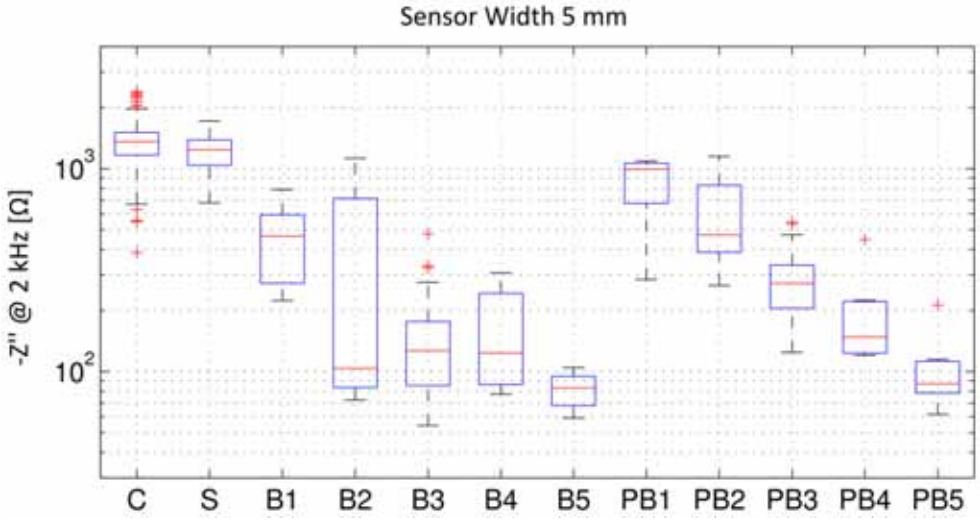

Figure 4-11 Boxplot representation of the experimental values of the epithelium permeability indicator proposed for each group studied: C Basalt measurements, S group treated with innocuous saline solution, B_x measurements performed just after the treatment and the PB_x measurements performed 15 minutes after the injury.

The experimental results of the proposed indicator (Imaginary part of the impedance measured at 2 kHz) are shown in Figure 4-11 for all groups using a Boxplot representation. As expected, the impedance measured before treatment (C) and the impedance measured in the control group (S), which was treated with innocuous saline solution, are in the same value range without significant statistical difference. Consequently, this range can be considered as the normality and can be associated to a healthy epithelium. For the rest of the groups, it is interesting to note that the values for the measurements performed 15 minutes after the injury (PB_x) are slightly higher than the measurements performed immediately after injury (B_x).

Moreover, their dispersion is drastically reduced, especially when the BAC concentration is lower than 0.05%. This fact can be attributed to a stabilization of the damage produced by the injury as it has been reported in a previous work (Kusano et al., 2010), where the impact of the BAC in the permeability and passive electrical properties could be observed just some seconds after its application. Moreover, it has been also reported that the tear produces a dilution of the applied BAC reducing the effects of the injury (Chetoni et al., 2003) which also contributes to the stabilization of the induced damage. Accordingly, and due to its stability and repeatability, the measurements performed 15 minutes after injury will be chosen in the succeeding analysis.

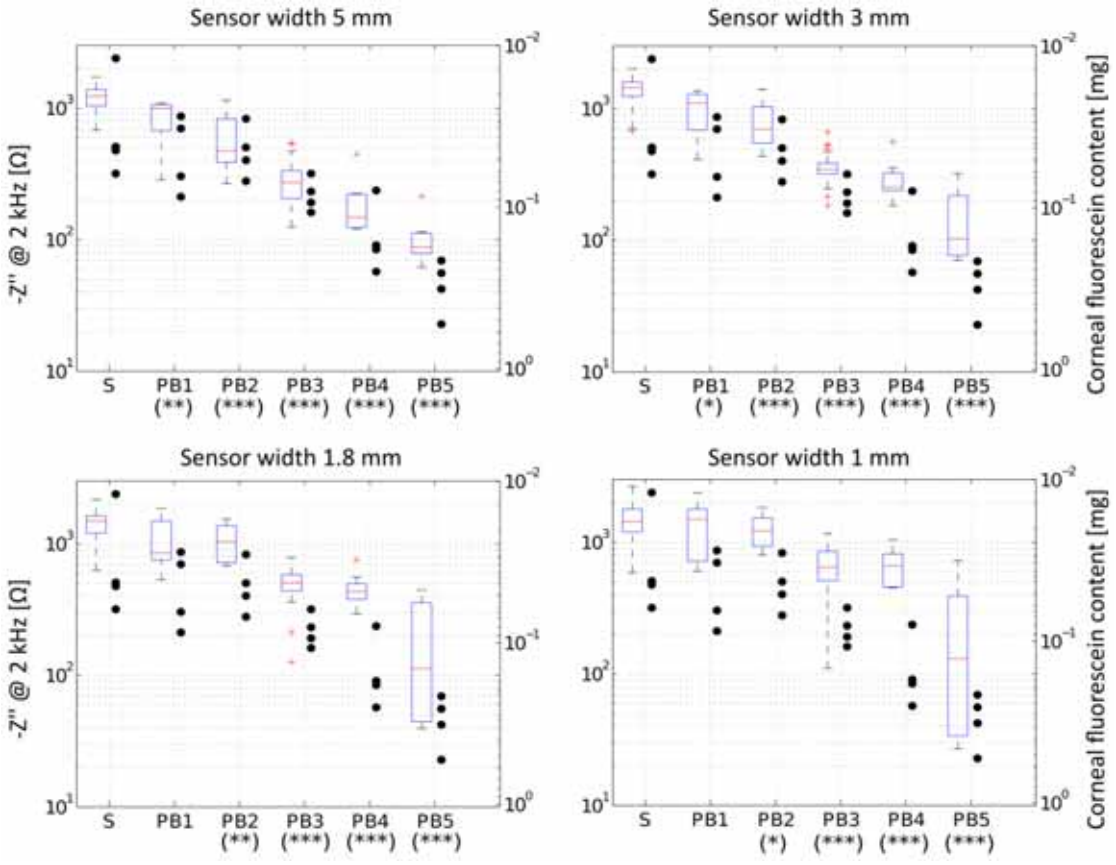

*Figure 4-12 Experimental results for the eyes treated with different BAC dilutions (S, PB_x) where the left Y-axis represents the imaginary part of the measured impedance at 2 kHz. These results are presented in a Boxplot which shows the mean value, the dispersion of the measurements grouped by quartiles (boxes and bars) and the outlier values (crosses). The right Y-axis represents the permeability to sodium fluorescein measurements of the corneal epithelium with the obtained values presented as points. The different graphs correspond to the results obtained using the different electrode configurations. (*** p<0.001; ** p<0.01; * p<0.1 with unpaired student's t-test)*

Figure 4-12 shows the values of the proposed indicator used to evaluate the epithelium permeability for the different electrode configurations. This data is compared with the results of the epithelial permeability to sodium fluorescein measurements, which are showed in the secondary axis. Concerning the fluorescein uptake measurements (same data plotted in all graphs of Figure 4-12 and showed in Table 4-2) it can be observed that the results correlate directly with the applied BAC concentration; a correlation that has been previously reported by other authors (Chen et al., 2011). In particular, it was observed a 2 fold increase in the case of

PB3 group (BAC at 0.05%), a 4 fold increase the case of PB4 group (BAC at 0.1%) and an 8 fold increase in the case of PB5 group (BAC at 0.2%). In addition, for lower BAC concentrations a slight difference between control and PB1 and PB2 groups was also observed (0.01% and 0.02% respectively). To summarize, it can be concluded that the applied experimental procedure produces a progressive increase in the epithelial permeability and thus, it can be considered suitable for the evaluation of the proposed impedance sensor.

Focusing on the data from the impedance measurements, a progressive decrease in their values is observed as the BAC concentration increases. In order to evaluate which sensor configuration has a better sensitivity, unpaired student's t-test has been performed by comparing all groups with the control group ($p<0.01$ was considered statistically significant). From this study, it can be concluded that in all the sensor configurations there is a significant difference between the groups corresponding to higher BAC concentrations (groups PB3, PB4 and PB5). However, for the lower BAC concentration groups (PB1 and PB2), only the 5 mm wide sensor is able to differentiate between them (e.g. control and PB1 group -BAC at 0.01%- can be differentiate within a significance level of $p<0.01\%$). These results are in accordance with the FEM simulations presented in previous chapter, where the 5 mm wide configuration presents a major contribution of the epithelium layer and minor contribution of the tear film. Thus, it can be concluded that the 5mm configuration is the most appropriate to use in order to detect any alteration in the epithelium permeability.

Table 4-2 Summary of the experimental data for the topical instillation of different BAC solutions. Data presented as mean ± Std from 4 eyes per group in the case of corneal fluorescein content, 10 eyes per BAC treated group and 50 eyes per NaCl group in the case of impedance measurements.

			Corneal fluorescein content [mg]		***-Z'' @ 2 kHz [kΩ]***	
Group caption	***Treatment***	***Concentration***	***Mean ± Std***	***Δ (%)***	***Mean ± Std***	***Δ (%)***
S	*NaCl*	0.9%	0.04 ± 0.02	0 %	1.22 ± 0.23	0 %
PB_1	*BAC*	0.0125 %	0.05 ± 0.02	32.5 %	0.85 ± 0.28	-30.3 %
PB_2		0.025 %	0.04 ± 0.01	20.0 %	0.58 ± 0.29	-52.5 %
PB_3		0.05 %	0.08 ± 0.02	120.0 %	0.28 ± 0.10	-77.0 %
PB_4		0.1 %	0.17 ± 0.07	327.5 %	0.19 ± 0.10	-84.4 %
PB_5		0.2 %	0.33 ± 0.14	725.0 %	0.10 ± 0.04	-91.8 %

Furthermore, the results obtained here can be compared with the results that have been already published by different authors. In particular, the reported values of *in vivo* TER measurements reported by Kusano et al. and Chen et al. (Kusano et al., 2010; Chen et al., 2012) for low BAC concentrations (up to 0.02 %) show similar trends as the one obtained with the non-invasive impedance measurement method that has been described in this dissertation. A significant decrease in the impedance values is observed in all cases, although the different measuring protocols and methods employed make it complex to compare the exact values of each work (Chetoni et al., 2003). Moreover, in a work from Uematsu et al.

(Uematsu et al., 2007) a decrease of around the 80% of the initial value in the case of BAC concentration of 0.05% is reported. This result is in accordance with the value obtained for this specific BAC concentration using the non-invasive method described in this dissertation and showed in Table 4-2.

4.3.4 Experimental results of the corneal epithelium wound healing

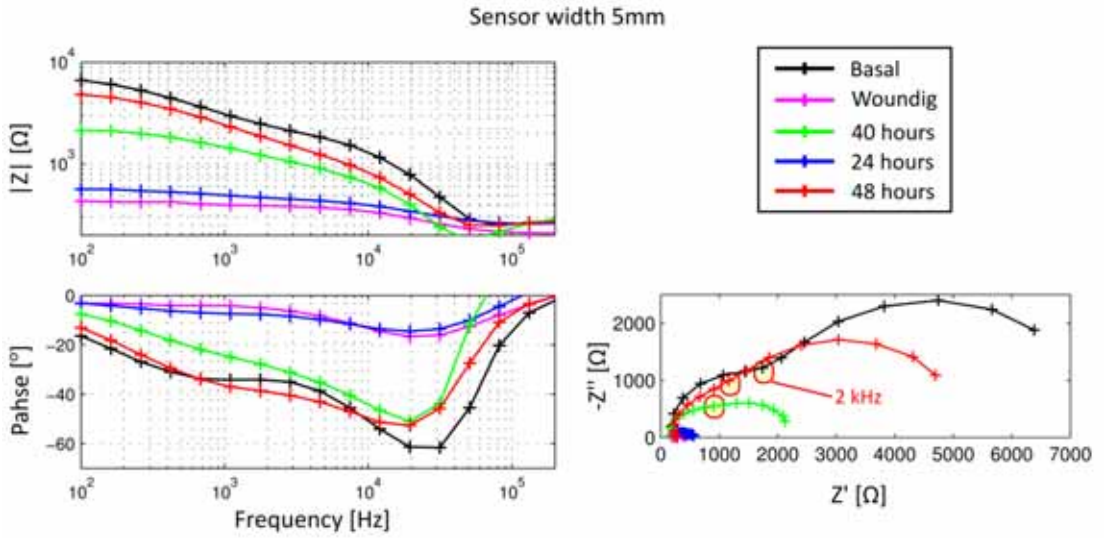

Figure 4-13 Experimental impedance measurements for the eyes insulted with different BAC dilutions, which are showed in a (Left) Bode and (right) Nyquist representation of the mean values for each group.

The impedance measurements performed during the corneal epithelium wound healing process are shown in Figure 4-13 in both Bode and Nyquist representation. These results are presented by plotting the mean of all the measurements for each group performed with the 5 mm electrode configuration. As expected, an increase, in both the impedance module and phase, proportional to the elapsed time from wounding can be clearly observed. Moreover, Figure 4-14 shows the results of the fluorescein staining test where it can be observed the evolution of the healing process along the time. It is interesting to note that the test performed after 48 hours of the wounding appears to be healthy.

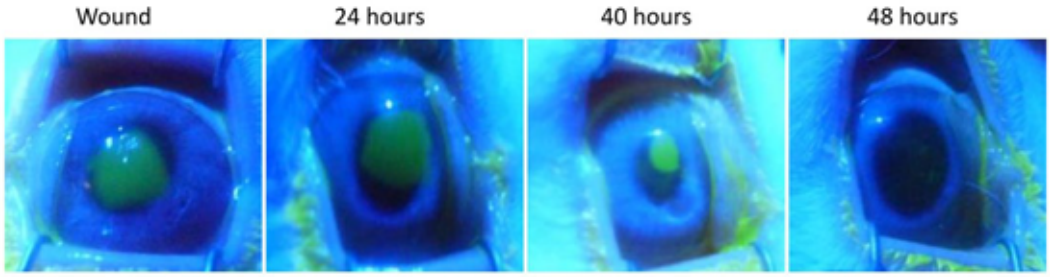

Figure 4-14 Images from the fluorescein test, wherein the corneal epithelial wound appear in bright green upon illumination by a blue cobalt light. It can be observed the evolution of the healing process along the time.

The values of imaginary part measured at 2 KHz, which has been proposed as an indicator of the epithelium permeability, are shown in Figure 4-15 in a boxplot representation for each time measured. Moreover, the impedance measurements are compared to the permeability to fluorescein measurements. Table 4-3 summarizes the data from both measurements. In this case, both measurements were performed in the same individuals and at the same time. As far as both measurements correspond to the same phenomena, a similar behavior is expected. To show this relation both logarithmic values are depicted in Figure 4-15, where a trend can be perceived although the variability of the data in both measurements methods. In particular, there is a lack of sensitivity of fluorescein quantification in corneas at 40 and 48 hours post wounding, which had very low fluorescein content. To better show this trend, a linear regression of the logarithmic values of both magnitudes is represented (dash line).

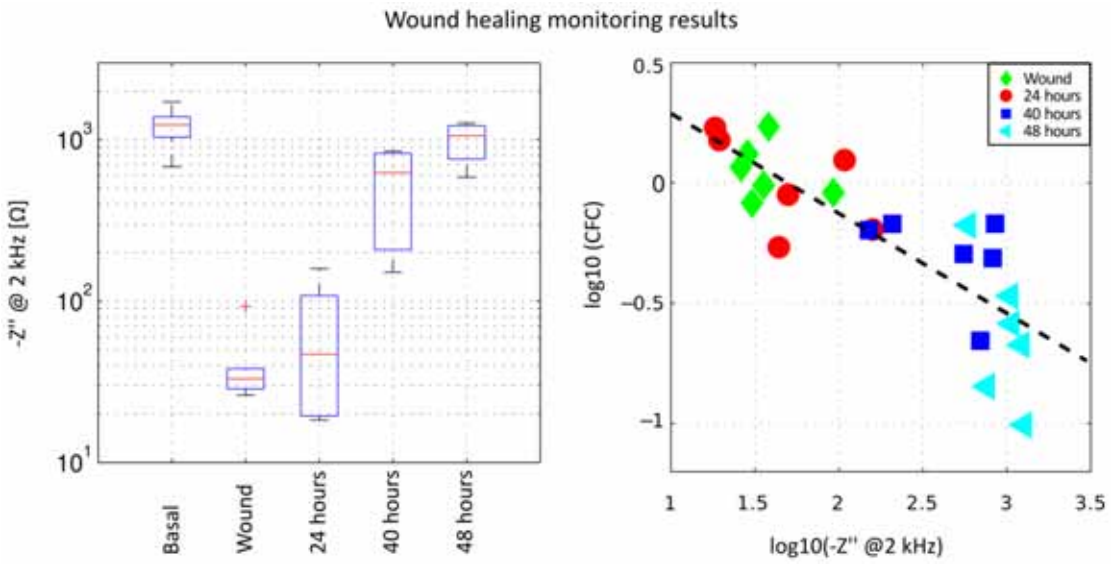

Figure 4-15 (Left) Boxplot representation of the imaginary part of the impedance measured at 2 kzHz for different times of the healing process. (Right) Representation of the logarithmic values of the Corneal Fluorescein Content (CFC) in function of the impedance imaginary part at 2 kHz. Dash line shows a linear regression of the logarithmic values of both magnitudes.

In addition, it is interesting to note that the value of the indicator proposed after wounding is almost null. As the n-heptanol removes all the epithelium cells, and therefore, no barrier exists, this fact denotes that the indicator proposed is mainly related with the corneal epithelium barrier function. Furthermore, it can be observed that the measurement performed

at 48 hours is lower than the basal measurement. In the same way, the CFC value at 48 hours is also higher than the basal value, which indicates that the healing process is not finished yet. However, in the fluorescein test performed at 48 hours (Figure 4-14), the corneal epithelium appears to be healthy. Therefore, it can be stated that the method proposed is more sensitive than the fluorescein test to assess the epithelium permeability.

Table 4-3 Summary of the experimentally obtained data. Data presented as mean ± std from 6 eyes per group.

Time		***Corneal fluorescein (CFC) [mg]***		***Impedance at 2 kHz [kΩ]***	
		Mean ± Std	***Δ (%)***	***Mean ± Std***	***Δ (%)***
Pre-wounding		0,11 ± 0,05	0	1,22 ± 0,23	0 %
Post-wounding	*15 minutes*	1,12 ± 0,33	918 %	0,04 ± 0,03	-96,7 %
	24 hours	1,00 ± 0,47	809 %	0,07 ± 0,06	-94,3 %
	40 hours	0,50 ± 0,17	354 %	0,55 ± 0,30	-54,9 %
	48 hours	0,24 ± 0,21	118 %	0,99 ± 0,27	-18,9 %

Moreover, the results can be compared with the results reported by Fukuda and Sasaki with a non-invasive method in a similar experimental procedure (Fukuda and Sasaki, 2012). Fukuda and Sasaki performed the impedance measurements at 1 kHz with two circular gold wire electrodes placed on the corneal surface. The results are presented as the percentage variation of the impedance modulus, the temporal evolution reported is similar to the results presented here. However, the variation measured after wounding is lower than the variation obtained with the method here presented (-50 % reported by Fukuda and Sasaki versus 96,7 % here obtained). Since the range of the variability is similar in both methods the higher variation obtained with the method presented here indicates that it is more sensible than the method presented by Fukuda and Sasaki.

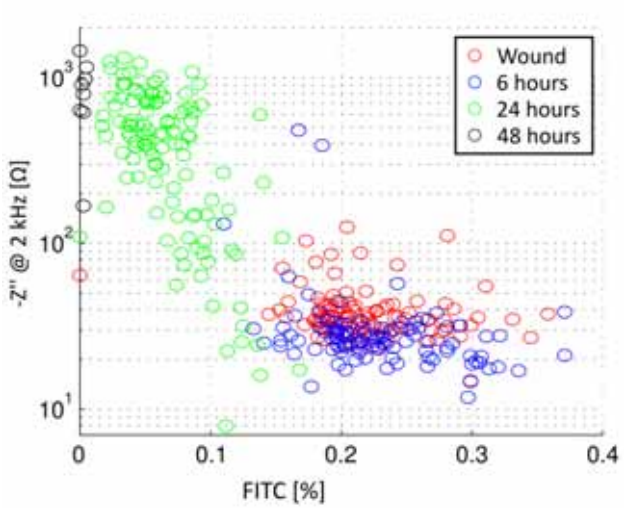

Figure 4-16 Value of the imaginary part measured at 2 kHz in function of the wound affected area evaluated with the fluorescein test (FITC) for each time evaluated. It is interesting to note that only exists correlation in the case of measurements performed at 24 hours.

In collaboration with the pharmaceutics company SALVAT S.A. the method developed was used to assess the behavior of different drugs in the healing process. As it is not the objective of this dissertation, the composition of these drugs is not described. Since the fluorescein test

is a non-destructive test and can be implemented in easy way, in this case, the impedance measurements are only compared with the wound affected area evaluated with the fluorescein test (FITC). Figure 4-16 shows the relation between both measurements, where it can be observed that both methods are only related in the case of measurements performed 24 hours after wounding. Therefore, it can be conclude that fluorescein test has more accuracy to evaluate the area affected by the wounding but its accuracy is substantially reduced to evaluate the epithelium permeability in advanced stages of the healing process.

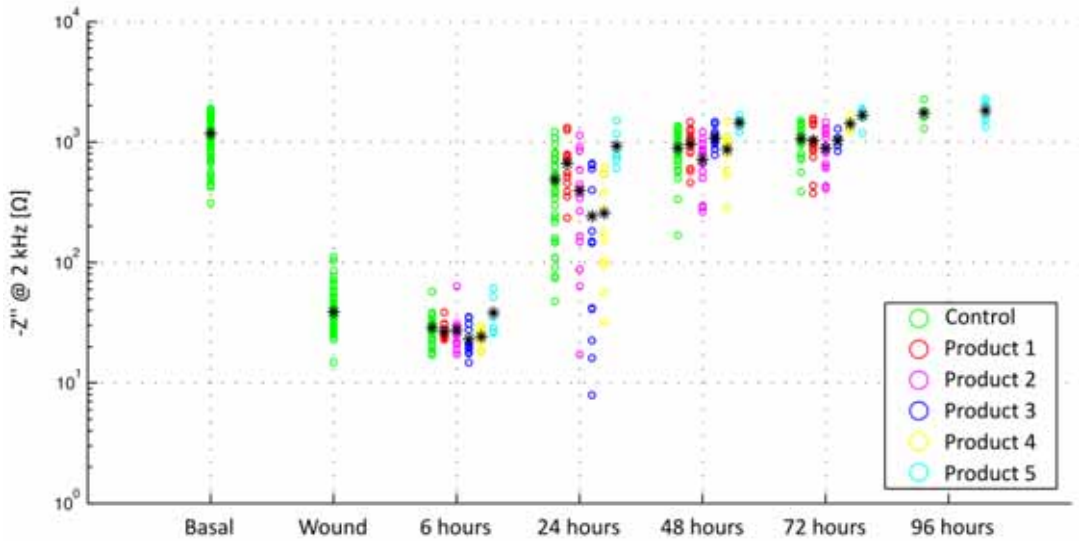

Figure 4-17 Scatter representation of the Imaginary part of the impedance measured at 2 kHz at different times of the healing process for the different products evaluated, where the black point indicate the mean value of each group. It can be observed that the product 5 presents a higher impedance values in all stages of the healing process, resulting in a quicker reestablishment of the epithelium barrier function.

Figure 4-17 shows the impedance measurements obtained for several products at different stages of the healing process. It can be observed that the product 5 presents a higher impedance values in all stages of the healing process, resulting in a quicker reestablishment of the epithelium barrier function. Moreover, the measurements performed at 72 hours and 96 hours after wounding presents a mean value similar to the basal measurement, confirming that at these times the healing process has been finished.

4.4 Conclusions

In previous chapter, a method to non-invasively assess corneal epithelial permeability through tetrapolar impedance measurements was presented and experimentally validated. In this chapter, a SU-8 based impedance sensor is presented. The flexibility of this novel sensing device dramatically improves the application method, ensuring the electric contact between the electrodes and the corneal surface without applying pressure. Furthermore, the influence of the tear film in the measurements can be reduced because of the increased separation between the electrodes. The imaginary part of the impedance measured at 2 kHz with the electrode configuration of 5 mm wide has been identified as the most feasible indicator of the epithelium permeability. From the obtained results it can be stated that with the presented

impedance sensor it is possible to discern between lower and time-dependent alterations in the corneal epithelium permeability after instillation of very low concentrated BAC solution (0.01%). Therefore, we conclude that the flexible sensing device presented here can be used as a non-invasive tool for assessing the corneal epithelial layer function. This new approach can be used for *in vivo* studies or in clinical practice, filling the gap existing for corneal function evaluation methods.

4.5 References

Bartko, J.J., 1966. The intraclass correlation coefficient as a measure of reliability. Psychol. Rep. 19, 3–11.

Bron, A.J., Tiffany, J.M., Gouveia, S.M., Yokoi, N., Voon, L.W., 2004. Functional aspects of the tear film lipid layer. Exp. Eye Res. 78, 347–360.

Burgalassi, S., Nicosia, N., Monti, D., Falcone, G., Boldrini, E., Fabiani, O., Lenzi, C., Pirone, A., Chetoni, P., 2011. Arabinogalactan as Active Compound in the Management of Corneal Wounds: In Vitro Toxicity and In Vivo Investigations on Rabbits. Curr. Eye Res. 36, 21–28.

Burgalassi, S., Raimondi, L., Pirisino, R., Banchelli, G., Boldrini, E., Saettone, M.F., 2000. Effect of xyloglucan (tamarind seed polysaccharide) on conjunctival cell adhesion to laminin and on corneal epithelium wound healing. Eur. J. Ophthalmol. 10, 71–76.

Calderón, E., Melero, A., Guimerà, A., 2009. Portable Device for Microelectrode Array Bio-impedance Measurements, in: Dössel, O., Schlegel, W.C. (Eds.), World Congress on Medical Physics and Biomedical Engineering, September 7 - 12, 2009, Munich, Germany, IFMBE Proceedings. Springer, pp. 883–886.

Chen, W., Hu, J., Zhang, Z., Chen, L., Xie, H., Dong, N., Chen, Y., Liu, Z., 2012. Localization and Expression of Zonula Occludins-1 in the Rabbit Corneal Epithelium following Exposure to Benzalkonium Chloride. PLoS ONE 7, e40893.

Chen, W., Li, Z., Hu, J., Zhang, Z., Chen, L., Chen, Y., Liu, Z., 2011. Corneal Alternations Induced by Topical Application of Benzalkonium Chloride in Rabbit. PLoS One 6.

Chetoni, P., Burgalassi, S., Monti, D., Saettone, M.F., 2003. Ocular toxicity of some corneal penetration enhancers evaluated by electrophysiology measurements on isolated rabbit corneas. Toxicol. Vitro Int. J. Publ. Assoc. BIBRA 17, 497–504.

Dunnett, C.W., 1955. A Multiple Comparison Procedure for Comparing Several Treatments with a Control. J. Am. Stat. Assoc. 50, 1096–1121.

Dupps Jr., W.J., Wilson, S.E., 2006. Biomechanics and wound healing in the cornea. Exp. Eye Res. 83, 709–720.

Fukuda, M., Sasaki, H., 2012. Quantitative evaluation of corneal epithelial injury caused by n-heptanol using a corneal resistance measuring device in vivo. Clin. Ophthalmol. Auckl. NZ 6, 585–593.

Grimnes, S., Martinsen, Ø.G., 2007. Sources of error in tetrapolar impedance measurements on biomaterials and other ionic conductors. J. Phys. Appl. Phys. 40, 9–14.

Grimnes, S., Martinsen, Ø.G., 2008. Bioimpedance and bioelectricity basics. Academic Press, New York.

Guimera, A., Calderon, E., Los, P., Christie, A.M., 2008. Method and device for bio-impedance measurement with hard-tissue applications. Physiol. Meas. 29, S279–S290.

Guimerà, A., Gabriel, G., Parramon, D., Calderón, E., Villa, R., 2009. Portable 4 Wire Bioimpedance Meter with Bluetooth Link, in: Dössel, O., Schlegel, W.C. (Eds.), World Congress on Medical Physics and Biomedical Engineering, September 7 - 12, 2009, Munich, Germany, IFMBE Proceedings. Springer, pp. 868–871.

Ivorra, A., Gómez, R., Noguera, N., Villa, R., Sola, A., Palacios, L., Hotter, G., Aguiló, J., 2003. Minimally invasive silicon probe for electrical impedance measurements in small animals. Biosens. Bioelectron. 19, 391–399.

Jl, A., Jj, P.-S., T, T., Kf, T., M, V., Rj, S., B, M., Rk, M., 1999. Postoperative inflammation, microbial complications, and wound healing following laser in situ keratomileusis. J. Refract. Surg. Thorofare NJ 1995 16, 523–538.

Keller, S., Blagoi, G., Lillemose, M., Haefliger, D., Boisen, A., 2008. Processing of thin SU-8 films. J. Micromechanics Microengineering 18.

Kusano, M., Uematsu, M., Kumagami, T., Sasaki, H., Kitaoka, T., 2010. Evaluation of acute corneal barrier change induced by topically applied preservatives using corneal transepithelial electric resistance in vivo. Cornea 29, 80–85.

Lorenz, H., Despont, M., Fahrni, N., LaBianca, N., Renaud, P., Vettiger, P., 1997. SU-8: A low-cost negative resist for MEMS. J. Micromechanics Microengineering 7, 121–124.

Marrese, C.A., 1987. Preparation of strongly adherent platinum black coatings. Anal. Chem. 59, 217–218.

Mokhtarzadeh, M., Casey, R., Glasgow, B.J., 2011. Fluorescein punctate staining traced to superficial corneal epithelial cells by impression cytology and confocal microscopy. Invest. Ophthalmol. Vis. Sci. 52, 2127–2135.

Shrout, P.E., Fleiss, J.L., 1979. Intraclass correlations: uses in assessing rater reliability. Psychol. Bull. 86, 420–428.

Talarico, E.F., 2010. Plasma membrane calcium-ATPase isoform four distribution changes during corneal epithelial wound healing. Mol. Vis. 16, 2259–2272.

Tiffany, J.M., 1994. Composition and Biophysical Properties of the Tear Film: Knowledge and Uncertainty, in: Sullivan, D.A. (Ed.), Lacrimal Gland, Tear Film, and Dry Eye Syndromes, Advances in Experimental Medicine and Biology. Springer US, pp. 231–238.

Uematsu, M., Kumagami, T., Kusano, M., Yamada, K., Mishima, K., Fujimura, K., Sasaki, H., Kitaoka, T., 2007. Acute Corneal Epithelial Change after Instillation of Benzalkonium Chloride Evaluated Using a Newly Developed in vivo Corneal Transepithelial Electric Resistance Measurement Method. Ophthalmic Res. 39, 308–314.

Versura, P., Profazio, V., Buzzi, M., Stancari, A., Arpinati, M., Malavolta, N., Campos, E.C., 2013. Efficacy of Standardized and Quality-Controlled Cord Blood Serum Eye Drop Therapy in the Healing of Severe Corneal Epithelial Damage in Dry Eye. Cornea 32, 412–418.

Vilares, R., Hunter, C., Ugarte, I., Aranburu, I., Berganzo, J., Elizalde, J., Fernandez, L.J., 2010. Fabrication and testing of a SU-8 thermal flow sensor. Sensors Actuators B Chem. 147, 411–417.

Wilson, G., Ren, H., Laurent, J., 1995. Corneal epithelial fluorescein staining. J. Am. Optom. Assoc. 66, 435–441.

Chapter 5

Ex vivo corneal endothelium permeability assessment during cold storage

The previous chapters of this dissertation are focused in the development of a method to non-invasive assessment of the corneal barrier function. In this chapter, the possibility to apply the proposed method to assess the endothelium barrier function of excised corneas has been studied. It can be accomplished by placing the cornea directly over the rigid impedance sensor, with the endothelium side in contact with the electrodes. This procedure will allow the assessment of the endothelium barrier function without removing the corneal epithelium, simplifying the experimental procedures required to perform the commonly used TER measurement methods. The developed method could be a helpful tool for evaluating the corneal functionality in eye banks, complementing the information provided by the endothelium cell density which is the currently gold standard parameter to determine its morphological state. Moreover, it also can be applied to monitor the behaviour of the preservation liquids used in the eye banks, improving its performance. To evaluate the feasibility of this method, changes in the rat corneal endothelium permeability during a preservation period of 7 days at 4ºC were monitored by impedance measurements and immunofluorescence. The obtained results show that the impairment of tight junction integrity could be detected by changes in impedance values that correlate with alteration observed after ZO-1 immunostaining. These successful results validate the capability of the proposed method to evaluate endothelium permeability in unmodified corneas. Moreover, these findings pave the way for developing a sensor able to measure the corneal endothelium functionality compatible with the current preservation protocols.

Most of the contents of this chapter have been published in the following contributions:

- C. Herrero, S. Marchán, E. Traver, R. Montava, M. Orzáez, M. Sancho, A. Guimerà, R. Villa, E. Pérez-Payá, C. Lagunas *"Inhibition of Apaf-1 as a potential therapeutic strategy to improve corneal quality"*. Annual Conference of European Association for Vision and Eye Research Conference (EVER 2012). **Acta Ophthalmologica** 90:0–0. doi: 10.1111/j.1755-3768.2012.3434.x

- A. Guimera, E. Traver, X. Illa, G. Gabriel, C. Herrero, C. Lagunas, MJ. Maldonado, R. Villa *"A new method for ex vivo corneal endothelium permeability assessment during cold storage through impedance measurements"*. **Physiological Measurement** Submitted.

5.1 Introduction

The corneal transplant is often the unique clinical alternative for treating its opacity. It is done by a surgical procedure called keratoplastya, which has been used along the last century to substitute a damaged cornea by a healthy one. In Spain, about of 3000 per year corneal transplants are performed. The viability of the graft transplanted depends upon of the proper endothelium functionality, since it plays the most important role in the corneal homeostasis. In humans, the corneal endothelium has a poor regenerative capacity. Therefore, methods to evaluate its physiological status are needed to assess the suitability of a given cornea for being transplanted. Currently, the endothelial cell density evaluated by confocal microscopy is the gold standard parameter used to accept a cornea for grafting (European Eye Bank Association, 2013). Since the cornea is preserved within liquids and cannot be extracted from the storage vial to perform the measurement, the accurately determination of this parameter usually takes a long time (about of 2 hours), being an expensive and tedious procedure.

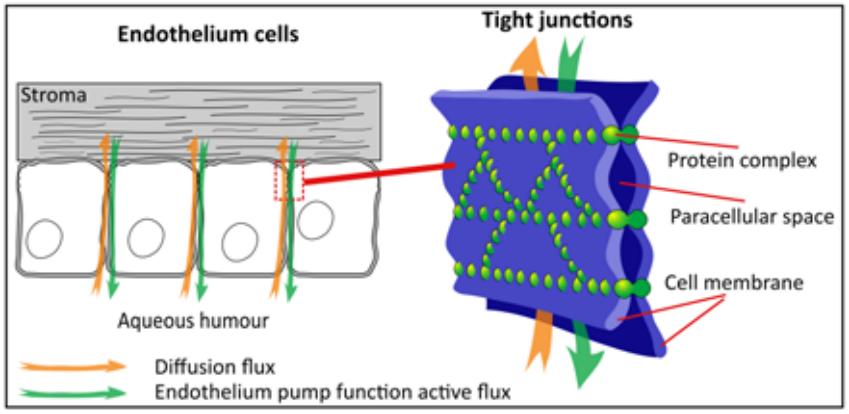

Figure 5-1 Schematic representation of tight junctions. It can be observed how the transmembrane proteins of adjacent cells join together, reducing the paracellular space, and consequently the fluid fluxes.

Besides, the use of endothelial cell density as graft viability indicator is under discussion (Lass et al., 2010), since it is not related directly to the endothelium barrier function, and therefore, to the grafting success. The tight junctions also play an important role in maintaining the endothelium barrier function, and thus in the corneal homeostasis (Srinivas, 2012). Therefore, to maintain the tight junctions integrity during the preservation time is important to guarantee the grafting viability. As it is shown in Figure 5-1, tight junctions are composed of a network of sealing strands. Each strand is formed from a row of transmembrane proteins embedded in plasma membranes, where its extracellular domain are joined directly one another. Thus, tight junctions join together the cytoskeletons of adjacent cells, reducing the paracellular space and forming a virtually impermeable barrier to fluids. Tight junctions are composed of several protein types such as claudins, occludins, actins or zonula occludens-1 (ZO-1). In addition, they are also involved in basic cellular processes like the regulation of cell growth, differentiation, and can been related to the cell viability (Balda and Matter, 1998).

Despite the key role of endothelial tight junctions in regulating corneal permeability, no methods for its evaluation are available in eye banks. Translayer Electrical Resistance (TER)

measurements have been consistently used in *in vitro* studies, allowing a rapid and quantitative evaluation of the endothelium permeability (Ma et al., 2007). In order to assess the corneal endothelium permeability by means of commonly used TER techniques, the corneal epithelium must be removed to avoid its influence in the measurement, as it has a much lower permeability than the corneal endothelium (Lim and Fischbarg, 1981; Kuang et al., 2001).

In this chapter, an alternative method to assess the endothelium permeability of excised corneas without removing the corneal epithelium is presented. Here, it is hypothesized that the tetrapolar impedance measurements developed in the previous chapters could be applied in the excised corneas to assess the endothelium permeability. In order to probe the feasibility of the proposed method, the previous presented rigid impedance sensor was used and the cornea was placed over it with the endothelium side in electric contact with the electrodes. The usefulness of the presented method to evaluate cornea permeability was analyzed in an *ex vivo* model of cornea preservation. The tight junction integrity was assessed by zona occludens (ZO-1) immunofluorescence and the results were correlated with the impedance measurements. The obtained results validate the capability of the proposed method to evaluate the endothelium permeability in unmodified corneas. Thus, the findings of this chapter give the guidelines for developing a sensor able to measure the corneal endothelium functionality in the eye banks, improving the assessment of the donor corneas. This new sensor should be compatible with the current preservation protocols. Moreover, since the proposed method allows the reduction of the experimental procedures it also will be a useful tool for studying the behavior of preservation liquids.

5.2 Materials and methods

5.2.1 Cornea preservation model

The experimental procedures were conducted under the supervision of the SALVAT S.A. ethics committee, conformed to the EU guidelines for handling and care of laboratory animals and following the guidelines of the ARVO Statement for the Use of Animals in Ophthalmic and Vision Research.

Female Lewis rats (>8 weeks old) were obtained from Charles River Laboratories (Germany) and were kept under controlled environmental conditions in ventilated cages with food and drinking water ad libitum. Rats were euthanized by CO_2 inhalation and eyeballs were excised and kept moistened in PBS. Corneas were immediately extracted with a 2 mm scleral ring around it to allow manipulation without endothelium harming. Finally, cold storage was performed at 4°C in a 24 multi-well plaque with 1 cornea per well in 1 ml of Eusol-C (CTC-001-01, Alchimia) during 3, 5 and 7 days. After the preservation period, corneas were rinsed from Eusol-C in PBS and used for impedance measurement or directly fixed in 1% formaldehyde (18814, Polysciences) for ZO-1 immunofluorescence. Freshly harvested corneas were used as negative control (day 0).

5.2.2 Sensor design and fabrication

As commented, the impedance sensor presented in Chapter 3 is now used to perform tetrapolar impedance measurements on excised corneas. The presented sensor was developed to evaluate the corneal barrier function *in vivo* by placing the electrodes on the corneal surface. For the case of excised corneas, the same principle can be applied to directly assess the corneal endothelium permeability, without removing the corneal epithelium. As can be observed in Figure 5-2B, the corneal endothelium is directly contacted with the sensor electrodes, and therefore, as in the case of the *in vivo* epithelium permeability measurements, the obtained impedance should be mainly affected by the endothelium electrical properties in the low frequency range. The sensor consists of ten electrodes which allow the implementation of various tetraploar configurations. Taking into account the reduced dimensions of the rat cornea (6 mm diameter and 100 µm thick), the one with the smallest distance between the pair of electrodes was chosen for this study (geometry scheme shown in Figure 5-2). The sensor was entirely fabricated in the clean room facilities at the Barcelona Microelectronic Institute IMB-CNM (CSIC) by means of standard photolithographic techniques using 500-µm-thick Pyrex® wafers as the substrate material. The whole fabrication process is described in Chapter 3.

5.2.3 Experimental setup

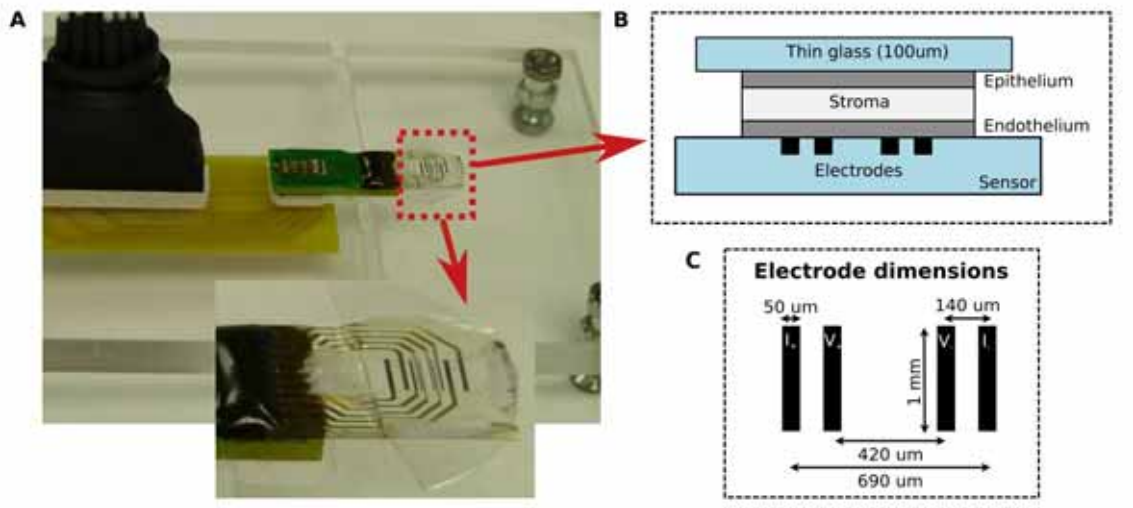

Figure 5-2 A) Image of the experimental setup. B) Schematic detail of the cornea collocation. C) Schematic representation of the electrodes with their dimensions.

As it is shown in Figure 5-2B, the excised cornea was directly placed over the sensor with the endothelium side in contact with the electrodes. Then, to ensure proper electric contact, the cornea was sandwiched by placing a thin glass over it. The final experimental setup was completed with a custom-made poly(methyl methacrylate) (PMMA) platform where the sensor and the connections of the measurement equipment were assembled (Figure 5-2A). It also allows the easy manipulation of the excised cornea, facilitating the supervision through optical equipment (i.e. magnifying glass). Impedance measurements were performed using a custom made tetrapolar impedance analysis system (Guimera et al., 2008; Guimerà et al.,

2009), which is able to measure the impedance over a frequency range from 100 Hz to 1 MHz. To ensure the correct sensor performance, before each measurement the system was tested. For that, a drop of saline solution (30 µl approx) was placed over the sensor.

5.2.4 ZO-1 immunofluorescence

Tight junction integrity was assessed by ZO-1 immunofluorescence. Corneas were rinsed in PBS for 5 minutes and incubated in PBS+0.2% Triton for 1 hour at room temperature (RT) and immediately after in PBS+ 1% BSA+ 5% donkey serum+0.05% Triton for 1 hour at RT. After rinsing corneas in PBS+0.05%Triton for 5 minutes, they were incubated overnight at 4ºC in rabbit anti-ZO-1 polyclonal antibody diluted 1/125 in PBS+0.05%Triton+0.5%BSA (402300, Invitrogen). After incubation and before measurement, corneas were rinsed three times in PBS+0.05 % Triton for 10 minutes and incubated for 1 hour at RT protected from light in donkey anti-rabbit IgG Alexa Fluor® 488 (A-21206, Invitrogen) diluted 1/400 in PBS+0.05%Triton+0.5%BSA. Finally, corneas were mounted with the endothelial side facing up in ProLong Gold Antifade (36934, Invitrogen) mounting media and observed with a fluorescence microscope (FSX100, Olympus). Images were analysed by quantitative image automation conducted by Wimasis software (Munich, Germany) obtaining tight junction area percentage and endothelial cell count.

5.3 Results and discussion

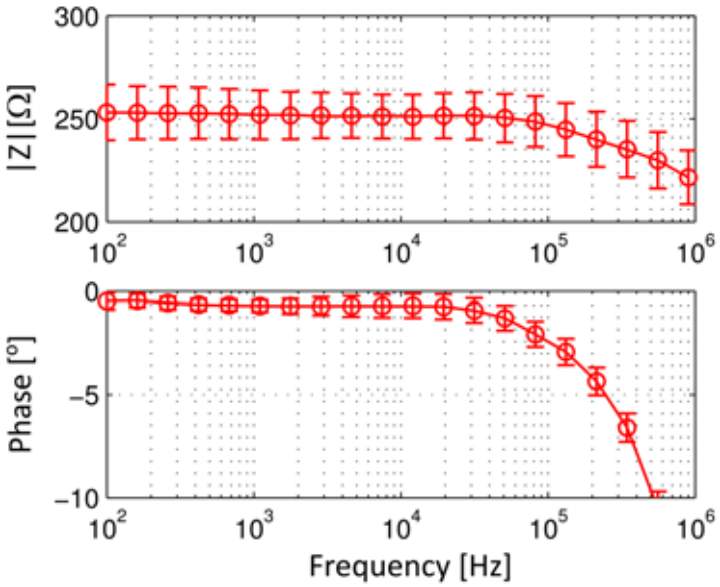

Figure 5-3 Bode representation of the impedance measurements of a NaCl 0.9 wt.% solution performed to test the system before the experimental usage (n=40).

As commented, the impedance sensor, and consequently the whole measurement system have been tested before each experimental usage. Figure 5-3 shows the impedance measurements of a NaCl 0.9 wt.% solution performed to ensure the correct behavior of the system. Ideally, in the analyzed frequency range, the impedance measured of a saline solution should be characterized by a flat modulus and 0º of phase shift (Grimnes and Martinsen, 2008) since it behaves as a pure resistance in the frequency range studied. However, the ideal

behavior cannot be accomplished at frequencies greater than 100 kHz, where a decrease in both modulus and phase can be clearly observed. This can be attributable to the capacitive coupling and current leakages of the wires, which are strongly manifested in high frequency range; therefore, the useful frequency band ranges from 100 Hz to 300 kHz. Moreover, the variation observed in the impedance modulus, can be attributable to variations in the thickness of the saline solution drop deposited over the sensor to perform the verification. However, it can be considered that the system works correctly in frequencies below 20 kHz since the phase shift values are close to 0º.

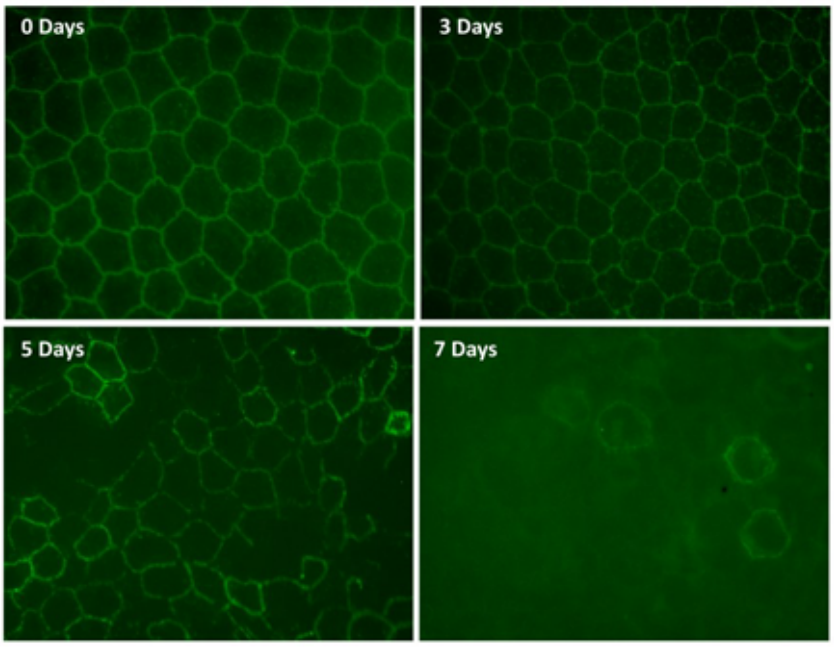

Figure 5-4 Images (40X) of corneal endothelium tight junctions by ZO-1 immunofluorescence after 0, 3, 5 and 7 days of cornea preservation at 4ºC. It can be observed how the tight junctions integrity is loosed with preservation time.

As commented, tight junctions create a paracellular structure responsible of maintaining the corneal endothelium barrier function (Figure 5-1). Endothelium tight junctions stained by ZO-1 immunofluorescence remain intact until 3 days of corneal preservation, as it is shown in Figure 5-4. Its disruption is partially observed at 5 days of preservation, and at 7 days, these unions can only be observed in isolated areas with lower intensity than in previous preservation times. Hence, longer preservation time leads to the complete loss of the tight junction integrity. Accordingly, experimental results of the impedance measurements for each group are depicted in a Bode representation in Figure 5-5. As it can be noted, the measured impedance modulus decreases progressively during cold storage. After 7 days, the impedance value is close to the saline solution ones, indicating that endothelium barrier function is completely impaired at this time. Moreover, a slight decrease in the phase value can also be observed with the preservation time. This behaviour can be explained by an increase of the extracellular current which results in a decrease of the capacitive effect produced by the cell membrane. Since the endothelium permeability is related with extracellular space, the impedance modulus measured at 100 Hz has been chosen as a proper indicator of endothelium permeability for these measurements. Thus, in Figure 5-5, the obtained values are shown in a Boxplot representation.

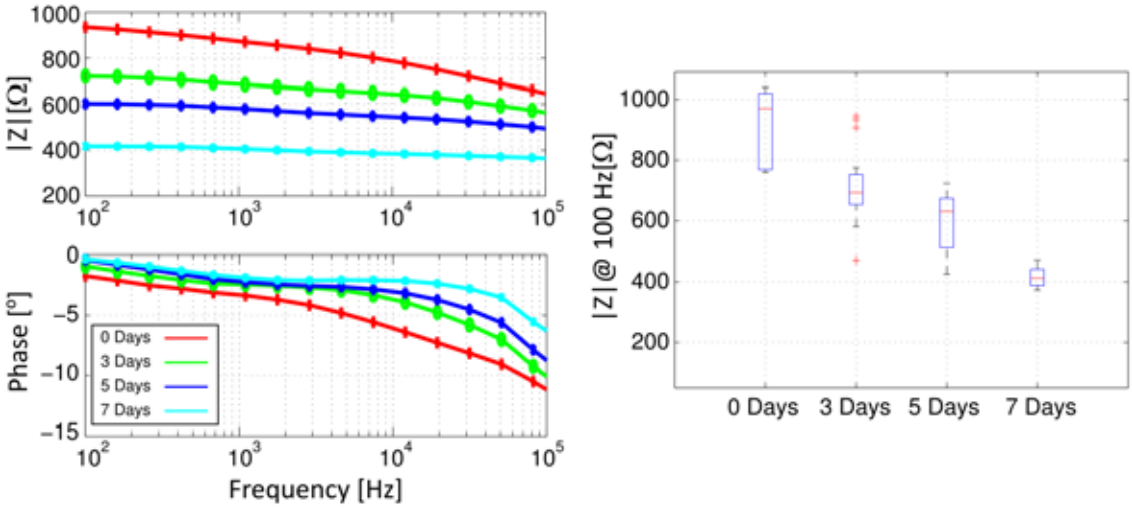

Figure 5-5 Experimental impedance measurements results for different preservation times. (Left) Bode representation of the mean values for each group (Right) Boxplot representation of the impedance modulus measured at 100 Hz. It shows the mean value, the dispersion of the measures grouped by quartiles (boxes and bars) and the outliers values (as crosses).

The tight junction area percentage and endothelial cell count were obtained through the quantitative analysis of the ZO-1 immunofluorescence images. These results are summarized together with the impedance measurement values in Table 5-1. From those values it can be firstly observed that the quantitative assessment of tight junction integrity correlates nicely with the corneal impedance (Figure 5-6), demonstrating that both parameters are intimately related and indicating that this novel method is a good indicator of tight junction integrity. Moreover, with the proposed method, variations in the integrity of the cornea are detected before they are observable by ZO-1 immunofluorescence (values at 3 days).

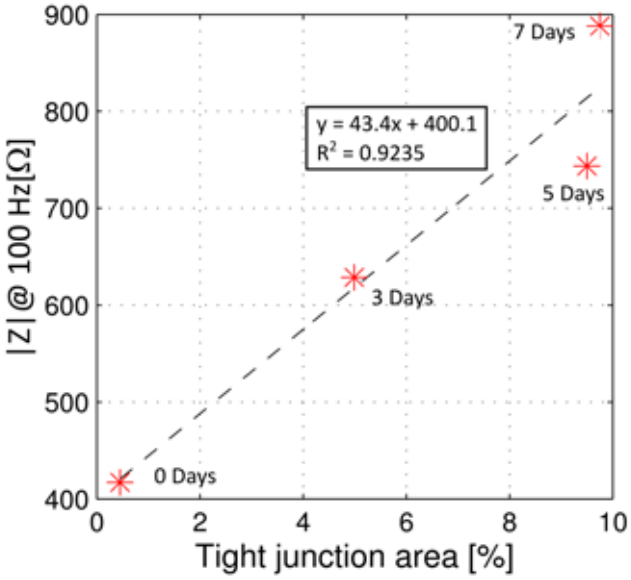

Figure 5-6 Representation of impedance modulus measured at 100 Hz versus tight junction area obtained through the quantitative analysis of the ZO-1 immunofluorescence images. The depicted values are the mean values for each group studied (Table 5-1). The dash line shows the linear regression.

Finally, the endothelial cell count, a parameter widely used to assess corneal quality in the eye banks does not correlate with tight junction values. The cell count maintains a constant

value until 5 days of cold storage and it falls abruptly at 7 days. Therefore, this parameter seems not to be an appropriate indicator of the endothelium barrier integrity.

Table 5-1. Summary of the experimental results. Impedance modulus measured at 100 Hz and quantification of tight junctions area and cell count determined by ZO-1 immunofluorescence image analysis for different preservation times.

Time	***|Z| @ 100 Hz [Ω]***		***Image quantification***		
				Cell Count	***Tight junction area [%]***
	n	*mean ± std*	*n*	*mean ± std*	*mean ± std*
0 day	10	925 ± 117	6	95 ±18	9.75 ± 0,75
3 days	10	718 ± 126	6	95 ±18	9.50 ± 0,85
5 days	10	601 ± 97	6	99 ±34	4.99 ± 3,34
7 days	10	417 ± 35	4	3 ±2	0.45 ± 0,42

In the literature, transendothelial electrical resistance (TER) had been evaluated *ex vivo* using freshly mounted preparations of desepitelialized rabbit corneas (Ma et al 2007). They also reported that TER decreases when endothelial tight junction disruption is induced, in their case by a Ca^{2+} chelator. Regarding the tight junction disruption time course, Kim et al. showed that human corneal endothelial permeability increased after longer preservation times (Kim et al., 1994), indicating that tight junction disruption may also occur in human corneas during cold storage. Moreover, Hsu et al. described that human corneas exhibited enlarged gaps in tight junctions after 2, 5 and 8 days of cold storage with no time-course effect (Hsu et al., 1999). In contrast, our results showed that in rat corneas cold storage induced a progressive impairment of tight junction integrity reaching nearly total disruption at 7 days of preservation. Thus, these results would suggest that in rat corneas tight junction disruption begins earlier and at a higher rate than in human corneas. It is noteworthy that storage mediums had been optimized for human cornea physiological conditions so this higher disruption rate in rat corneas could be due to physiological differences between species.

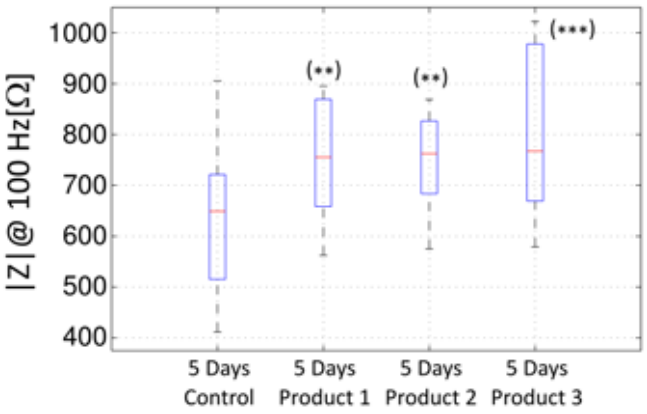

*Figure 5-7 Boxplot representation of the impedance modulus measured at 100 Hz after 5 days of preservation with different products. (*** p<0.001; ** p<0.01 with unpaired student's t-test)*

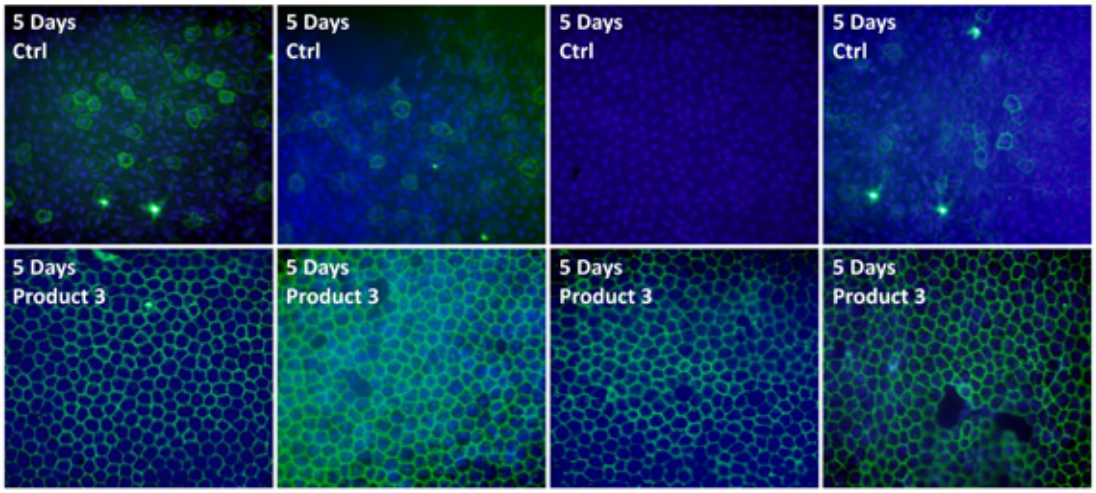

Figure 5-8 Images (40X) of ZO-1 immunofluorescence (green) for tight junctions staining and DAPI immunofluorescence (blue) for cells staining. Results for endothelium of four different corneas preserved at 4ºC during 5 days with DMSO at 0.1% (Control) or with product 3.

In collaboration with the pharmaceutics company SALVAT S.A. the method developed was used to assess the behavior of different drugs in the preservation process. As it is not the objective of this dissertation, the composition of these drugs is not described. Figure 5-7 shows the impedance results obtained with different products after 5 days of cold storage. From this results it can be observed that the product 3 presents a higher impedance values than the other products evaluated, being close to the obtained in the freshly harvest corneas. Moreover, Figure 5-8 shows the images (40X) of immunofluorescence results, where the thigh junctions are stained in green and cells are stained in blue. In accordance with the impedance measurements, the images of the corneas preserved with the product 3 present a higher tight junctions integrity than the conserved in a control solution. Therefore, these results confirm the ability of the presented method to assess the tight junction integrity.

These promising results together with the possibility of this method to be used in complete cornea without the need of desepithelization, pave the way to develop a new system that evaluates the endothelium permeability in human corneas during its preservation before grafting. To make possible this new development, the impedance sensor device must be manufactured with the same curvature of the human cornea. To achieve this goal, the flexible substrate presented in the previous chapter seems to be a feasible alternative. This improvement may avoid damaging the cornea during the measurement. It should be also taken into account the influence of the current leakages through the preservation liquids. To make possible the compatibility of this new system with the preservation protocols, the effect of these current in the measurements should be minimized. This new system would complete the current assessment method of cornea quality based on the cell count with the endothelium barrier function measurement, which is of great importance due to its key role preventing the stroma hydration and keeping corneal transparency.

5.4 Conclusions

In this chapter, a novel method to assess endothelium permeability of rat excised corneas has been presented and validated in a corneal preservation model. The method allows the measurement of the passive electrical properties of the corneal endothelium without removing the epithelium, maintaining the integrity of the cornea and simplifying the experimental procedures. The impedance measurements, performed by placing the whole cornea over four electrodes, were sensitive enough to detect variations in the endothelium permeability with even more resolution than the obtained when using immunofluorescence techniques. Thus, we can conclude that the sensor presented here can be used for *ex vivo* studies, and for the first time to the best of our knowledge, the feasibility of a non-destructive method for assessing endothelium layer function has been demonstrated. Moreover, the presented results pave the way to apply this new method in the assessment of corneas during its preservation in eye banks.

5.5 References

Balda, M.S., Matter, K., 1998. Tight junctions. J. Cell Sci. 111, 541–547.

European Eye Bank Association, 2013. Technical Guidelines for Ocular Tissue reference.

Grimnes, S., Martinsen, Ø.G., 2008. Bioimpedance and bioelectricity basics. Academic Press, New York.

Guimera, A., Calderon, E., Los, P., Christie, A.M., 2008. Method and device for bio-impedance measurement with hard-tissue applications. Physiol. Meas. 29, S279–S290.

Guimerà, A., Gabriel, G., Parramon, D., Calderón, E., Villa, R., 2009. Portable 4 Wire Bioimpedance Meter with Bluetooth Link, in: Dössel, O., Schlegel, W.C. (Eds.), World Congress on Medical Physics and Biomedical Engineering, September 7 - 12, 2009, Munich, Germany, IFMBE Proceedings. Springer, pp. 868–871.

Hsu, J.K., Cavanagh, H.D., Jester, J.V., Ma, L., Petroll, W.M., 1999. Changes in corneal endothelial apical junctional protein organization after corneal cold storage. Cornea 18, 712–720.

Kim, K.S., Edelhauser, H.F., Holley, G.P., Geroski, D.H., Lynn, M., Walsh, G.E., 1994. Corneal endothelial permeability of human tissue after storage in Optisol. Am. J. Ophthalmol. 117, 385–393.

Kuang, K., Li, Y., Wen, Q., Wang, Z., Li, J., Yang, Y., Iserovich, P., Reinach, P.S., Sparrow, J., Diecke, F.P., Fischbarg, J., 2001. Corneal endothelial NKCC: molecular identification, location, and contribution to fluid transport. Am. J. Physiol. Cell Physiol. 280, C491–499.

Lass, J.H., Sugar, A., Benetz, B.A., Beck, R.W., Dontchev, M., Gal, R.L., Kollman, C., Gross, R., Heck, E., Holland, E.J., Mannis, M.J., Raber, I., Stark, W., Stulting, R.D., 2010. Endothelial cell density to predict endothelial graft failure after penetrating keratoplasty. Arch. Ophthalmol. 128, 63–69.

Lim, J.J., Fischbarg, J., 1981. Electrical properties of rabbit corneal endothelium as determined from impedance measurements. Biophys. J. 36, 677–695.

Ma, L., Kuang, K., Smith, R.W., Rittenband, D., Iserovich, P., Diecke, F.P.J., Fischbarg, J., 2007. Modulation of tight junction properties relevant to fluid transport across rabbit corneal endothelium. Exp. Eye Res. 84, 790–798.

Srinivas, S.P., 2012. Cell signaling in regulation of the barrier integrity of the corneal endothelium. Exp. Eye Res. 95, 8–15.

Chapter 6

Conclusions & Future perspectives

The principal conclusions of this dissertation are described in this chapter.

In addition, ongoing tasks intended for applying the developed method to endothelial permeability assessment are also detailed. Here are also described the improvements that should be implemented in order to enable the use of the developed method in the clinical practice.

6.1 Conclusions

Methods to assess the permeability of corneal layers in *in vitro* conditions are well-established, however, it is difficult to find out methods to assess it in *in vivo* conditions, and thus, to be used in clinical practice. The feasibility of a novel method to assess the corneal barrier function through non-invasive impedance measurements has been studied in this thesis. The rationale for this approach was that ion fluxes have a large impact on the passive electrical properties of living tissues. The main conclusions of the work described in this dissertation are:

1) The numerical study of impedance measurements performed with a four-electrodes setup placed on the corneal surface demonstrates that the proposed method is indeed sufficiently sensitive to assess the endothelial and epithelial permeability. The contribution of each corneal layer to the total measured impedance depends on the analyzed frequency. Three frequency ranges can be discerned: impedance measurements at the low frequency band (<1 kHz) are mainly affected by the epithelium layer, the intermediate frequency band (from 1 kHz to 100 kHz) can be considered as a transition zone where the endothelium reaches its maximum contribution, and measurement at the high frequency band (> 100 kHz) are mainly affected by the stroma and the aqueous humour.

2) An impedance sensor on a Pyrex® substrate has been designed and fabricated using standard microelectronic technologies and following the guidelines from numerical study. The developed sensor has been characterized and experimentally validated by pharmacologically increasing the epithelial permeability of rabbit's cornea. The obtained results are related with the alterations observed by corneal histopathological evaluation and fluorescein staining techniques.

3) A measurement method for assessing the endothelial permeability of excised corneas without removing the corneal epithelium has been developed. It is based on the impedance sensor mentioned above and it very significantly simplifies the existing procedures for assessing endothelial permeability. The developed method has been experimentally validated by monitoring a corneal preservation procedure. The obtained results indicate that the measured impedance changes are related with the condition of the endothelial tight junctions as observed by immunostaining image techniques. This implies that impedance measurements provide complementary information to that provided by endothelial cell count, which is the currently used parameter for assessing the viability of a cornea to be grafted.

4) The use of the impedance sensors on a Pyrex® substrate requires the application of a reasonable pressure to flatten the corneal surface and ensure a proper electric contact with the electrodes. In fact, proper contact can only be achieved with the closest electrode configuration (1 mm electrode separation) which results in a severe limitation of sensitivity.

5) Use of a flexible polymer (SU-8) as a substrate improves the usability and performance of the developed impedance sensor since no pressure is required to flatten the cornea. With this new implementation, proper electric contact for all the studied electrode configurations (up to 5 mm electrode separation) can be ensured.

6) It has been experimentally deducted that most of the variations in the obtained impedance measurements are due to the variations in the tear film thickness between the sensor and the corneal surface. This is in accordance with the numerical study, which shows that the contribution of the tear film is considerable across the whole spectrum, being higher at low frequency range and for the closest electrode configuration. It has been experimentally found that the impedance values obtained with the widest electrode configuration (5 mm separation) present a lower dispersion than the closest configurations.

7) From the analysis of the experimental results, it has been found that the imaginary part of the impedance measured at 2 kHz using the 5 mm electrode configuration is the most consistent indicator to quantify the epithelial permeability. This indicator has been validated by pharmacologically increasing the epithelial permeability of rabbit's cornea. The obtained results are related with corneal fluorescein uptake measurements; a destructive method directly related to the epithelial permeability. Small epithelium alterations that cannot be observed with macroscopic diagnostic techniques, such as fluorescein staining, can be detected using the proposed method.

8) The improvement regarding usability provided by the flexible substrate allows the use of the sensor in non-anesthetised animals. Therefore, it simplifies the experimental procedures to monitor different processes, such as the corneal epithelium wound healing, which are of especial interest for drug development.

9) The excellent obtained results together with the non-invasiveness of the sensor enable the current use of the developed method in the clinical practice.

6.2 Work in progress

6.2.1 In vivo assessment of endothelial permeability

As already mentioned, the corneal homeostasis depends upon epithelial and endothelial permeability, which maintains the stroma hydration level, and therefore, the corneal transparency. The main objective of this thesis was the development of a system able to assess the epithelial and endothelial permeability in a non-invasive way. As it has been described in this dissertation, the feasibility of the proposed method for the case of epithelial permeability has been experimentally demonstrated. However, the capability of the proposed method to assess the endothelial permeability has not been validated yet. Although the numerical study described in Chapter 1 shows that the corneal endothelium can be assessed by the proposed method, the experimental validation of those results has not been achieved. Ongoing tasks to achieve this goal are briefly described following.

The reported methods to experimentally increase the endothelial permeability are based on topical administration of BAC solutions (Chen et al., 2011). This procedure also induces epithelial damage, and therefore, it would be difficult to isolate the impact of the endothelial permeability in the obtained impedance. Therefore, the lack of reported experimental procedures to induce an increase of the endothelial permeability in *in vivo* conditions without damaging the epithelium made necessary the development of those procedures. Thus, in collaboration with the biomedical partners (IOBA and SALVAT S.A.), two experimental protocols to increase the endothelial permeability in *in vivo* conditions have been studied. The first one consists in intra-cameral administration of a BAC 0.05% solution, while the second one consists in a mechanical abrasion of the endothelium layer produced by inserting a needle through the sclera in the interior chamber. However, first experimental results showed very low repeatability. Moreover, the impossibility to quantify the damage produced make difficult the determination of robust conclusions about the feasibility of the proposed method.

Those incongruous results may be caused by the reduced space of the rabbit's intra-cameral space since the used procedures may produce an alteration in the aqueous humour volume and pressure. This fact has been suggested as possible cause of the obtained incongruous results. Therefore, the use of other animal models has been explored. In particular, and considering that the morphological structure of the pig's eyes is similar to the human one it has been chosen as a feasible model.

Experimental uses of big animals requires of specific facilities which limit its implementation. Therefore, in collaboration with the Institut Clínic del Tòrax of Hospital Clínic de Barcelona, the possibility to apply the above commented experimental procedure in pigs was studied. Then, our experimentation has been adapted to be performed at the same time but without interfering the cardiovascular experimental procedures performed by the clinical investigators. Moreover, this experimentation has been done under the supervision of the ethics committee of Hospital Clinic de Barcelona, conformed to the UE guidelines for handling and care of laboratory animals.

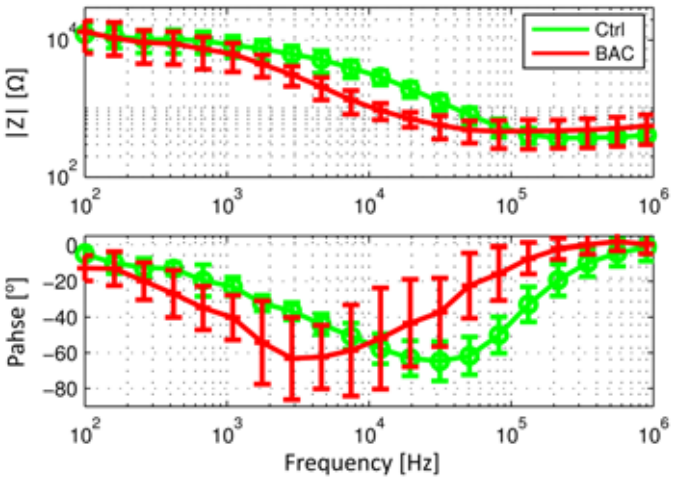

Figure 6-1 Experimental impedance measurements for the pig's eyes insulted with intra-cameral administration of BAC 0.05% solution. The results are presented as mean values and standard deviation, where each group is composed of 12 measurements resulting from three repeated measurements performed over 4 eyes.

The obtained results on pig's eyes are presented as mean values and standard deviation in Figure 6-1, where each group is composed of 12 measurements resulting from three repeated measurements performed over 4 eyes. It can be clearly observed a decrease in the impedance modulus measured at intermediate frequencies (from 1 kHz to 100 kHz) in the measurements performed 45 minutes after the BAC solution application. Although these satisfactory results, the induced damage could not be quantified by the corneal pachymetry measurements, and therefore, the affirmation that this variation is due to the increase of the endothelium permeability cannot be stated at all. Therefore, to validate the capability of the proposed method to assess the corneal endothelium permeability more experimental studies should be performed. These new studies should be focused on the development of experimental techniques to quantify the induced damage in order to correlate it with the impedance measurements.

6.2.2 Clinical assay

The consistent results described in this dissertation, together with the non-invasiveness of the developed impedance sensor have enabled the transfer of the proposed method to the clinical practice. For that, the developed system has been validated as a class II medical device by the Electromagnetic Compatibility Group (GCEM) of Polytechnic University of Catalonia (UPC) after filling the electrical safety and electromagnetic compatibility requirements of the UNE-EN 60601-1. Figure 6-2 shows the whole medical device, which is based on the system presented in the Chapter 4 and composed of a tetrapolar impedance analysis system, the tetrapolar multiplexor module and a disposable impedance sensor. It allows the acquisition and storage of the impedance measurements autonomously. It implements functions to check the proper performance of the impedance sensor after measuring it in a physiologic saline solution. Finally, the impedance senor is placed over the corneal surface after instillation of a topical anesthetic in order to reduce the involuntary ocular movements.

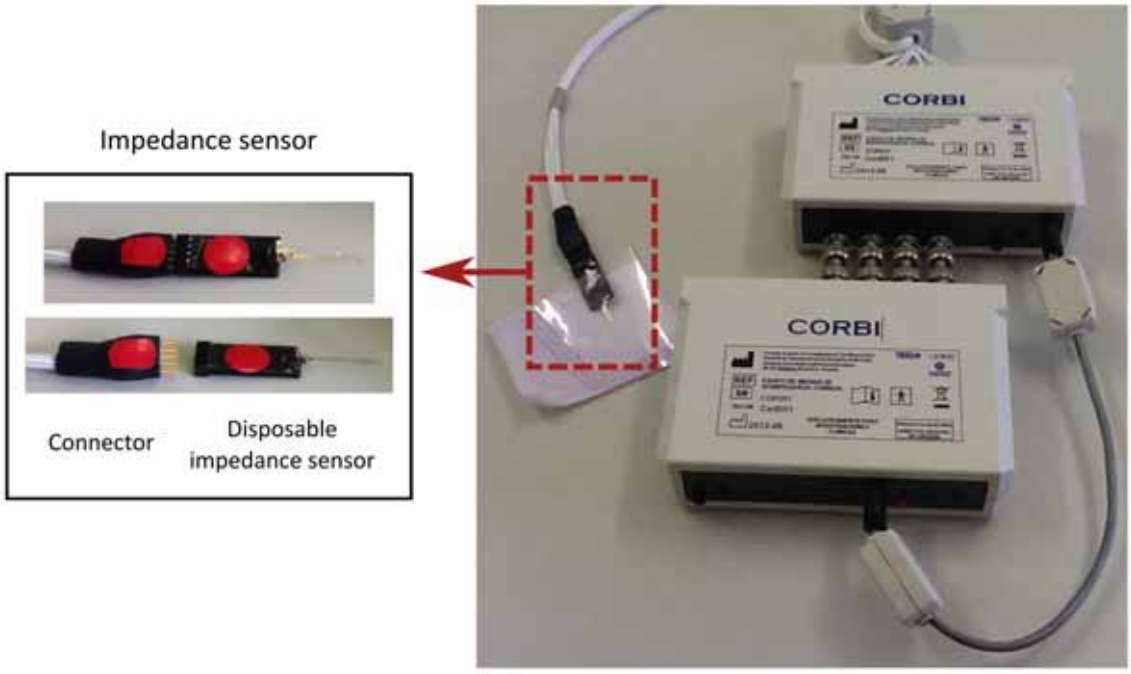

Figure 6-2 Image of the developed system homologated as a class II medical device by the AEMPS. It is composed by the tetrapolar impedance analysis system, the tetrapolar multiplexer module and the impedance sensor. The impedance sensor can be easily attached as a disposable part.

To evaluate the feasibility of the system in the clinical practice, a clinical assay formed by two kinds of patients and carried out in collaboration with IOBA and SALVAT S.A., has been authorized by the AEMPS. The first group is composed of cataract surgery patients as, in some cases, this clinical practice may produce damage in the corneal endothelium (Bourne et al., 2004; Díaz-Valle et al., 1998; Ventura et al., 2001). Moreover, the use of several topical drugs during the intervention can also produce an increase in the epithelium permeability (Holden et al., 1982). In order to monitor each patient, the impedance measurement is performed before the surgical procedure and several times after the intervention (1 day, 1 week, 2 weeks and 4 months). The second group is composed of patients who wear contact lenses as it has also been reported that its wearing can lead in alterations of the corneal barrier function (Lin et al., 2002; McNamara et al., 1998).

The clinical assay is still ongoing, and therefore, final conclusions cannot be stated. However, it is interesting to show some preliminary results for the cataract surgery patients. In Figure 6-3, the obtained impedance measurements are compared with the previously presented measurements of rabbits. The results are presented as the average values of basal measurements, 20 eyes for the case of humans and 100 eyes for the case of rabbits. It can be observed that the impedance modulus is lower for the case of human. Thus, it could suggest that the human's permeability is larger than the rabbit's permeability in healthy conditions. Moreover, it can be clearly observed than the rabbit's corneal impedance spectrum presents two relaxations, where the one with lower frequency is associated to the corneal epithelium and the other one to the corneal endothelium. In contrast, the human's corneal impedance spectrum only presents one relaxation. More studies should be carried out to explain the reason of these differences.

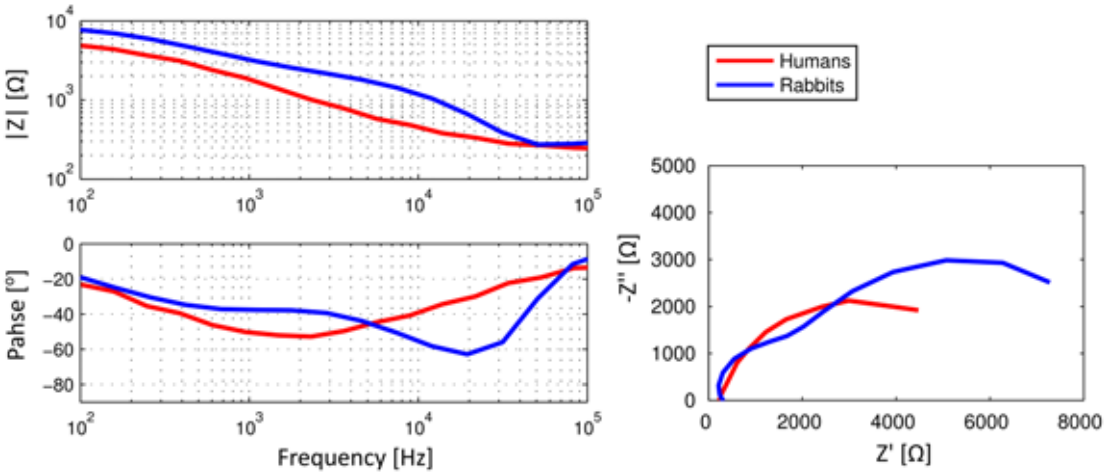

Figure 6-3 Comparison of the experimental impedance measurements for humans (red line) and rabbits (blue line). The results are presented as the average values of the basal measurement, 20 eyes for the case of humans and 100 eyes for the case of rabbits

To perform a preliminary analysis of the data obtained in the clinical assay, the impedance spectrum has been fitted to the Cole-Cole equation (Grimnes and Martinsen, 2008), obtaining consistent fittings. Figure 6-4 depicts in a Boxplot representation the Ro parameter of the Cole-Cole equation obtained from the measurements of the patients submitted to cataracts surgery. The Ro parameter is related with the impedance modulus at low frequency, and therefore, can be related with the permeability of the corneal epithelium. As can be observed, the measurements performed 1 day before the surgery tend to be lower than the other measurements. Then, it can be suggested that this tendency may be related with the use of several ophthalmologic drugs during the surgical procedure.

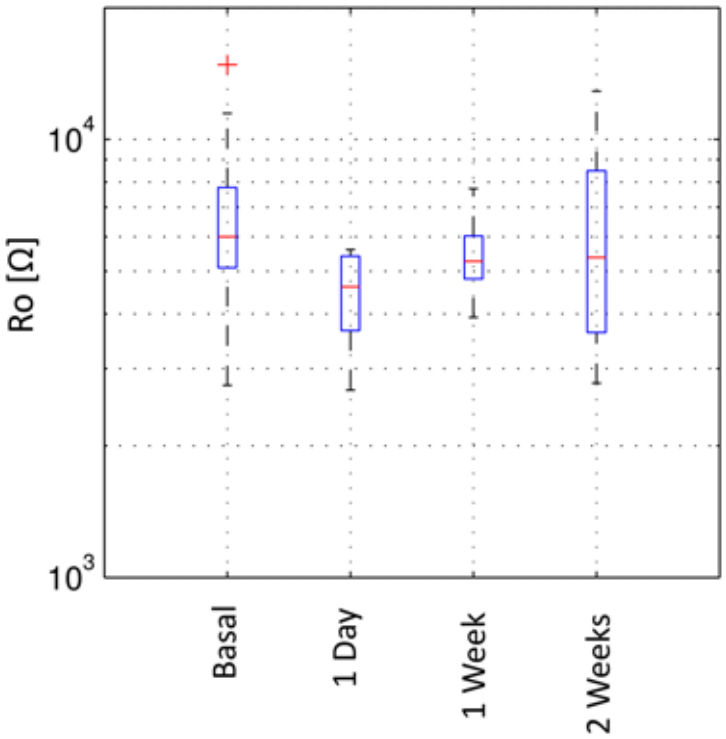

Figure 6-4 Boxplot representation of the Ro parameter for the measurements obtained in the clinical assay for the cataracts surgery patients. Each group is composed by 10 values.

6.3 Future perspectives

Concerning to the development of a system to assess the endothelium permeability of excised corneas, the obtained results pave the way to develop a new system that could evaluate endothelium permeability in human corneas during the preservation time and before grafting. This new system would complete the current assessment method of cornea quality based on cell count with the endothelium barrier function measurement, which is of great importance due to its key role preventing the stroma hydration and keeping corneal transparency. Future work on this field will be focused on developing an impedance sensor device with the same curvature of the human cornea. To achieve this goal, the flexible substrate presented in Chapter 4 together with the use of rapid prototyping techniques seems to be a feasible alternative. This improvement will avoid damaging the cornea during the measurement. Furthermore, since the cornea cannot be extracted from the storage vial to perform the measurement, the effect of the current leakages through the preservation liquids in the measured impedance should be studied and minimized in order to make possible the compatibility of this new system with the actual preservation protocols.

Preliminary results of the clinical assay validate the capability of the developed medical device to assess the epithelial permeability in the clinical practice. However, some improvements in the developed system could increase its performance and the measurements consistency. These improvements should be focused in the reduction of the measurement acquisition time, which will reduce the influence of involuntary ocular movements and increase the usability of the sensor.

Moreover, in order to validate the sensitivity of the developed method in the clinical practice, the performed measurements should be compared with permeability to fluorescein measurements. This is the unique method to directly evaluate the epithelial permeability that can be used in the clinical practice. However, due to the low repeatability and the time required to perform the measurement, its use is limited to experimental purposes (Bourne and McLaren, 2004; McNamara et al., 1997). In the context of the INDREYE project, the possibility to use the developed system to assess the dry eye syndrome will be studied. In addition, and for this case, the obtained measurements will be compared with the flourophotometer measurements.

6.4 References

Bourne, R.R.., Minassian, D.C., Dart, J.K.., Rosen, P., Kaushal, S., Wingate, N., 2004. Effect of cataract surgery on the corneal endothelium: Modern phacoemulsification compared with extracapsular cataract surgery. Ophthalmology 111, 679–685.

Bourne, W.M., McLaren, J.W., 2004. Clinical responses of the corneal endothelium. Exp. Eye Res. 78, 561–572.

Chen, W., Li, Z., Hu, J., Zhang, Z., Chen, L., Chen, Y., Liu, Z., 2011. Corneal Alternations Induced by Topical Application of Benzalkonium Chloride in Rabbit. PLoS One 6.

Díaz-Valle, D., Sánchez, J.M.B. del C., Castillo, A., Sayagués, O., Moriche, M., 1998. Endothelial damage with cataract surgery techniques. J. Cataract Refract. Surg. 24, 951–955.

Grimnes, S., Martinsen, Ø.G., 2008. Bioimpedance and bioelectricity basics. Academic Press, New York.

Holden, B.A., Polse, K.A., Fonn, D., Mertz, G.W., 1982. Effects of cataract surgery on corneal function. Invest. Ophthalmol. Vis. Sci. 22, 343–350.

Lin, M.C., Graham, A.D., Fusaro, R.E., Polse, K.A., 2002. Impact of Rigid Gas-Permeable Contact Lens Extended Wear on Corneal Epithelial Barrier Function. Invest. Ophthalmol. Vis. Sci. 43, 1019–1024.

McNamara, N., Fusaro, R., Brand, R., Polse, K., Srinivas, S., 1997. Measurement of corneal epithelial permeability to fluorescein. A repeatability study. Invest. Ophthalmol. Vis. Sci. 38, 1830–1839.

McNamara, N.A., Polse, K.A., Fukunaga, S.A., Maebori, J.S., Suzuki, R.M., 1998. Soft lens extended wear affects epithelial barrier function. Ophthalmology 105, 2330–2335.

Ventura, A.C.S., Wälti, R., Böhnke, M., 2001. Corneal thickness and endothelial density before and after cataract surgery. Br. J. Ophthalmol. 85, 18–20.

Publications

Publications in indexed journals

1) A. Guimerà, A. Ivorra, G. Gabriel, R. Villa *"Non-invasive assessment of corneal endothelial permeability by means of electrical impedance measurements"*. **Medical Engineering & Physics** (2010) 32:1107–1115. doi: 10.1016/j.medengphy.2010.07.016

2) A. Guimerà, G. Gabriel, M. Plata-Cordero, L. Montero, M.J. Maldonado, R. Villa *"A non-invasive method for an in vivo assessment of corneal epithelium permeability through tetrapolar impedance measurements"*. **Biosensors and Bioelectronics** (2012) 31:55–61. doi: 10.1016/j.bios.2011.09.039

3) L. Montero, G. Gabriel, A. Guimerà, R. Villa, K.K. Gleason, S. Borrós *"Increasing biosensor response through hydrogel thin film deposition: Influence of hydrogel thickness"*. **Vacuum** (2012) 86:2102–2104. doi: 10.1016/j.vacuum.2012.06.002

4) A. Guimera, X. Illa, E. Traver, S. Marchan, C. Herrero, C. Lagunas, M.J. Maldonado, A. Ivorra, R. Villa *"In vivo assessment of corneal barrier function through non-invasive impedance measurements using a flexible probe"*. **Journal of Physics: Conference Series** (2013) 434:012072. doi: 10.1088/1742-6596/434/1/012072

5) A. Guimerà, X. Illa, E. Traver, M. Plata-Cordero, J. Yeste, C. Herrero, C. Lagunas, M.J. Maldonado, R. Villa *"Flexible probe for in vivo quantification of corneal epithelium permeability through non-invasive tetrapolar impedance measurements".* **Biomedical Microdevices** (2013) 15:849–858. doi: 10.1007/s10544-013-9772-x

Contributions in conferences

- Conference: 20th World Congress on Biosensors (Biosensors 2010)
  Location: Glasgow (United Kingdom) Year: 2009
  Type of Contribution: **Poster.**
  Authors: A. Guimerà, G. Gabriel, R. Villa
  Title: *"A corneal electrical model for a non-invasive assessment of corneal endothelial permeability"*.

- Conference: European Association for Vision and Eye Research Conference (EVER 2012)
  Location: Nice (France) Year: 2012
  Type of Contribution: **Oral.**
  Authors: C. Herrero, S. Marchán, E. Traver, R. Montava, M. Orzáez, M. Sancho, A. Guimerà, R. Villa, E. Pérez-Payá, C. Lagunas
  Title: *"Inhibition of Apaf-1 as a potential therapeutic strategy to improve corneal quality"*.
  Reference: Acta Ophthalmologica 90:0–0. doi: 10.1111/j.1755-3768.2012.3434.x

- Conference: 25th International Conference on Electrical Bio-Impedance (ICEBI 2013)
  Location: Heilbad Heiligenstadt (Germany) Year: 2013
  Type of Contribution: **Oral.**
  Authors: A. Guimera, X. Illa, E. Traver, S. Marchan, C. Herrero, C. Lagunas, M.J. Maldonado, A. Ivorra, R. Villa
  Title: *"Flexible probe for in vivo quantification of corneal epithelium permeability through non-invasive tetrapolar impedance measurements"*.

- Conference: European Academy of Optemetry and Optics (EAOO 2013)
  Location: Malaga (Spain) Year: 2013
  Type of Contribution: **Poster.**
  Authors: A. del Río, M. Plata-Cordero, A. Guimerà, E. Traver, R. Martín, R. Villa, C. Herrero, C. Lagunas, M. J. Maldonado
  Title: *"A new non-invasive method to assess corneal integrity based on bioimpedance measurements"*.

Patents

- Title: *"Non-invasive sensor for determining determining characteristics of the cornea, device including said sensor and use thereof ".*
  PCT number: PCT/ES2011/070131
  Priority date: 2 March 2010
  Authors: A. Guimerà, R. Villa, G. Gabriel, M.J. Maldonado

Abbreviations and symbols

List of abbreviations and symbols used throughout the dissertation

ARVO	Association for Research in Vision and Ophthalmology
Au	Gold
BAC	benzalkonium chloride
BI	Bioimpedance
BSA	Bovine serum albumin
CFC	Corneal Fluorescein Content
CMRR	Common Mode Rejection Ratio
CORBI	Development of a new noninvasive diagnostic method of the cornea based on bioimpedance measurement using micro-nano-technologies
CPE	Constant Phase Element
CSIC	Consejo Superior de Investigaciones Científicas
FEM	Finite Elements Method
FITC	Fluorescein test
GEMAT	Grup d'enginyeria de Materials, Institut Químic de Sarrià
H	Health status parameter for the endothelial and epithelial layer
I	Current
i	Complex number (-1)1/2
ICC	Intraclass Correlation Coefficient
IgG	Immunoglobulin G
IMB-CNM	Institut de Microelectrònica de Barcelona, Centro Nacional de Microelectrónica
IOBA	Instituto de Oftalmobiologia Aplicada, Valladolid
IPA	Isopropyl alcohol
J	Current density
MINECO	Ministerio de Economía y Competitividad
N_2	Nitrogen
NaCl	Sodium chloride
Ni	Nickel
O_2	Oxygen
OCT	Ocular Coherence Tomography
p	Confidence interval

PBS	Phosphate buffered saline
PCB	Printed circuit board
PGMEA	propylene glycol methyl ether acetate
pHEMA	Poly(2-hydroxyethyl methacrylate)
Pt	Platinum
RT	Room temperature
S	Sensitivity
Si	Silicon
Si_3N_4	Silicon nitride
SiO_2	Silicon dioxide
SU-8	Epoxy-based negative photoresist
TBPO	TerButylPerOctoate
TER	Translayer Electrical Resistance
Ti	Titanium
UE	European Union
UV	Ultraviolet
V	Voltage or voltage units (Volts)
Z	Impedance (complex number)
ZIF	Zero insertion force
ZO-1	Zonula Occludens 1
ρ	Resistivity
σ	Conductivity
ω	Angular frequency
ε_r	Relative permittivity
ε_o	Permittivity of the vacuum

List of figures